

# Non-hermitian Green's function theory with $N$ -body interactions: the coupled-cluster similarity transformation

Christopher J. N. Coveney<sup>1,\*</sup> and David P. Tew<sup>2,†</sup>

<sup>1</sup>*Department of Physics, University of Oxford, Oxford OX1 3PJ, United Kingdom*

<sup>2</sup>*Physical and Theoretical Chemistry Laboratory,  
University of Oxford, South Parks Road, United Kingdom*

(Dated: March 11, 2025)

## Abstract

We present the diagrammatic theory of the irreducible self-energy and Bethe-Salpeter kernel that naturally arises within the Green's function formalism for a general  $N$ -body non-hermitian interaction. In this work, we focus specifically on the coupled-cluster self-energy generated by the similarity transformation of the electronic structure Hamiltonian. We develop the biorthogonal quantum theory to construct dynamical correlation functions where the time-dependence of operators is governed by a non-hermitian Hamiltonian. We extend the Gell-Mann and Low theorem to include non-hermitian interactions and to generate perturbative expansions of many-body Green's functions. We introduce the single-particle coupled-cluster Green's function and derive the perturbative diagrammatic expansion for the non-hermitian coupled-cluster self-energy in terms of the 'non-interacting' reference Green's function,  $\tilde{\Sigma}[G_0]$ . From the equation-of-motion of the single-particle coupled-cluster Green's function, we derive the self-consistent renormalized coupled-cluster self-energy,  $\tilde{\Sigma}[\tilde{G}]$ , and demonstrate its relationship to the perturbative expansion of the self-energy,  $\tilde{\Sigma}[G_0]$ . Subsequently, we show that the usual electronic self-energy can be recovered from the coupled-cluster self-energy by neglecting the effects of the similarity transformation. We show how the coupled-cluster ground state energy is related to the coupled-cluster self-energy and provide an overview of the relationship between approximations for the coupled-cluster self-energy, IP/EA-EOM-CCSD and the  $G_0W_0$  approximation. As a result, we introduce the CC- $G_0W_0$  self-energy by leveraging the connections between Green's function and coupled-cluster theory. Finally, we derive the diagrammatic expansion of the coupled-cluster Bethe-Salpeter kernel.

---

\* [christopher.coveney@physics.ox.ac.uk](mailto:christopher.coveney@physics.ox.ac.uk)

† [david.tew@chem.ox.ac.uk](mailto:david.tew@chem.ox.ac.uk)

## I. INTRODUCTION

The Green's function formalism is one of the major pillars in the *ab initio* theory of many interacting particles [1–3]. Green's function theory is based on the analysis of  $N$ -point dynamical correlation functions, with the single-particle Green's function occupying the central position. A significant conceptual and computational advantage of Green's functions is that they provide a simultaneous description of ground and excited state many-body correlation. Knowledge of the single-particle Green's function gives access to the exact addition and removal energies, ground state expectation value of any single-particle observable and, for two-body interactions, the exact ground state energy of the system. Similarly, knowledge of the  $N$ -body Green's function yields ground and excited state properties of  $N$ -body observables.

Direct computation of the single-particle Green's function scales exponentially with the number of interacting particles, requiring knowledge of exact eigenstates of the full many-body Hamiltonian containing different numbers of particles. However, the single-particle Green's function can also be constructed from the Dyson equation. The Dyson equation relates a known, reference Green's function to the exact, interacting Green's function through the irreducible self-energy. The irreducible self-energy contains all the many-body interactions a single-particle experiences as it propagates through the system. The self-energy itself depends on the exact Green's function such that the Green's function formalism constitutes a self-consistent theory [4]. The self-energy can be expressed either as a perturbative or self-consistent Feynman diagrammatic expansion. For systems of particles governed by a two-body interaction, theories of the self-energy have been well established and extensively explored in nuclear and condensed matter systems [3, 5–11]. Only recently, in the context of nuclear theory, has the Green's function formalism been extended to include three-body interactions [12, 13]. Until now, the development of the Green's function formalism in the context of non-hermitian  $N$ -body interactions has been entirely unexplored.

Another central pillar in the *ab initio* theory of many interacting particles is coupled-cluster (CC) theory [14, 15]. Coupled-cluster theory is directly concerned with obtaining ground state properties of a system of many interacting particles. It is based on a size-extensive reformulation of the configuration interaction that leads to hierarchical and systematically controllable sets of equations that are, in principle, exact. CC theory is formu-

lated in terms of the non-hermitian similarity transformed Hamiltonian. The CC similarity transformation is determined by the ground state CC amplitude equations. In general, when the CC transformation is not truncated, the similarity transformed Hamiltonian is an  $N$ -body non-hermitian operator that possesses different left and right eigenstates. Excited state properties are then obtained from linear response theory on the CC ground state ansatz, referred to as equation-of-motion coupled-cluster (EOM-CC) theory.

Until now, attempts at combining coupled-cluster and Green's function methods have been largely centered around direct construction of the electronic single-particle Green's function using the eigenstates and eigenvalues resulting from ground state and IP/EA-EOM-CC theory [16–20]. This approach has led to many practical advantages over conventional many-body Green's function techniques for computing spectral functions and charged excitation energies [20–23]. However, these approaches to combining coupled-cluster with Green's function theory do not connect to a diagrammatic construction of the irreducible coupled-cluster self-energy [24]. Further, the connections to the coupled-cluster Bethe-Salpeter equation for neutral and two-particle excitation energies remain largely unexplored. The reason for this is that the formalism required to generate expressions for non-hermitian self-energies corresponding to higher-body non-hermitian Hamiltonians has not yet been developed. Recently, there has been increasing interest in understanding and exploring the connections between coupled-cluster and Green's function theories based on the approximate  $G_0W_0$  self-energy [25–28]. This work has been crucial in furthering the conceptual understanding of the nature of the many-body self-energy in the context of wavefunction based approaches. However, Green's function theory is centered about universal relationships between the exact single-particle Green's function and irreducible self-energy functional,  $\Sigma[G]$  [3]. To fully understand the relationship between the functional-diagrammatic framework of Green's function theory and the coupled-cluster similarity transformation it is necessary to develop new methods to construct the self-energy generated by a higher than two-body, non-hermitian interaction Hamiltonian.

In this work, we generalize the conventional formulation of Green's function theory, based on hermitian two-body (and recently three-body [12]) interactions, to include up to  $N$ -body hermitian and/or non-hermitian interactions. We present the diagrammatic theory of the self-energy generated by a non-hermitian  $N$ -body interaction, focusing specifically on the coupled-cluster similarity transformed Hamiltonian. This formalism unifies and combines

the techniques of CC and Green’s function theory, thereby furthering the conceptual understanding of ground and excited state many-body correlation in the context of condensed matter and nuclear physics. Our approach is based on taking the coupled-cluster similarity transformed Hamiltonian as the fundamental interaction Hamiltonian. This change of perspective unveils the derivation of the resulting theory of the self-energy and single-particle Green’s function that naturally arise within the context of coupled-cluster theory.

The diagrammatic content of the irreducible self-energy depends on whether it is expanded with respect to the non-interacting or exact Green’s function. Expansion of the electronic self-energy with respect to the exact Green’s function gives rise to self-consistent renormalization and leads to the GF2 and *GW* approximations [4, 29–36]. In the case of a two-body interaction, the interaction lines/vertices appearing in irreducible self-energy diagrams are ‘bare’, exhibiting no dependence on the form of the Green’s function itself. Whilst it is true that Hedin’s equations introduce the screened interaction  $W$ , which is also a functional of the single-particle Green’s function, this is a choice that is not fundamentally necessary to construct the self-consistent self-energy expansion. However, in the presence of higher-body interactions, the interaction lines/vertices appearing in the self-energy expansion are fundamentally dependent on which Green’s function the self-energy is expanded with respect to. For example, if the self-energy is expanded with respect to the non-interacting Green’s function,  $G_0$ , it is composed of one-particle irreducible diagrams that are constructed from effective interactions that arise when normal-ordering the Hamiltonian with respect to the reference state. However, to construct the self-energy as a functional of the exact Green’s function requires effective interactions that arise when normal-ordering the Hamiltonian with respect to the exact ground state. It is a fundamental consequence of the Green’s function formalism that interaction vertices of the self-energy are dressed by the Green’s function. However, this consideration has been entirely unexplored in the context of non-hermitian interactions and coupled-cluster theory. This analysis is not only crucial to construct the correct renormalized self-energy functional but also to generate the correct diagrams of the Bethe-Salpeter kernel which arise by taking the functional derivative of the renormalized self-energy with respect to the exact Green’s function.

This paper is organized as follows. In Section II, we present a brief summary of the key results presented in this paper. In Section III, we provide an overview of the conventional Green’s function formalism. Here, we touch on the fundamental principles of Green’s

function theory and considerations that must be made when constructing the irreducible self-energy. In Section IV, we review the biorthogonal quantum theory in order to discuss the pictures of quantum mechanics in the presence of a non-hermitian Hamiltonian. Here, we define the biorthogonal Schrodinger, Heisenberg and Interaction pictures, extending the Gell-Mann and Low theorem to include non-hermitian interactions. In Section V, we define the single-particle Green's function and Dyson equation for a system governed by an  $N$ -body non-hermitian Hamiltonian. We demonstrate the generalization of effective interactions required to construct the non-hermitian irreducible self-energy as a functional of the exact Green's function. In Section VI, we provide an overview of coupled-cluster theory and the similarity transformed Hamiltonian. In Section VII we discuss the coupled-cluster representation of the electronic Green's function which leads us to define the genuine single-particle coupled-cluster Green's function. In Section VIII, we derive the perturbative expansion of the single-particle coupled-cluster Green's function, thereby defining the irreducible coupled-cluster self-energy. In Section IX, we derive the diagrammatic perturbation expansion of the irreducible coupled-cluster self-energy, demonstrating its relationship to the conventional electronic self-energy. In Section X, we construct the non-perturbative renormalized coupled-cluster self-energy from the equation-of-motion of the single-particle coupled-cluster Green's function. Here, we describe how the perturbative expansion is recovered from the self-consistent renormalization procedure. In Section XI, we demonstrate the relationship between the coupled-cluster self-energy and the coupled-cluster ground state energy. In Section XII, we use the spectral representation of the coupled-cluster self-energy to derive the associated coupled-cluster Dyson supermatrix. Here, we also introduce several different approximations for the coupled-cluster self-energy that may be readily implemented. In Section XIII, we demonstrate the relationship between the coupled-cluster self-energy, IP/EA-EOM-CCSD and the  $G_0W_0$  approximation. This motivates us to introduce CC- $G_0W_0$  theory that combines aspects of Green's function theory and Hedin's equations with coupled-cluster theory. Finally, in Section XIV, we derive the relationship between the coupled-cluster self-energy and the Bethe-Salpeter kernel. We present our conclusions and outlook for future work in Section XV.

Throughout this work, indices and wavevectors  $i\mathbf{k}_i, j\mathbf{k}_j, \dots$  denote occupied (valence band) spin-orbitals and  $a\mathbf{k}_a, b\mathbf{k}_b, \dots$  will denote virtuals (conduction band). A mixture of latin and greek indices  $p\mathbf{k}_p, q\mathbf{k}_q, \alpha\mathbf{k}_\alpha, \dots$  is used to denote general spin-orbitals. The





contribute at second-order as they evaluate to zero due to the coupled-cluster amplitude equations. The third-order diagrams of the electronic self-energy are given by

$$\Sigma^{(3)}[G] = \text{[Diagram 1]} + \text{[Diagram 2]} \quad (6)$$

For the coupled-cluster self-energy, we see the appearance of many more diagrams at third-order which demonstrate the presence of two and three-body effective interactions (introduced by the coupled-cluster similarity transformation) which are themselves also functionals of  $\tilde{G}$ , as defined in Section X. The three-body interaction  $\tilde{\chi}_{pqr,stu}[\tilde{G}]$ , is also defined in Section X. The diagrams are as follows:

$$\tilde{\Sigma}^{(3)}[\tilde{G}] = \text{[Diagram 1]} + \text{[Diagram 2]} + \text{[Diagram 3]} + \text{[Diagram 4]} + \text{[Diagram 5]} + \text{[Diagram 6]} + \text{[Diagram 7]} + \text{[Diagram 8]} + \text{[Diagram 9]} + \text{[Diagram 10]} \quad (7)$$

We see that the first two diagrams are topologically identical to the electronic case, containing correlation effects only due to the two-body effective interaction. There are no

higher-body terms that contribute to the coupled-cluster self-energy at third-order as all vanish due to the amplitude equations.

Within Green's function theory, the ground state electronic correlation energy is obtained from the electronic Green's function and self-energy through the Galitskii-Migdal formula

$$E_c = -\frac{i}{2} \lim_{\eta \rightarrow 0^+} \sum_{pq} \int_{-\infty}^{\infty} \frac{d\omega}{2\pi} e^{i\eta\omega} \Sigma_{pq}^c(\omega) G_{qp}(\omega). \quad (8)$$

This formula is exact because the electronic structure Hamiltonian is a two-body operator. In coupled-cluster theory, the ground state correlation energy is found directly from the first-order contribution to the static self-energy

$$E_c^{\text{CC}} = \frac{1}{2} \sum_i \left( \tilde{\Sigma}_{ii}^{\infty(0)} + \sum_a h_{ia} t_i^a \right), \quad (9)$$

as derived in Section XI, and is equivalent to the Galitskii-Migdal formula for the electronic correlation energy for a two-body interaction [24].

From the spectral representation of the coupled-cluster self-energy, in Section XII we derive the coupled-cluster Dyson supermatrix [24]

$$\tilde{\mathbf{D}}^{\text{CC}} = \begin{pmatrix} \mathbf{f} + \tilde{\Sigma}^{\infty} & \tilde{\mathbf{U}} & \tilde{\mathbf{V}} \\ \tilde{\mathbf{U}} & \bar{\mathbf{K}}^> + \bar{\mathbf{C}}^> & 0 \\ \tilde{\mathbf{V}} & 0 & \bar{\mathbf{K}}^< + \bar{\mathbf{C}}^< \end{pmatrix}. \quad (10)$$

The upper left block,  $\mathbf{f} + \tilde{\Sigma}^{\infty}$ , is defined over the spin-orbital space and the off-diagonal matrices  $\tilde{\mathbf{U}}/\bar{\mathbf{U}}$ ,  $\tilde{\mathbf{V}}/\bar{\mathbf{V}}$  couple the single-particle states to many-particle excited state configurations. The  $\bar{\mathbf{K}}^{\lessgtr} + \bar{\mathbf{C}}^{\lessgtr}$  matrices contain the interactions between the different excited state configurations. The eigenvalues of the coupled-cluster Dyson supermatrix are the exact ionization and electron affinities of the system.

We arrive at CC- $G_0W_0$  theory by employing the ground-state ring CCD (rCCD) approximation [38] whilst truncating the interaction matrices to consist of 2p1h/2h1p excitations:

$$\tilde{\mathbf{D}}^{\text{CC-}G_0W_0} = \begin{pmatrix} f_{pq} + \tilde{\Sigma}_{pq}^{\infty\text{rCCD}} & \chi_{pi,ab}^{\text{rCCD}} & \chi_{pa,ij}^{\text{rCCD}} \\ \chi_{ab,qi}^{\text{rCCD}} & \bar{\Lambda}_{iab,jcd}^{G_0W_0>} & 0 \\ \chi_{ij,qa}^{\text{rCCD}} & 0 & \bar{\Lambda}_{ija,klb}^{G_0W_0<} \end{pmatrix}. \quad (11)$$

Here  $\tilde{\Sigma}_{pq}^{\infty\text{rCCD}}$  is the static component of the coupled-cluster self-energy evaluated in the rCCD approximation and  $\chi_{pq,rs}^{\text{rCCD}}$  is the rCCD two-body interaction that arises when normal-ordering the similarity transformed Hamiltonian with respect to the reference determinant. The interaction matrices are given by  $\bar{\Lambda}_{iab,jcd}^{G_0W_0>} = (\epsilon_a \delta_{bd} \delta_{ij} + H_{ib,jd}^{\text{RPA}}) \delta_{ac}$  and  $\bar{\Lambda}_{ija,klb}^{G_0W_0<} =$

$(\epsilon_i \delta_{jl} \delta_{ab} - H_{ja,lb}^{\text{RPA}}) \delta_{ik}$ , respectively, where  $H^{\text{RPA}}$  is the RPA Hamiltonian. All matrix elements are defined in Section XII.

In Section XIV, we define the coupled-cluster Bethe-Salpeter kernel as the functional derivative of the coupled-cluster self-energy with respect to the single-particle coupled-cluster Green's function. The electronic BSE kernel is given by  $\Xi = i \frac{\delta \Sigma}{\delta G}$ , with the coupled-cluster equivalent  $\tilde{\Xi} = i \frac{\delta \tilde{\Sigma}}{\delta \tilde{G}}$ . The electronic BSE kernel is given by the diagram series (up to second-order in the bare interaction)

$$\Xi_{pq,rs}[G] = \begin{array}{c} \begin{array}{c} p \\ \bullet \end{array} \text{---} \begin{array}{c} q \\ \bullet \end{array} \begin{array}{c} s \\ \bullet \end{array} \\ + \\ \begin{array}{c} p \\ \bullet \end{array} \begin{array}{c} s \\ \bullet \end{array} \\ \begin{array}{c} \uparrow \\ \downarrow \end{array} \\ \begin{array}{c} r \\ \bullet \end{array} \begin{array}{c} q \\ \bullet \end{array} \\ + \\ \begin{array}{c} p \\ \bullet \end{array} \begin{array}{c} q \\ \bullet \end{array} \\ \begin{array}{c} \uparrow \\ \downarrow \end{array} \\ \begin{array}{c} r \\ \bullet \end{array} \begin{array}{c} s \\ \bullet \end{array} \\ + \\ \begin{array}{c} p \\ \bullet \end{array} \begin{array}{c} s \\ \bullet \end{array} \\ \begin{array}{c} \uparrow \\ \downarrow \end{array} \\ \begin{array}{c} q \\ \bullet \end{array} \begin{array}{c} r \\ \bullet \end{array} \\ \text{---} \end{array} + \dots \quad (12)$$

The analogous coupled-cluster BSE kernel (up to second-order) is given by the series

$$\tilde{\Xi}_{pq,rs}[\tilde{G}] = \begin{array}{c} \begin{array}{c} p \\ \bullet \end{array} \text{---} \begin{array}{c} q \\ \bullet \end{array} \begin{array}{c} s \\ \bullet \end{array} \\ + \\ \begin{array}{c} p \\ \bullet \end{array} \begin{array}{c} s \\ \bullet \end{array} \\ \begin{array}{c} \uparrow \\ \downarrow \end{array} \\ \begin{array}{c} r \\ \bullet \end{array} \begin{array}{c} q \\ \bullet \end{array} \\ + \\ \begin{array}{c} p \\ \bullet \end{array} \begin{array}{c} q \\ \bullet \end{array} \\ \begin{array}{c} \uparrow \\ \downarrow \end{array} \\ \begin{array}{c} r \\ \bullet \end{array} \begin{array}{c} s \\ \bullet \end{array} \\ + \\ \begin{array}{c} p \\ \bullet \end{array} \begin{array}{c} s \\ \bullet \end{array} \\ \begin{array}{c} \uparrow \\ \downarrow \end{array} \\ \begin{array}{c} q \\ \bullet \end{array} \begin{array}{c} r \\ \bullet \end{array} \\ \text{---} \\ + \\ \begin{array}{c} p \\ \bullet \end{array} \begin{array}{c} s \\ \bullet \end{array} \\ \begin{array}{c} \uparrow \\ \downarrow \end{array} \\ \begin{array}{c} q \\ \bullet \end{array} \begin{array}{c} r \\ \bullet \end{array} \\ \text{---} \\ + \\ \begin{array}{c} p \\ \bullet \end{array} \begin{array}{c} q \\ \bullet \end{array} \\ \begin{array}{c} \uparrow \\ \downarrow \end{array} \\ \begin{array}{c} r \\ \bullet \end{array} \begin{array}{c} s \\ \bullet \end{array} \\ \text{---} \\ + \\ \begin{array}{c} p \\ \bullet \end{array} \begin{array}{c} q \\ \bullet \end{array} \\ \begin{array}{c} \uparrow \\ \downarrow \end{array} \\ \begin{array}{c} r \\ \bullet \end{array} \begin{array}{c} s \\ \bullet \end{array} \\ \text{---} \\ \text{---} \end{array} + \dots \quad (13)$$

Within coupled-cluster theory, derivation of the BSE kernel is significantly more complicated than for the electronic case as the interaction lines are also functionals of  $\tilde{G}$ . Therefore, one must also take functional derivatives of all interaction and Green's function lines of the self-energy to obtain the correct expression for the BSE kernel. The last four diagrams of the

CC-BSE kernel above result from the functional derivative of the two-body interaction with respect to the Green's function to yield the three-body interaction. The series of CC-BSE diagrams generated is clearly related to EE-EOM-CC theory once further approximations are made to define an effective BSE kernel in terms of a single frequency.

### III. REVIEW OF CONVENTIONAL GREEN'S FUNCTION THEORY

In this section, we present an overview of the conventional formulation of many-body quantum field theory where the Hamiltonian is hermitian. This is necessary in order to provide a complete description of the forthcoming non-hermitian theory.

#### A. The pictures of Quantum Mechanics

Let us assume that we have a hermitian Hamiltonian  $H$ , that contains no explicit time-dependence. The Schrödinger equation is therefore

$$i \frac{\partial}{\partial t} |\Psi_S(t)\rangle = H |\Psi_S(t)\rangle . \quad (14)$$

Given an initial state  $|\Psi_S(0)\rangle$ , we write the formal solution in terms of the time-evolution operator as

$$|\Psi_S(t)\rangle = \exp(-iHt) |\Psi_S(0)\rangle . \quad (15)$$

In the Schrödinger representation of quantum mechanics, all operators are time-independent and the time-dependence enters via the state vector,  $|\Psi_S(t)\rangle$ . Alternatively, we can use the Heisenberg picture where we instead define time-dependent operators and stationary state vectors. This formulation corresponds more intuitively to the classical picture where observables such as position and momentum vary with time. The state-vector in the Heisenberg representation is time-independent and given by  $|\Psi_H\rangle = |\Psi_S(0)\rangle$ . Heisenberg operators are related to Schrödinger operators via [1, 2]

$$O_H(t) = \exp(iHt) O_S \exp(-iHt) . \quad (16)$$

Finally, we have the Interaction picture where we assume that the Hamiltonian may be written as a sum of two terms  $H = H_0 + H_1$ , where  $H_0$  is the reference Hamiltonian. The

interaction state vector is written as

$$|\Psi_I(t)\rangle = \exp(iH_0t) |\Psi_S(t)\rangle . \quad (17)$$

This time-dependent unitary transformation results in the Interaction state vector obeying the Schrödinger equation

$$i \frac{\partial}{\partial t} |\Psi_I(t)\rangle = H_1(t) |\Psi_I(t)\rangle \quad (18)$$

where  $H_1(t) = \exp(iH_0t)O_S \exp(-iH_0t)$ . The formal solution of the Interaction state vector Schrödinger equation is given by [1]

$$\begin{aligned} |\Psi_I(t)\rangle &= U(t, t_0) |\Psi_I(t_0)\rangle \\ &= \mathcal{T} \left\{ \exp \left( -i \int_{t_0}^t dt' H_1(t') \right) \right\} |\Psi_I(t_0)\rangle \end{aligned} \quad (19)$$

where  $\mathcal{T}$  represents the time-ordering operator. Clearly we have  $|\Psi_H\rangle = |\Psi_I(0)\rangle$ , with the relationship between Heisenberg and Interaction picture operators as

$$O_H(t) = U(0, t)O_I(t)U(t, 0) \quad (20)$$

where we have used the unitarity of the time-evolution operator. All three pictures coincide at  $t = 0$ .

## B. The ground state in quantum field theory: Gell-Mann and Low theorem

To derive the Gell-Mann and Low theorem requires the introduction of the explicitly time-dependent adiabatic ‘switching-on’ Hamiltonian as

$$H(t) = H_0 + e^{-\eta|t|}H_1, \quad (21)$$

where  $\eta$  is a positive infinitesimal. At large times, this Hamiltonian reduces to the reference and at  $t = 0$  it corresponds to the full Hamiltonian of our system. All previous results on the relationships between state vectors in the pictures of quantum mechanics hold and we immediately write

$$|\Psi_H\rangle = U_\eta(0, t_0) |\Psi_I(t_0)\rangle , \quad (22)$$

where  $U_\eta$  is given by replacing  $H_1(t')$  in Eq. 19 with  $e^{-\eta|t'|}H_1(t')$ . Letting the time  $t_0$  approach  $-\infty$ , whilst taking the physical limit as  $\eta \rightarrow 0$  of Eq. 22, requires the introduction

of the Gell-Mann and Low theorem on the ground state of quantum field theory [1, 39]. The theorem states that if the quantity

$$\frac{|\Psi_0\rangle}{\langle\Phi_0|\Psi_0\rangle} = \lim_{\eta\rightarrow 0} \frac{U_\eta(0, \pm\infty)|\Phi_0\rangle}{\langle\Phi_0|U_\eta(0, \pm\infty)|\Phi_0\rangle} \quad (23)$$

converges, then it is an eigenstate of the full Hamiltonian such that

$$H \frac{|\Psi_0\rangle}{\langle\Phi_0|\Psi_0\rangle} = E \frac{|\Psi_0\rangle}{\langle\Phi_0|\Psi_0\rangle}. \quad (24)$$

In this way an eigenstate of the full Hamiltonian is generated adiabatically from  $|\Phi_0\rangle$  as the interaction is switched on. If  $|\Phi_0\rangle$  is the ground state of the reference Hamiltonian, then the eigenstate generated from this procedure is usually the true ground state. However, this is not always the case. Importantly, the limits of the numerator and denominator as  $\eta \rightarrow 0$  in Eq. 23 do not exist separately [39]. The theorem only asserts that if the limit of their ratio exists, then the eigenstate is well defined and is an eigenstate of the full Hamiltonian. In quantum field theory, where the particle number is no longer a ‘good quantum number’, the Gell-Mann and Low theorem provides the central key to find the ground state and construct propagators perturbatively.

### C. The single-particle Green’s function and irreducible self-energy

At equilibrium and at zero temperature, the single-particle Green’s function is defined as

$$iG_{pq}(t_1 - t_2) = \frac{\langle\Psi_0|\mathcal{T}\{a_p(t_1)a_q^\dagger(t_2)\}|\Psi_0\rangle}{\langle\Psi_0|\Psi_0\rangle}, \quad (25)$$

where  $a_p^\dagger(t)/a_p(t)$  create/annihilate electrons in spin-orbital  $|\phi_p\rangle$  in the Heisenberg representation,  $\mathcal{T}$  is the time-ordering operator and  $|\Psi_0\rangle$  is the exact ground state. In general, regardless of whether the Hamiltonian is a two-body operator or higher, the single-particle Green’s function contains information on the following observables:

1. The exact single-particle excitation spectrum.
2. The ground state expectation value of any *single-particle* operator.
3. The exact ground-state energy (in the case of a two-body interaction).

The single-particle Green's function is related to the one-body reduced density matrix by

$$\gamma_{pq} = -iG_{qp}(t_1 - t_1^+) = \langle \Psi_0 | a_p^\dagger a_q | \Psi_0 \rangle , \quad (26)$$

where the notation  $t_1^+ = \lim_{\eta \rightarrow 0^+} t_1 + \eta$  indicates evaluation of time argument from above.

Using the Gell-Mann and Low theorem (Eq. 23), we construct the perturbative expansion for the Green's function as

$$\begin{aligned} iG_{pq}(t_1 - t_2) &= \lim_{\eta \rightarrow 0} \frac{\langle \Phi_0 | \mathcal{T} \{ S_\eta a_p(t_1) a_q^\dagger(t_2) \} | \Phi_0 \rangle}{\langle \Phi_0 | S_\eta | \Phi_0 \rangle} \\ &= \lim_{\eta \rightarrow 0} \langle \Phi_0 | \mathcal{T} \{ S_\eta a_p(t_1) a_q^\dagger(t_2) \} | \Phi_0 \rangle_{\mathcal{C}} \end{aligned} \quad (27)$$

where  $S_\eta = \mathcal{T} \left\{ \exp \left( -i \int_{-\infty}^{\infty} dt e^{-\eta|t|} H_1(t) \right) \right\}$  and the subscript  $\mathcal{C}$  corresponds to retaining only the connected diagrams in the expansion using Goldstone's theorem [1].

The number of diagrams (terms) generated by Eq. 27 at each order is reduced by collecting all *one-particle irreducible* (1PI) diagrams in the expansion. 1PI diagrams are diagrams that cannot be divided into different sub-diagrams by cutting a single propagator line and their complete set defines the irreducible self-energy kernel,  $\Sigma_{pq}(\omega)$ . All reducible diagrams are then generated by the geometric Dyson series

$$G_{pq}(\omega) = G_{pq}^0(\omega) + \sum_{rs} G_{pr}^0(\omega) \Sigma_{rs}(\omega) G_{sq}(\omega) . \quad (28)$$

Here,  $G_{pq}^0(\omega)$  is the 'non-interacting' propagator that results from independent-particle propagation corresponding to time evolution under the action of the one-body reference operator  $H_0$ . The Dyson equation allows us to move away from direct Green's function perturbation theory and instead focus on the reduced set of diagrams that constitute the self-energy. In general, the self-energy is composed of a static component and a dynamical contribution

$$\Sigma_{pq}(\omega) = \Sigma_{pq}^\infty + \Sigma_{pq}^F(\omega) + \Sigma_{pq}^B(\omega) \quad (29)$$

where  $\Sigma_{pq}^\infty$  is the static component and  $\Sigma_{pq}^F(\omega)/\Sigma_{pq}^B(\omega)$  are the forward/backward time dynamical contributions.

The set of diagrams that constitute the irreducible self-energy may be expressed with respect to the reference Green's function  $G_0$ , or the exact Green's function,  $G$ . If the self-energy is expanded in terms of the exact Green's function, this restricts the self-energy diagrams to be only those which are 1PI, skeleton and interaction-irreducible. Skeleton

diagrams are self-energy diagrams that cannot be separated into two pieces by cutting a single fermion line twice at two different points [3]. Interaction-irreducible diagrams are self-energy diagrams that are constructed from the effective interactions that arise when normal-ordering the Hamiltonian with respect to the exact ground state [12, 13]. Expressing the self-energy with respect to the exact Green's function  $\Sigma[G]$ , is referred to as self-consistent renormalization and considerably reduces the number of diagrams constituting the self-energy expansion. It is also crucial to construct the functional  $\Sigma[G]$  to correctly derive the BSE kernel. For example, the effective interactions corresponding to the two-body Hamiltonian

$$H = \sum_{pq} h_{pq} a_p^\dagger a_q + \frac{1}{(2!)^2} \sum_{pq,rs} v_{pq,rs} a_p^\dagger a_q^\dagger a_s a_r \quad (30)$$

are given by normal-ordering  $H$  with respect to the exact ground state  $|\Psi_0\rangle$ . This gives

$$H = E_0^N + \sum_{pq} F_{pq} \{a_p^\dagger a_q\} + \frac{1}{(2!)^2} \sum_{pq,rs} V_{pq,rs} \{a_p^\dagger a_q^\dagger a_s a_r\} \quad (31)$$

where the effective interactions that are used to construct interaction-irreducible diagrams are defined by

$$\begin{aligned} F_{pq} &= h_{pq} + \sum_{rs} v_{pr,qs} \gamma_{rs} \\ &= f_{pq} + \sum_{rs} v_{pr,qs} (\gamma_{rs} - \gamma_{rs}^{\text{ref}}) \\ &= f_{pq} + \Sigma_{pq}^\infty, \end{aligned} \quad (32a)$$

where  $f_{pq} = h_{pq} + \sum_{rs} v_{pr,qs} \gamma_{rs}^{\text{ref}}$  is the Fock operator,  $\gamma_{rs} = \langle \Psi_0^N | a_r^\dagger a_s | \Psi_0^N \rangle$  is the exact one-particle reduced density matrix and  $\gamma_{rs}^{\text{ref}} = \langle \Phi_0 | a_r^\dagger a_s | \Phi_0 \rangle$  is the reference one-particle reduced density matrix. The two-body effective interaction is

$$V_{pq,rs} = v_{pq,rs} \cdot \quad (32b)$$

Here  $v_{pq,rs}$  is the antisymetrized two-body interaction and  $E_0^N = \langle \Psi_0^N | H | \Psi_0^N \rangle$  is the exact ground state energy. The notation  $\{\dots\}$  indicates a string of operators that is normal-ordered with respect to the exact ground state.

By the relationship between the one-particle reduced density matrix and the Green's function (Eq. 26), we see that the contribution  $\Sigma_{pq}^\infty$  to the one-body effective interaction is

the exact static component of the self-energy

$$\Sigma_{pq}^{\infty} = \sum_{rs} v_{pr,qs} \left( \gamma_{rs} - \gamma_{rs}^{\text{ref}} \right) \quad (33)$$

and depends self-consistently on the exact Green's function [3, 4].

In the case of a two-body interaction Hamiltonian, the effective two-body interaction is the same as the 'bare' two-body interaction. This is because there are no higher-body terms present that may dress this interaction. Therefore, the irreducible self-energy may be expressed in terms of the 1PI, skeleton and interaction-irreducible diagrams constructed from the bare two-body interaction using exact propagators. The two-body effective interaction is unchanged from the bare one. Therefore, we are usually not concerned with the effective interactions that arise when normal-ordering  $H$ , as the self-consistent expansion for the self-energy is unchanged when using the 'bare' two-body interaction.

However, generating the effective interactions for a three-body Hamiltonian is more involved. Consider the three-body Hamiltonian

$$H = \sum_{pq} h_{pq} a_p^{\dagger} a_q + \frac{1}{(2!)^2} \sum_{pq,rs} v_{pq,rs} a_p^{\dagger} a_q^{\dagger} a_s a_r + \frac{1}{(3!)^2} \sum_{pqr,stu} w_{pqr,stu} a_p^{\dagger} a_q^{\dagger} a_r^{\dagger} a_u a_t a_s . \quad (34)$$

Normal-ordering this Hamiltonian with respect to the exact ground state gives

$$H = E_0^N + \sum_{pq} F_{pq} \{a_p^{\dagger} a_q\} + \frac{1}{(2!)^2} \sum_{pq,rs} V_{pq,rs} \{a_p^{\dagger} a_q^{\dagger} a_s a_r\} + \frac{1}{(3!)^2} \sum_{pqr,stu} W_{pqr,stu} \{a_p^{\dagger} a_q^{\dagger} a_r^{\dagger} a_u a_t a_s\} \quad (35)$$

where the effective interactions are now

$$\begin{aligned} F_{pq} &= h_{pq} + \sum_{rs} v_{pr,qs} \gamma_{rs} + \frac{1}{(2!)^2} \sum_{rs,tu} W_{prs,qtu} \Gamma_{rs,tu} \\ &= f_{pq} + \sum_{rs} v_{pr,qs} \left( \gamma_{rs} - \gamma_{rs}^{\text{ref}} \right) + \frac{1}{(2!)^2} \sum_{rs,tu} W_{prs,qtu} \Gamma_{rs,tu} \\ &= f_{pq} + \Sigma_{pq}^{\infty} \end{aligned} \quad (36a)$$

with

$$V_{pq,rs} = v_{pq,rs} + \sum_{tu} W_{pqt,rsu} \gamma_{tu} \quad (36b)$$

and

$$W_{pqr,stu} = w_{pqr,stu} , \quad (36c)$$

where  $W_{pqr,stu}$  is the anti-symmetrized three-body interaction and  $\Gamma_{pq,rs} = \langle \Psi_0^N | a_p^\dagger a_q^\dagger a_s a_r | \Psi_0^N \rangle$  is the exact two-body reduced density matrix. Here, we clearly see that generating the self-consistent renormalized 1PI, skeleton and interaction-irreducible diagrams for  $\Sigma[G]$  corresponding to a three-body Hamiltonian is more involved [12]. The exact static contribution to the self-energy:

$$\Sigma_{pq}^\infty = \sum_{rs} v_{pr,qs} \left( \gamma_{rs} - \gamma_{rs}^{\text{ref}} \right) + \frac{1}{(2!)^2} \sum_{rs,tu} W_{prs,qtu} \Gamma_{rs,tu} , \quad (37)$$

now involves the two-particle reduced density matrix contracted with the three-body interaction. The effective two-body interaction is significantly modified. It includes the contraction of the bare three-body interaction with the exact one-particle reduced density matrix. The effective two-body interaction is now a functional of the single-particle Green's function,  $V[G]$ . Therefore the self-energy functional  $\Sigma[G]$ , is constructed only from skeleton diagrams using the effective interactions,  $V$  and  $W$ , with exact propagators [12, 13]. In the case of a three-body interaction, this greatly reduces the number of terms in the diagrammatic expansion and this procedure is absolutely necessary when expressing the self-energy as a functional of the exact Green's function. When there are three-body interactions present, the ground state energy is no longer directly obtainable from knowledge of the single-particle Green's function and self-energy [12].

This concludes our summary of the standard results that are pertinent to the similarity transformed formulation.

#### IV. BIORTHOGONAL QUANTUM THEORY

In this section, we will review aspects of biorthogonal quantum theory, as well as the biorthogonal Schrödinger and Heisenberg pictures. We present the biorthogonal interaction picture and the extension of the Gell-Mann and Low theorem to biorthogonal quantum theory.

Suppose we have a diagonalizable non-hermitian Hamiltonian  $\bar{H}$  with eigenstates  $\{|\Psi_n\rangle\}$  and eigenvalues  $\{E_n\}$  such that

$$\bar{H} |\Psi_n\rangle = E_n |\Psi_n\rangle \quad \Rightarrow \quad \langle \Psi_n | \bar{H}^\dagger = \langle \Psi_n | E_n^* . \quad (38)$$

The eigenstates of the hermitian adjoint  $\bar{H}^\dagger$  are

$$\bar{H}^\dagger |\Phi_n\rangle = \mathcal{E}_n |\Phi_n\rangle \Rightarrow \langle \Phi_n | \bar{H} = \langle \Phi_n | \mathcal{E}_n^* . \quad (39)$$

The set  $\{|\Psi_n\rangle\}$  is complete in the Hilbert space, with  $\langle \Phi_n | \Psi_m \rangle = \delta_{nm}$ ,  $E_n = \mathcal{E}_n^* \forall n$ . Completeness of  $\{|\Psi_n\rangle\}$  implies the completeness of  $\{|\Phi_n\rangle\}$  [40, 41]. The eigenstates of  $\bar{H}$  are generally not orthogonal [40]. The basis set  $\{|\Phi_m\rangle\}_{m=1}^N$  is referred to as the biorthonormal basis associated with  $\{|\Psi_n\rangle\}_{n=1}^N$  [40–42]. A general state

$$|\Psi\rangle = \sum_{n=1}^N C_n |\Psi_n\rangle , \quad (40)$$

has an *associated state* and a dual state

$$|\tilde{\Psi}\rangle := \sum_{n=1}^N C_n |\Phi_n\rangle \Rightarrow \langle \tilde{\Psi} | = \sum_{n=1}^N C_n^* \langle \Phi_n | . \quad (41)$$

The state dual to  $|\Psi\rangle$  is given by  $\langle \tilde{\Psi} |$  and the associated state is given by its hermitian conjugate:  $|\tilde{\Psi}\rangle$ . The biorthogonal inner product is defined as

$$\langle \Psi, \Psi \rangle_{bo} = \langle \tilde{\Psi} | \Psi \rangle = \sum_{nm} C_m^* C_n \langle \Phi_m | \Psi_n \rangle = \sum_n |C_n|^2 . \quad (42)$$

where  $\langle \cdot, \cdot \rangle_{bo}$  denotes the biorthogonal inner product. Under the biorthogonal inner product, the set of states,  $\{|\Psi_n\rangle | \Phi_n\rangle\}_{n=1}^N$  forms a complete biorthogonal system. A generic operator,  $A$ , can be represented in the biorthogonal basis as

$$A = \sum_{nm} a_{nm} |\Psi_n\rangle \langle \Phi_m | , \quad (43)$$

with  $a_{nm} = \langle \Phi_n | A | \Psi_m \rangle$ . The expectation value of an observable in a pure state  $|\Psi\rangle$  is defined as

$$\langle A \rangle = \frac{\langle \tilde{\Psi} | A | \Psi \rangle}{\langle \tilde{\Psi} | \Psi \rangle} , \quad (44)$$

and if the operator is biorthogonally hermitian with  $a_{nm} = a_{mn}^*$ , the expectation value of the observable will be real. Non-hermitian quantum mechanics can also be formulated in terms of conventional quantum theory where the Hilbert space is endowed with a nontrivial metric. This is known as pseudo-hermitian quantum theory (see Appendix B) [40, 43, 44].

Within non-hermitian quantum theory, time evolution of states and operators must be formulated carefully. This is due to the fact that the left and right states are related to each other by a non-trivial metric and therefore evolve under different Hamiltonians.

### A. Biorthogonal Schrödinger and Heisenberg pictures

The time-dependent Schrödinger equation is written as

$$i \frac{\partial}{\partial t} |\Psi_S(t)\rangle = \bar{H} |\Psi_S(t)\rangle \quad (45)$$

where  $\bar{H}$  is a time-independent, pseudo-hermitian Hamiltonian that necessarily possesses a real spectrum [44]. The formal solution is given by

$$|\Psi_S(t)\rangle = U(t, 0) |\Psi_S(0)\rangle , \quad (46)$$

where  $U(t, 0) = \exp(-i\bar{H}t)$ . The time-evolution operator  $U$  is not unitary, but we retain the nomenclature of the hermitian formulation. The associated states necessarily obey the conjugate equation

$$i \frac{\partial}{\partial t} |\tilde{\Psi}_S(t)\rangle = \bar{H}^\dagger |\tilde{\Psi}_S(t)\rangle \quad (47)$$

yielding the formal solution

$$|\tilde{\Psi}_S(t)\rangle = \tilde{U}^\dagger(t, 0) |\tilde{\Psi}_S(0)\rangle , \quad (48)$$

where  $|\tilde{\Psi}_S(0)\rangle$  is the associated state of  $|\Psi_S(0)\rangle$  and  $\tilde{U}^\dagger(t, 0) = \exp(-i\bar{H}^\dagger t)$ . This ensures that the norm of the state is preserved under time-evolution as  $\langle \tilde{\Psi}_S(t) | \Psi_S(t) \rangle = \langle \tilde{\Psi}_S(0) | \Psi_S(0) \rangle$ . Clearly, we see that *associated states* evolve according to a different Hamiltonian ( $\bar{H}^\dagger$ ) [45].

The Heisenberg states are given by extension of the usual relationship:  $|\Psi_H\rangle = |\Psi_S(0)\rangle$  and  $|\tilde{\Psi}_H\rangle = |\tilde{\Psi}_S(0)\rangle$ . An arbitrary matrix element in the biorthogonal theory within the Schrödinger representation is given by

$$\langle \tilde{\Psi}'_S(t) | O_S | \Psi_S(t) \rangle = \langle \tilde{\Psi}'_H | \tilde{U}(t, 0) O_S U(t, 0) | \Psi_H \rangle . \quad (49)$$

Therefore, a general operator in the Heisenberg representation is given by

$$O_H(t) = \exp(i\bar{H}t) O_S \exp(-i\bar{H}t) . \quad (50)$$

It should be noted that the same form is obtained in the pseudo-hermitian theory with respect to the  $\tau$ -inner product [46]. Now that we have defined the biorthogonal Schrödinger and Heisenberg pictures, we introduce the biorthogonal Interaction picture.

## B. Biorthogonal Interaction picture

Assume that a time-independent diagonalizable non-hermitian Hamiltonian  $\bar{H}$  may be expressed as the sum of two non-hermitian terms  $\bar{H}_0$  and  $\bar{H}_1$  such that

$$\bar{H} = \bar{H}_0 + \bar{H}_1 . \quad (51)$$

Let us define the interaction state vector in the Hilbert space as

$$|\Psi_I(t)\rangle = \exp(i\bar{H}_0 t) |\Psi_S(t)\rangle \quad (52)$$

and it's associated state as

$$|\tilde{\Psi}_I(t)\rangle = \exp(i\bar{H}_0^\dagger t) |\tilde{\Psi}_S(t)\rangle . \quad (53)$$

This transformation leads to the following Schrödinger equations for the interaction state vector

$$i \frac{\partial}{\partial t} |\Psi_I(t)\rangle = \bar{H}_1(t) |\Psi_I(t)\rangle \quad (54a)$$

and its associated state

$$i \frac{\partial}{\partial t} |\tilde{\Psi}_I(t)\rangle = \bar{H}_1^\dagger(t) |\tilde{\Psi}_I(t)\rangle \quad (54b)$$

where  $\bar{H}_1(t) = \exp(i\bar{H}_0 t) \bar{H}_1 \exp(-i\bar{H}_0 t)$  and  $\bar{H}_1^\dagger(t)$  is the hermitian adjoint. An arbitrary matrix element in the Schrödinger picture is

$$\langle \tilde{\Psi}'_S(t) | O_S | \Psi_S(t) \rangle = \langle \tilde{\Psi}'_I(t) | \exp(i\bar{H}_0 t) O_S \exp(-i\bar{H}_0 t) | \Psi_I(t) \rangle \quad (55)$$

which requires a general operator to be defined in the biorthogonal interaction picture as

$$O_I(t) = \exp(i\bar{H}_0 t) O_S \exp(-i\bar{H}_0 t) . \quad (56)$$

In order to find an expression for the time-evolution operator in the biorthogonal interaction picture, from Eqs 54a and 54b, we immediately find that

$$\begin{aligned} |\Psi_I(t)\rangle &= \mathcal{T} \left\{ \exp \left( -i \int_{t_0}^t dt' \bar{H}_1(t') \right) \right\} |\Psi_I(t_0)\rangle \\ &= U(t, t_0) |\Psi_I(t_0)\rangle \end{aligned} \quad (57)$$

and

$$\begin{aligned} |\tilde{\Psi}_I(t)\rangle &= \mathcal{T} \left\{ \exp \left( -i \int_{t_0}^t dt' \bar{H}_1^\dagger(t') \right) \right\} |\tilde{\Psi}_I(t_0)\rangle \\ &= \tilde{U}^\dagger(t, t_0) |\tilde{\Psi}_I(t_0)\rangle . \end{aligned} \quad (58)$$

These relations ensure that the biorthogonal norm of the interaction state-vector is time-independent. As a result, the general relationship between the biorthogonal interaction and Heisenberg pictures is given by

$$\begin{aligned} |\Psi_H\rangle &= U(0, t_0) |\Psi_I(t_0)\rangle \\ |\tilde{\Psi}_H\rangle &= \tilde{U}^\dagger(0, t_0) |\tilde{\Psi}_I(t_0)\rangle \\ O_H(t) &= U(0, t) O_I(t) U(t, 0) . \end{aligned} \quad (59)$$

### C. Extension of the Gell-Mann and Low theorem

Exact eigenstates of the full non-hermitian Hamiltonian can be generated adiabatically by introducing the time-dependent Hamiltonian

$$\bar{H} = \bar{H}_0 + e^{-\eta|t|} \bar{H}_1 , \quad (60)$$

where  $\eta$  is a positive infinitesimal. Here we have made the implicit assumption that  $\bar{H}$  can be partitioned as the sum of two diagonalizable non-hermitian Hamiltonians  $\bar{H}_0$  and  $\bar{H}_1$ . At very large times, the Hamiltonian reduces to  $\bar{H}_0$  and at  $t = 0$ , the Hamiltonian is the full non-hermitian Hamiltonian. The general solution for the interaction and associated states is given by

$$\begin{aligned} |\Psi_I(t)\rangle &= U_\eta(t, t_0) |\Psi_I(t_0)\rangle \\ |\tilde{\Psi}_I(t)\rangle &= \tilde{U}_\eta^\dagger(t, t_0) |\tilde{\Psi}_I(t_0)\rangle \end{aligned} \quad (61)$$

where the time-evolution operator now takes the form

$$U_\eta(t, t_0) = \mathcal{T} \left\{ \exp \left( -i \int_{t_0}^t dt' e^{-\eta|t'|} \bar{H}_1(t') \right) \right\} , \quad (62)$$

with the analogous form for  $\tilde{U}_\eta^\dagger(t, t_0)$ . As  $t_0 \rightarrow -\infty$ , the interaction state vector reduces to a stationary eigenstate of the reference Hamiltonian  $\bar{H}_0$ , written as

$$\bar{H}_0 |\Phi_0\rangle = E^{(0)} |\Phi_0\rangle \quad ; \quad \bar{H}_0^\dagger |\tilde{\Phi}_0\rangle = E^{(0)} |\tilde{\Phi}_0\rangle \quad (63)$$

where  $E^{(0)}$  is real. Therefore, we have a time-independent state vector as  $t_0 \rightarrow -\infty$ . We immediately write

$$|\Psi_H(\eta)\rangle = U_\eta(0, -\infty) |\Phi_0\rangle , \quad (64a)$$

with the associated state

$$|\tilde{\Psi}_H(\eta)\rangle = \tilde{U}_\eta^\dagger(0, -\infty) |\tilde{\Phi}_0\rangle . \quad (64b)$$

Next we require the physical limit as  $\eta \rightarrow 0$ . To do this, we extend the Gell-Mann and Low theorem (see Appendix A) such that if the limits of the quantities

$$\frac{|\Psi_0\rangle}{\langle \tilde{\Phi}_0 | \Psi_0 \rangle} \equiv \lim_{\eta \rightarrow 0^+} \frac{U_\eta(0, -\infty) |\Phi_0\rangle}{\langle \tilde{\Phi}_0 | U_\eta(0, -\infty) |\Phi_0\rangle} \quad (65a)$$

and

$$\frac{|\tilde{\Psi}_0\rangle}{\langle \Phi_0 | \tilde{\Psi}_0 \rangle} \equiv \lim_{\eta \rightarrow 0^+} \frac{\tilde{U}_\eta^\dagger(0, -\infty) |\tilde{\Phi}_0\rangle}{\langle \Phi_0 | \tilde{U}_\eta^\dagger(0, -\infty) |\tilde{\Phi}_0\rangle} \quad (65b)$$

exist, then they are the ‘right’ and ‘left’ eigenstates of the full Hamiltonian  $\bar{H}$ , such that

$$\bar{H} \frac{|\Psi_0\rangle}{\langle \tilde{\Phi}_0 | \Psi_0 \rangle} = E \frac{|\Psi_0\rangle}{\langle \tilde{\Phi}_0 | \Psi_0 \rangle} ; \quad \bar{H}^\dagger \frac{|\tilde{\Psi}_0\rangle}{\langle \Phi_0 | \tilde{\Psi}_0 \rangle} = E \frac{|\tilde{\Psi}_0\rangle}{\langle \Phi_0 | \tilde{\Psi}_0 \rangle} . \quad (66)$$

As a result, the ground state energy shift is given by

$$\Delta E = \frac{\langle \tilde{\Phi}_0 | \bar{H}_1 | \Psi_0 \rangle}{\langle \tilde{\Phi}_0 | \Psi_0 \rangle} = \frac{\langle \Phi_0 | \bar{H}_1^\dagger | \tilde{\Psi}_0 \rangle}{\langle \Phi_0 | \tilde{\Psi}_0 \rangle} , \quad (67)$$

where  $\Delta E = E - E^{(0)}$ . Importantly, the limit as  $\eta \rightarrow 0$  of both the numerators and denominators of Eqs 65a and 65b do not separately exist. The proof is analogous to the original proof presented for the Hermitian case and applies equally to the state obtained from evolving from  $t = +\infty$  [1, 39]. Using our definition, the associated state is written as

$$\begin{aligned} \frac{\langle \tilde{\Psi}_0 |}{\langle \tilde{\Psi}_0 | \Phi_0 \rangle^*} &= \lim_{\eta \rightarrow 0^+} \frac{\langle \tilde{\Phi}_0 | \tilde{U}_\eta(0, -\infty)}{\langle \tilde{\Phi}_0 | \tilde{U}_\eta(0, -\infty) | \Phi_0 \rangle^*} \\ &= \lim_{\eta \rightarrow 0^+} \frac{\langle \tilde{\Phi}_0 | U_\eta(-\infty, 0)}{\langle \tilde{\Phi}_0 | U_\eta(-\infty, 0) | \Phi_0 \rangle^*} . \end{aligned} \quad (68)$$

Therefore, the state obtained from the adiabatic procedure is an eigenstate of the full non-hermitian Hamiltonian, which may be obtained from either evolving ‘forward’ or ‘backward’ in time.

By making use of the extended Gell-Mann and Low theorem, we can construct perturbative expressions for time-dependent correlation functions in the usual way by evolving on the right from  $-\infty$  and on the left from  $+\infty$  as follows

$$\begin{aligned}
\mathcal{R}(t_1, t_2, \dots, t_n) &= \frac{\langle \tilde{\Psi}_0 | \mathcal{T} \{ O_H(t_1) O_H(t_2) \cdots O_H(t_n) \} | \Psi_0 \rangle}{\langle \tilde{\Psi}_0 | \Psi_0 \rangle} \\
&= \lim_{\eta \rightarrow 0^+} \frac{\langle \tilde{\Phi}_0 | \mathcal{T} \left\{ \exp \left( -i \int_{-\infty}^{\infty} dt e^{-\eta|t|} \bar{H}_1(t) \right) O_I(t_1) O_I(t_2) \cdots O_I(t_n) \right\} | \Phi_0 \rangle}{\langle \tilde{\Phi}_0 | \mathcal{T} \left\{ \exp \left( -i \int_{-\infty}^{\infty} dt e^{-\eta|t|} \bar{H}_1(t) \right) \right\} | \Phi_0 \rangle}.
\end{aligned} \tag{69}$$

Making use of the linked diagram theorem [1, 14], we rewrite this equation as

$$\mathcal{R}(t_1, t_2, \dots, t_n) = \lim_{\eta \rightarrow 0^+} \langle \tilde{\Phi}_0 | \mathcal{T} \left\{ \exp \left( -i \int_{-\infty}^{\infty} dt e^{-\eta|t|} \bar{H}_1(t) \right) O_I(t_1) O_I(t_2) \cdots O_I(t_n) \right\} | \Phi_0 \rangle_{\mathcal{C}} \tag{70}$$

where the subscript  $\mathcal{C}$  indicates that only connected diagrams contribute to the expansion. If we choose the partitioning such that the reference Hamiltonian is hermitian, *i.e.*  $H_0 = H_0^\dagger$ , the results above hold and we have

$$\mathcal{R}(t_1, t_2, \dots, t_n) = \lim_{\eta \rightarrow 0^+} \langle \Phi_0 | \mathcal{T} \left\{ \exp \left( -i \int_{-\infty}^{\infty} dt e^{-\eta|t|} \bar{H}_1(t) \right) O_I(t_1) O_I(t_2) \cdots O_I(t_n) \right\} | \Phi_0 \rangle_{\mathcal{C}} \tag{71}$$

where now the left and right states of the hermitian reference are simply related to each other via hermitian conjugation.

## V. N-BODY NON-HERMITIAN INTERACTIONS AND EFFECTIVE INTERACTIONS

In this section, we define the single-particle Green's function for the case of an  $N$ -body non-hermitian interaction Hamiltonian and discuss the construction of the non-hermitian irreducible self-energy that emerges. Suppose we have an  $N$ -body non-hermitian Hamiltonian

$$\begin{aligned}
\bar{H} &= \sum_{pq} \bar{h}_{pq} a_p^\dagger a_q + \frac{1}{(2!)^2} \sum_{pq,rs} \bar{v}_{pq,rs} a_p^\dagger a_q^\dagger a_s a_r + \frac{1}{(3!)^2} \sum_{pqr,stu} \bar{w}_{pqr,stu} a_p^\dagger a_q^\dagger a_r^\dagger a_u a_t a_s \\
&+ \frac{1}{(4!)^2} \sum_{pqrs, tuvz} \bar{u}_{pqrs, tuvz} a_p^\dagger a_q^\dagger a_r^\dagger a_s^\dagger a_z a_v a_u a_t + \frac{1}{(5!)^2} \sum_{pqrsn, tuvzm} \bar{k}_{pqrsn, tuvzm} a_p^\dagger a_q^\dagger a_r^\dagger a_s^\dagger a_n^\dagger a_m a_z a_v a_u a_t + \cdots
\end{aligned} \tag{72}$$

with right and left eigenstates given by  $\bar{H} |\Psi_0^N\rangle = E_0^N |\Psi_0^N\rangle$  and  $\bar{H}^\dagger |\tilde{\Psi}_0^N\rangle = E_0^N |\tilde{\Psi}_0^N\rangle$ . The single-particle Green's function is defined as the biorthogonal expectation value

$$i\tilde{G}_{pq}(t_1, t_2) = \langle \tilde{\Psi}_0^N | \mathcal{T} \{ a_p(t_1) a_q^\dagger(t_2) \} | \Psi_0^N \rangle \quad (73)$$

where the time-dependence of the field-operators is given by  $a_p(t_1) = e^{i\bar{H}t_1} a_p e^{-i\bar{H}t_1}$  defined in the biorthogonal Heisenberg picture. The notation  $\tilde{G}$  is used to indicate that the Green's function is defined with respect to the biorthogonal inner product. Using the extended Gell-Mann and Low theorem, we write the perturbative expansion for the Green's function as

$$i\tilde{G}_{pq}(t_1, t_2) = \langle \tilde{\Phi}_0 | \mathcal{T} \left\{ \exp \left( -i \int_{-\infty}^{\infty} dt \bar{H}_1(t) \right) a_p(t_1) a_q^\dagger(t_2) \right\} | \Phi_0 \rangle_c, \quad (74)$$

with the time-dependence of the field operators is now defined in the biorthogonal interaction picture  $a_p(t_1) = e^{i\bar{H}_0 t_1} a_p e^{-i\bar{H}_0 t_1}$ , where  $\bar{H}_0 = \sum_{pq} \bar{h}_{pq} a_p^\dagger a_q$  and  $\bar{H}_1 = \bar{H} - \bar{H}_0$ . Here,  $|\Phi_0\rangle$  and  $|\tilde{\Phi}_0\rangle$  are the right and left ground eigenstates of  $\bar{H}_0$ , respectively. Eq. 74 immediately implies the geometric Dyson series

$$\tilde{G}_{pq}(\omega) = \tilde{G}_{pq}^0(\omega) + \sum_{rs} \tilde{G}_{pr}^0(\omega) \tilde{\Sigma}_{rs}(\omega) \tilde{G}_{sq}(\omega). \quad (75)$$

The non-hermitian self-energy is also composed of static and dynamical contributions as

$$\tilde{\Sigma}_{pq}(\omega) = \tilde{\Sigma}_{pq}^\infty + \tilde{\Sigma}_{pq}^F(\omega) + \tilde{\Sigma}_{pq}^B(\omega), \quad (76)$$

and is a functional of the exact single-particle Green's function,  $\tilde{\Sigma}[\tilde{G}]$ . The 1PI, skeleton and interaction-irreducible diagrams that make up the self-energy are obtained from the effective interactions. In this case, the one-body term is given by

$$\begin{aligned} \bar{F}_{pq} &= \bar{h}_{pq} + \sum_{rs} \bar{v}_{pr,qs} \tilde{\gamma}_{rs} + \frac{1}{(2!)^2} \sum_{rs,tu} \bar{w}_{prs,qtu} \tilde{\Gamma}_{rs,tu} + \frac{1}{(3!)^2} \sum_{rst,uvw} \bar{u}_{prst,quvw} \tilde{\Gamma}_{rst,uvw} + \dots \\ &= \bar{f}_{pq} + \sum_{rs} \bar{v}_{pr,qs} \left( \tilde{\gamma}_{rs} - \tilde{\gamma}_{rs}^{\text{ref}} \right) + \frac{1}{(2!)^2} \sum_{rs,tu} \bar{w}_{prs,qtu} \tilde{\Gamma}_{rs,tu} + \frac{1}{(3!)^2} \sum_{rst,uvw} \bar{u}_{prst,quvw} \tilde{\Gamma}_{rst,uvw} + \dots \\ &= \bar{f}_{pq} + \tilde{\Sigma}_{pq}^\infty, \end{aligned} \quad (77a)$$

where  $\bar{f}_{pq}$  is the non-hermitian Fock operator, the exact one-particle reduced density matrix is defined as  $\tilde{\gamma}_{pq} = \langle \tilde{\Psi}_0^N | a_p^\dagger a_q | \Psi_0^N \rangle$  and the biorthogonal reference one-particle reduced density

matrix is  $\tilde{\gamma}_{pq}^{\text{ref}} = \langle \tilde{\Phi}_0 | a_p^\dagger a_q | \Phi_0 \rangle$ . The two-body effective interaction is obtained as

$$\bar{V}_{pq,rs} = \bar{v}_{pq,rs} + \sum_{tu} \bar{w}_{pqt,rsu} \tilde{\gamma}_{tu} + \frac{1}{(2!)^2} \sum_{tu,vz} \bar{u}_{pqtu,rsvz} \tilde{\Gamma}_{tu,vz} + \dots \quad (77b)$$

with the three-body effective interaction

$$\bar{W}_{pqr,stu} = \bar{w}_{pqr,stu} + \sum_{vx} \bar{u}_{pqr,svx} \tilde{\gamma}_{vx} + \frac{1}{(2!)^2} \sum_{vw,lo} \bar{k}_{pqr,svw,stu,lo} \tilde{\Gamma}_{vw,lo} + \dots \quad (77c)$$

The four-body effective interaction is

$$\bar{U}_{pqrs,tuvo} = \bar{u}_{pqrs,tuvo} + \sum_{yx} \bar{k}_{pqrs,xy,tuvo} \tilde{\gamma}_{yx} + \dots \quad (77d)$$

This procedure is continued up to the  $N$ -body interaction. The two-particle biorthogonal reduced density matrix is defined as  $\tilde{\Gamma}_{pq,rs} = \langle \tilde{\Psi}_0^N | a_p^\dagger a_q^\dagger a_s a_r | \Psi_0^N \rangle$  and so on for the higher-body equivalents. These interactions arise when normal-ordering  $\bar{H}$  with respect to the biorthogonal ground state expectation value,  $E_0^N = \langle \tilde{\Psi}_0^N | \bar{H} | \Psi_0^N \rangle$ .

In analogy with the conventional hermitian case, we immediately find the exact static component of the self-energy  $\tilde{\Sigma}^\infty[\tilde{G}]$  as the remainder of the one-body effective interaction,  $\bar{F} - \bar{f}$ :

$$\tilde{\Sigma}_{pq}^\infty = \sum_{rs} \bar{v}_{pr,qs} \left( \tilde{\gamma}_{rs} - \tilde{\gamma}_{rs}^{\text{ref}} \right) + \frac{1}{(2!)^2} \sum_{rs,tu} \bar{w}_{prs,qtu} \tilde{\Gamma}_{rs,tu} + \frac{1}{(3!)^2} \sum_{rst,uvw} \bar{u}_{prst,quvw} \tilde{\Gamma}_{rst,uvw} + \dots \quad (78)$$

To construct the self-energy functional self-consistently, it must be composed of the effective interactions  $\bar{V}$ ,  $\bar{W}$ ,  $\bar{U}$  and so on, which are required in order to generate interaction-irreducible self-energy diagrams. Therefore, it is these effective interactions that appear as vertices in the self-consistent expression of the self-energy functional,  $\tilde{\Sigma}[\tilde{G}]$ . Importantly, all effective interactions up to the  $N$ -body term are explicitly functionals of the single-particle Green's function. The perturbative expansion for the self-energy  $\tilde{\Sigma}[\tilde{G}_0]$  is obtained by expanding both the propagators and effective interactions with respect to the reference Green's function,  $\tilde{G}_0$ . For the remainder of this work we will focus on generating the interaction-irreducible self-energy diagrams arising resulting from the coupled-cluster similarity transformed Hamiltonian. However, the analysis presented in this work is general and can be applied to any  $N$ -body hermitian or non-hermitian interaction Hamiltonian.

## VI. OVERVIEW OF COUPLED-CLUSTER THEORY

Within coupled-cluster theory, the following ansatz is made for the exact ground state wavefunction of a system of  $N$  interacting particles

$$|\Psi_0^N\rangle = e^T |\Phi_0\rangle \quad (79)$$

where  $|\Phi_0\rangle$  is the reference determinant. The wave operator  $T$ , creates all excitations with respect to the reference determinant and is defined as

$$T = \sum_{ia} t_i^a a_a^\dagger a_i + \frac{1}{(2!)^2} \sum_{ijab} t_{ij}^{ab} a_a^\dagger a_b^\dagger a_j a_i + \frac{1}{(3!)^2} \sum_{ijkabc} t_{ijk}^{abc} a_a^\dagger a_b^\dagger a_c^\dagger a_k a_j a_i + \dots \quad (80)$$

where  $\{t_i^a, t_{ij}^{ab}, t_{ijk}^{abc}, \dots\}$  are the cluster amplitudes. Using the CC ansatz, we write the non-hermitian CC eigenvalue problem for the right and left eigenstates of the similarity transformed Hamiltonian as

$$\bar{H} |\Phi_0\rangle = E_0^{\text{CC}} |\Phi_0\rangle \quad ; \quad \langle \tilde{\Psi}_0 | \bar{H} = \langle \tilde{\Psi}_0 | E_0^{\text{CC}} \quad , \quad (81)$$

where

$$\bar{H} = e^{-T} H e^T \quad (82)$$

is the similarity transformed Hamiltonian and  $H$  is the bare Hamiltonian. Here, we see that the reference  $|\Phi_0\rangle$  is the right eigenstate of the similarity transformed Hamiltonian. The left eigenstate is given by  $\langle \tilde{\Psi}_0 | = \langle \Phi_0 | (\mathbb{1} + \Lambda)$ .  $\Lambda$  is the de-excitation operator defined as

$$\Lambda = \sum_{ai} \lambda_a^i a_i^\dagger a_a + \frac{1}{(2!)^2} \sum_{abij} \lambda_{ab}^{ij} a_i^\dagger a_j^\dagger a_b a_a + \frac{1}{(3!)^2} \sum_{abcijk} \lambda_{abc}^{ijk} a_i^\dagger a_j^\dagger a_k^\dagger a_c a_b a_a + \dots \quad (83)$$

where  $\{\lambda_a^i, \lambda_{ab}^{ij}, \lambda_{abc}^{ijk}, \dots\}$  are the de-excitation amplitudes. The excitation, de-excitation amplitudes and ground state energy are obtained from minimization of the coupled-cluster Lagrangian [15]

$$\mathcal{L}_0^{\text{CC}}(\mathbf{t}, \lambda) = \langle \tilde{\Psi}_0 | \bar{H} | \Phi_0 \rangle = \langle \Phi_0 | \bar{H} | \Phi_0 \rangle + \sum_{\mu} \lambda_{\mu} \langle \Phi_{\mu} | \bar{H} | \Phi_0 \rangle \quad , \quad (84)$$

where  $|\Phi_{\mu}\rangle$  represents the manifold of excited Slater determinants given by  $|\Phi_i^a\rangle = a_a^\dagger a_i |\Phi_0\rangle$  etc. Minimization of the Lagrangian gives rise to the excitation and de-excitation amplitude equations

$$\frac{\partial \mathcal{L}_0^{\text{CC}}}{\partial \lambda_{\mu}} = \langle \Phi_{\mu} | \bar{H} | \Phi_0 \rangle = 0 \quad (85a)$$

$$\frac{\partial \mathcal{L}_0^{\text{CC}}}{\partial t_\mu} = \langle \Phi_0 | \bar{H} \tau_\mu | \Phi_0 \rangle + \sum_\nu \lambda_\nu \langle \Phi_\nu | [\bar{H}, \tau_\mu] | \Phi_0 \rangle = 0 \quad (85\text{b})$$

where  $\tau_\mu$  is the excitation operator associated with the cluster amplitude  $t_\mu$ . Once the excitation amplitudes are determined, the ground state energy is simply given by

$$E_0^{\text{CC}} = \langle \tilde{\Psi}_0 | \bar{H} | \Phi_0 \rangle = \langle \Phi_0 | \bar{H} | \Phi_0 \rangle . \quad (86)$$

When  $T$  is not truncated, the ground state energy obtained from this procedure is formally exact. Importantly, the reference state  $|\Phi_0\rangle$  can be constructed such that the singles amplitudes,  $t_i^a$ , are zero by construction. This approach is referred to as Brueckner coupled-cluster theory (BCC) and implies that the reference state has maximum overlap with the exact ground state. Brueckner coupled-cluster theory uses spin-orbitals that are determined by unitary rotation using the singles amplitude equations [47–49]. In terms of the cluster amplitudes and general spin-orbitals, the coupled-cluster ground state energy corresponding to the electronic structure Hamiltonian is given by

$$E_0^{\text{CC}} = E_0^{\text{ref}} + \frac{1}{4} \sum_{ijab} \langle ij || ab \rangle (t_{ij}^{ab} + 2t_i^a t_j^b) + \sum_{ia} f_{ia} t_i^a, \quad (87)$$

where  $E_0^{\text{ref}}$  is the energy of the reference.

The similarity transformed Hamiltonian  $\bar{H}$  possesses the same spectrum as the electronic structure Hamiltonian,  $H$ . In EOM-CC theory, the charged excitation energies are obtained by diagonalization of the similarity transformed Hamiltonian in the basis of all Slater determinants containing  $(N \pm 1)$ -electrons. Focusing on the removal energies, the IP-EOM-CC eigenvalue problem can be written as

$$[\bar{H}, R_\nu^{\text{IP}}] |\Phi_0\rangle = -\varepsilon_\nu^{N-1} R_\nu^{\text{IP}} |\Phi_0\rangle, \quad (88)$$

where  $R_\nu^{\text{IP}} |\Phi_0\rangle$  is the right  $(N - 1)$ -particle eigenstate of  $\bar{H}$ ,  $|\Psi_\nu^{N-1}\rangle$ . In IP-EOM-CC theory, the operator creates all determinants consisting of  $(N - 1)$  electrons:

$$R_\nu^{\text{IP}} = \sum_i r_i(\nu) a_i + \sum_{i < j, a} r_{ij}^a(\nu) a_a^\dagger a_j a_i + \dots \quad (89)$$

The IP-EOM-CC eigenvalue problem is written in matrix form in terms of the non-Hermitian supermatrix:

$$\bar{\mathbf{H}}^{\text{IP-EOM-CC}} = - \begin{pmatrix} \langle \Phi_i | \bar{H}_N | \Phi_j \rangle & \langle \Phi_i | \bar{H}_N | \Phi_{kl}^a \rangle & \dots \\ \langle \Phi_{mn}^b | \bar{H}_N | \Phi_j \rangle & \langle \Phi_{mn}^b | \bar{H}_N | \Phi_{kl}^a \rangle & \dots \\ \vdots & \vdots & \ddots \end{pmatrix}, \quad (90)$$

where  $\bar{H}_N = \bar{H} - E_0^{\text{CC}}$ . An analogous supermatrix for the EA-EOM-CC eigenvalue problem can also be constructed.

### A. The similarity transformed Hamiltonian

The full similarity transformed Hamiltonian is an  $N$ -body operator written as

$$\begin{aligned} \bar{H} &= \bar{h} + \bar{V} + \bar{W} + \dots \\ &= \sum_{pq} \bar{h}_{pq} a_p^\dagger a_q + \frac{1}{(2!)^2} \sum_{pq,rs} \bar{h}_{pq,rs} a_p^\dagger a_q^\dagger a_s a_r + \frac{1}{(3!)^2} \sum_{pqr,stu} \bar{h}_{pqr,stu} a_p^\dagger a_q^\dagger a_r^\dagger a_u a_t a_s + \dots, \end{aligned} \quad (91)$$

where  $\{\bar{h}_{pq}, \bar{h}_{pq,rs}, \bar{h}_{pqr,stu}, \dots\}$  are the one-body, antisymmetrized two-body, three-body and so on matrix elements. Using the notation of Ref. [24], normal-ordering this Hamiltonian with respect to the reference determinant gives [14]

$$\begin{aligned} \bar{H} &= E_0^{\text{CC}} + \sum_{pq} F_{pq} \{a_p^\dagger a_q\}_0 + \frac{1}{(2!)^2} \sum_{pq,rs} \chi_{pq,rs} \{a_p^\dagger a_q^\dagger a_s a_r\}_0 \\ &+ \frac{1}{(3!)^2} \sum_{pqr,stu} \chi_{pqr,stu} \{a_p^\dagger a_q^\dagger a_r^\dagger a_u a_t a_s\}_0 + \dots \end{aligned} \quad (92)$$

where the notation  $\{\dots\}_0$  indicates normal-ordering with respect to the reference,  $|\Phi_0\rangle$ . The set of effective interaction matrix elements  $\{F_{pq}, \chi_{pq,rs}, \chi_{pqr,stu}, \dots\}$ , up to the four-body effective interaction, can be found in Refs 14 and 50. We can also normal-order the Hamiltonian with respect to the biorthogonal expectation value  $\langle \Phi_0 | \Phi_0 \rangle_{bo} := \langle \tilde{\Psi}_0 | \Phi_0 \rangle$ , as defined in Section IV, yielding

$$\begin{aligned} \bar{H} &= E_0^{\text{CC}} + \sum_{pq} \tilde{F}_{pq} \{a_p^\dagger a_q\} + \frac{1}{(2!)^2} \sum_{pq,rs} \tilde{\Xi}_{pq,rs} \{a_p^\dagger a_q^\dagger a_s a_r\} \\ &+ \frac{1}{(3!)^2} \sum_{pqr,stu} \tilde{\chi}_{pqr,stu} \{a_p^\dagger a_q^\dagger a_r^\dagger a_u a_t a_s\} + \dots \end{aligned} \quad (93)$$

The relationship between all matrix elements  $\{\bar{h}_{pq}, \bar{h}_{pq,rs}, \bar{h}_{pqr,stu}, \dots\}, \{F_{pq}, \chi_{pq,rs}, \chi_{pqr,stu}, \dots\}$  and  $\{\tilde{F}_{pq}, \tilde{\Xi}_{pq,rs}, \tilde{\chi}_{pqr,stu}, \dots\}$  is derived in Appendix C and described in Ref. [24]. The coupled-cluster amplitude equations are given by the effective interaction elements  $\{F_{ai}, \chi_{ab,ij}, \chi_{abc,ijk}, \dots\}$  which all evaluate to zero at convergence [14]. Since these effective interaction elements vanish, the interaction elements  $\{\tilde{F}_{ai}, \tilde{\Xi}_{ab,ij}, \tilde{\chi}_{abc,ijk}, \dots\}$  also evaluate to zero. All effective interaction matrix elements with four or more lines below the vertex,

apart from the two-body terms  $\chi_{ij,ab}$  and  $\tilde{\Xi}_{ij,ab}$ , vanish as a result of the coupled-cluster similarity transformation. Finally, it is useful to split the similarity transformed Hamiltonian into two terms

$$\begin{aligned}\bar{H} &= F + \bar{H}_1 \\ &= \sum_{pq} f_{pq} a_p^\dagger a_q + \sum_{pq} (\bar{h}_{pq} - f_{pq}) a_p^\dagger a_q + \frac{1}{(2!)^2} \sum_{pq,rs} \bar{h}_{pq,rs} a_p^\dagger a_q^\dagger a_s a_r \\ &\quad + \frac{1}{(3!)^2} \sum_{pqr,stu} \bar{h}_{pqr,stu} a_p^\dagger a_q^\dagger a_r^\dagger a_u a_t a_s + \dots\end{aligned}\tag{94}$$

where  $F$  is the Fock operator and  $\bar{H}_1 = \bar{H} - F$ , is the  $N$ -body operator containing all the interactions and effects introduced by the similarity transformed Hamiltonian. The analysis of the effective interactions generated by the CC similarity transformed Hamiltonian will be crucial when constructing the perturbative and renormalized expansions of the coupled-cluster self-energy in Sections IX and X.

## VII. THE COUPLED-CLUSTER REPRESENTATION OF THE ELECTRONIC GREEN'S FUNCTION

The single-particle electronic Green's function of the hermitian, two-body electronic structure Hamiltonian  $H$ , is defined as

$$iG_{pq}(t_1 - t_2) = \langle \Psi_0^N | \mathcal{T} \{ a_p(t_1) a_q^\dagger(t_2) \} | \Psi_0^N \rangle\tag{95}$$

where  $|\Psi_0^N\rangle$  is the exact  $N$ -electron ground state wavefunction and the time-dependence of the field operators is governed by the electronic structure Hamiltonian:  $a_p(t) = e^{iHt} a_p e^{-iHt}$ .

Attempts at combining coupled-cluster theory with the Green's function formalism have largely focused on *direct computation* of Eq. 95 for the electronic Green's function using coupled-cluster theory [16–19]. The coupled-cluster representation of the time-domain electronic Green's function is obtained from the biorthogonal theory developed in Section IV and is written as

$$i\bar{G}_{pq}(t_1 - t_2) = \langle \tilde{\Psi}_0 | \mathcal{T} \{ \bar{a}_p(t_1) \bar{a}_q^\dagger(t_2) \} | \Phi_0 \rangle ,\tag{96}$$

where  $\bar{a}_p(t_1) = \exp(i\bar{H}t) \bar{a}_p \exp(-i\bar{H}t)$ ,  $\bar{a}_q^\dagger(t_1) = \exp(i\bar{H}t) \bar{a}_q^\dagger \exp(-i\bar{H}t)$  with  $\bar{a}_p = e^{-T} a_p e^T$  and  $\bar{a}_p^\dagger = e^{-T} a_p^\dagger e^T$ , respectively. The notation  $\bar{G}$  is chosen to distinguish the coupled-

cluster representation of the electronic Green's function from the electronic Green's function, denoted by  $G$ . Performing the similarity transformation on the operators leads to

$$\begin{aligned}\bar{a}_p(t_1) &= a_p(t_1) + e^{i\bar{H}t_1}[a_p, T]e^{-i\bar{H}t_1} \\ &= a_p(t_1) + [a_p, T](t_1) ,\end{aligned}\tag{97}$$

where  $[a_p, T](t_1) = e^{i\bar{H}t_1}[a_p, T]e^{-i\bar{H}t_1}$ . Inserting this relation into the time-ordered expectation value gives

$$\begin{aligned}i\bar{G}_{pq}(t_1 - t_2) &= \langle \tilde{\Psi}_0 | \mathcal{T} \{ a_p(t_1) a_q^\dagger(t_2) \} | \Phi_0 \rangle + \langle \tilde{\Psi}_0 | \mathcal{T} \{ [a_p, T](t_1) a_q^\dagger(t_2) \} | \Phi_0 \rangle \\ &\quad + \langle \tilde{\Psi}_0 | \mathcal{T} \{ a_p(t_1) [a_q^\dagger, T](t_2) \} | \Phi_0 \rangle + \langle \tilde{\Psi}_0 | \mathcal{T} \{ [a_p, T](t_1) [a_q^\dagger, T](t_2) \} | \Phi_0 \rangle .\end{aligned}\tag{98}$$

Due to the commutator of the creation/annihilation operators with  $T$ , it is clear that the coupled-cluster representation of the electronic single-particle Green's function is in fact a collection of 'many-particle' Green's functions of specified time-orderings, including up to the  $N$ -body Green's function. However, the occupied-virtual part of the coupled-cluster representation of the electronic Green's function is in fact a single-particle propagator:

$$i\bar{G}_{ia}(t_1 - t_2) = \langle \tilde{\Psi}_0 | \mathcal{T} \{ \bar{a}_i(t_1) \bar{a}_a^\dagger(t_2) \} | \Phi_0 \rangle = \langle \tilde{\Psi}_0 | \mathcal{T} \{ a_i(t_1) a_a^\dagger(t_2) \} | \Phi_0 \rangle .\tag{99}$$

This is because  $[a_i, T] = [a_a^\dagger, T] = 0$ . Although the full coupled-cluster representation of the electronic Green's function is a complicated combination of many-body Green's functions, the many-particle coupled-cluster Green's functions are explicitly coupled to each other through their equations of motion (see Section X) and it is exactly this hierarchy of coupled many-body Green's functions that we want to decouple by introduction of the coupled-cluster self-energy.

The spectral form of the coupled-cluster representation of the electronic Green's function we first presented by Nooijen and Snijders [16, 17] and can be obtained from our analysis by taking the Fourier transform of Eq. 96 to give:

$$\bar{G}_{pq}(\omega) = \sum_{\mu} \frac{\langle \tilde{\Psi}_0 | \bar{a}_p | \Psi_{\mu}^{N+1} \rangle \langle \tilde{\Psi}_{\mu}^{N+1} | \bar{a}_q^\dagger | \Phi_0 \rangle}{\omega - \varepsilon_{\mu}^{N+1} + i\eta} + \sum_{\nu} \frac{\langle \tilde{\Psi}_0 | \bar{a}_q^\dagger | \Psi_{\nu}^{N-1} \rangle \langle \tilde{\Psi}_{\nu}^{N-1} | \bar{a}_p | \Phi_0 \rangle}{\omega - \varepsilon_{\nu}^{N-1} - i\eta} ,\tag{100}$$

where  $\varepsilon_{\mu}^{N+1} = E_{\mu}^{N+1} - E_0^N$  and  $\varepsilon_{\nu}^{N-1} = E_0^N - E_{\nu}^{N-1}$  are the exact addition and removal energies of the system of interacting electrons, within a complete basis when  $T$  is not truncated. In principle, knowledge of the exact coupled-cluster representation of the electronic Green's

function gives the exact single-particle spectrum, coupled-cluster ground state energy as well as the non-hermitian one-particle reduced density matrix

$$\bar{\gamma}_{pq} = -i\bar{G}_{qp}(t - t^+) = \langle \tilde{\Psi}_0 | \bar{a}_p^\dagger \bar{a}_q | \Phi_0 \rangle . \quad (101)$$

However, it should be noted that calculation of the ground state energy at any level of approximation for the coupled-cluster representation of the electronic Green's function results in a different ground state energy from that obtained at the same level of approximation of the ground state coupled-cluster equations [16, 17, 28].

Formally the Dyson equation for the coupled-cluster representation of the electronic Green's function is written as

$$\bar{G}_{pq}(\omega) = G_{pq}^0(\omega) + \sum_{rs} G_{pr}^0(\omega) \bar{\Sigma}_{rs}(\omega) \bar{G}_{sq}(\omega) . \quad (102)$$

However, it is important to note that the 'self-energy',  $\bar{\Sigma}$ , is not the same object as the electronic self-energy,  $\Sigma$  [24]. This is because  $\bar{\Sigma}$  is an object that connects  $G_0$  to  $\bar{G}$  rather than  $G$  of the hermitian electronic structure Hamiltonian. As a result the coupled-cluster self-energy is non-hermitian. Due to the fact that the coupled-cluster representation of the electronic Green's function introduces a fundamental coupling to every  $N$ -particle Green's function, the 'self-energy'  $\bar{\Sigma}$  entering Eq. 102 cannot be defined in the diagrammatic way as the set of all 1PI diagrams. Therefore, the coupled-cluster representation of the electronic Green's function,  $\bar{G}$ , does not concern the diagrammatic coupled-cluster self-energy and therefore does not fully connect Green's function and coupled-cluster theories.

## VIII. THE SINGLE-PARTICLE COUPLED-CLUSTER GREEN'S FUNCTION AND THE COUPLED-CLUSTER SELF-ENERGY

In this work, we take the similarity transformed Hamiltonian as the fundamental interaction Hamiltonian and use the biorthogonal formulation for non-hermitian Hamiltonians to define the *single-particle* coupled-cluster Green's function (SP-CCGF) as

$$i\tilde{G}_{pq}(t_1 - t_2) = \langle \tilde{\Psi}_0 | \mathcal{T} \{ a_p(t_1) a_q^\dagger(t_2) \} | \Phi_0 \rangle , \quad (103)$$

where the time-dependence of the operators is governed by the similarity transformed Hamiltonian,  $\bar{H}$  via Eq. 50. We note that  $\bar{G}_{ia}(\omega) = \tilde{G}_{ia}(\omega)$ . This is a single-particle propagator

that remains coupled to all higher-order many-body Green's function through its equation-of-motion. It will subsequently be shown that this propagator also contains the exact charged excitation spectrum as well as the coupled-cluster ground-state correlation energy through its associated self-energy. As we will show, this change of perspective allows us to define the irreducible coupled-cluster self-energy directly using techniques from Green's function theory. In the following we refer to  $G$  as the electronic Green's function,  $\bar{G}$  as the coupled-cluster representation of the electronic Green's function and  $\tilde{G}$  as the single-particle coupled-cluster Green's function.

### A. Lehmann representation of the single-particle coupled-cluster Green's function

The explicit *single-particle* coupled-cluster Green's function is defined in Eq. 103. By expanding the time-ordered product, resolving the identity of  $(N \pm 1)$ -particle eigenstates of  $\bar{H}$  and taking the Fourier transform, we find the Lehmann representation of the SP-CCGF:

$$\tilde{G}_{pq}(\omega) = \sum_{\mu} \frac{\langle \tilde{\Psi}_0 | a_p | \Psi_{\mu}^{N+1} \rangle \langle \tilde{\Psi}_{\mu}^{N+1} | a_q^{\dagger} | \Phi_0 \rangle}{\omega - \varepsilon_{\mu}^{N+1} + i\eta} + \sum_{\nu} \frac{\langle \tilde{\Psi}_0 | a_q^{\dagger} | \Psi_{\nu}^{N-1} \rangle \langle \tilde{\Psi}_{\nu}^{N-1} | a_p | \Phi_0 \rangle}{\omega - \varepsilon_{\nu}^{N-1} - i\eta}. \quad (104)$$

We immediately see that the SP-CCGF contains the exact single-particle spectrum and we will subsequently show how the associated self-energy also contains the exact ground state energy. The only difference between the SP-CCGF and the coupled-cluster representation of the electronic Green's function (Eq. 100) arises in the form of the residues, which in the coupled-cluster representation are different due to the explicit contribution of the higher-order  $N$ -particle Green's functions. We introduce the residues of the coupled-cluster propagator defined in Eq. 104 as  $\bar{Y}_p^{\mu} = \langle \tilde{\Psi}_{\mu}^{N+1} | a_p^{\dagger} | \Phi_0 \rangle$ ,  $\tilde{Y}_p^{\mu} = \langle \tilde{\Psi}_0 | a_p | \Psi_{\mu}^{N+1} \rangle$ ,  $\bar{X}_p^{\nu} = \langle \tilde{\Psi}_{\nu}^{N-1} | a_p | \Phi_0 \rangle$  and  $\tilde{X}_p^{\nu} = \langle \tilde{\Psi}_0 | a_p^{\dagger} | \Psi_{\nu}^{N-1} \rangle$ , and re-write the single-particle coupled-cluster Green's function as

$$\tilde{G}_{pq}(\omega) = \sum_{\mu} \frac{\tilde{Y}_p^{\mu} \bar{Y}_q^{\mu}}{\omega - \varepsilon_{\mu}^{N+1} + i\eta} + \sum_{\nu} \frac{\tilde{X}_q^{\nu} \bar{X}_p^{\nu}}{\omega - \varepsilon_{\nu}^{N-1} - i\eta}. \quad (105)$$

The four blocks of the SP-CCGF are given by:

$$\tilde{G}_{ij}(\omega) = \sum_{\nu} \frac{\tilde{X}_j^{\nu} \bar{X}_i^{\nu}}{\omega - \varepsilon_{\nu}^{N-1} - i\eta} \quad (106a)$$

$$\tilde{G}_{ab}(\omega) = \sum_{\mu} \frac{\tilde{Y}_a^{\mu} \bar{Y}_b^{\mu}}{\omega - \varepsilon_{\mu}^{N+1} + i\eta} \quad (106b)$$

$$\tilde{G}_{ia}(\omega) = \sum_{\mu} \frac{\tilde{Y}_i^{\mu} \bar{Y}_a^{\mu}}{\omega - \varepsilon_{\mu}^{N+1} + i\eta} + \sum_{\nu} \frac{\tilde{X}_a^{\nu} \bar{X}_i^{\nu}}{\omega - \varepsilon_{\nu}^{N-1} - i\eta} \quad (106c)$$

$$\tilde{G}_{ai}(\omega) = 0. \quad (106d)$$

Note that  $\bar{Y}_i^{\mu} = \bar{X}_a^{\nu} = 0$ . Therefore, we see that the occupied block contains only backward time contributions, the virtual block contains only forward time contributions, the occupied–virtual block contains both forward and backward time contributions and that the virtual–occupied block vanishes.

## B. The single-particle coupled-cluster Green’s function and self-energy

The perturbative expression for the SP-CCGF is given by

$$i\tilde{G}_{pq}(t_1 - t_2) = \langle \Phi_0 | \mathcal{T} \left\{ \exp \left( -i \int_{-\infty}^{\infty} dt \bar{H}_1(t) \right) a_p(t_1) a_q^{\dagger}(t_2) \right\} | \Phi_0 \rangle_c, \quad (107)$$

where the operators are implicitly defined in the Heisenberg picture in the first equality and the interaction picture in the perturbative expansion:  $a_p(t_1) = e^{iFt} a_p e^{-iFt}$ . We have dropped the implicit limit of  $\eta \rightarrow 0$ . This procedure was outlined in Section IV and results in a diagrammatic perturbation theory for the Green’s function. Following the standard procedure, outlined in Section III, the set of diagrams generated by Eq. 107 is reduced by collecting all 1PI diagrams and performing a geometric series summation through the coupled-cluster Dyson equation

$$\tilde{G}_{pq}(\omega) = G_{pq}^0(\omega) + \sum_{rs} G_{pr}^0(\omega) \tilde{\Sigma}_{rs}(\omega) \tilde{G}_{sq}(\omega), \quad (108)$$

where  $G_{pq}^0(\omega)$  is the reference Green’s function of the Fock operator and  $\tilde{\Sigma}_{pq}(\omega)$  is the coupled-cluster self-energy. As  $\tilde{G}_{ia} = \bar{G}_{ia}$ , it should be noted that  $\tilde{\Sigma}_{ia} = \bar{\Sigma}_{ia}$ .

From the Lehmann representation of the coupled-cluster Green’s function (Eq. 104), we immediately identify the spectral form of the coupled-cluster self-energy as [24]

$$\begin{aligned} \tilde{\Sigma}_{pq}(\omega) &= \tilde{\Sigma}_{pq}^{\infty} + \tilde{\Sigma}_{pq}^{\text{F}}(\omega) + \tilde{\Sigma}_{pq}^{\text{B}}(\omega) \\ &= \tilde{\Sigma}_{pq}^{\infty} + \sum_{JJ'} \tilde{U}_{pJ} \left[ (\omega + i\eta) \mathbb{1} - (\bar{\mathbf{K}}^{\text{>}} + \bar{\mathbf{C}}^{\text{>}}) \right]_{JJ'}^{-1} \bar{U}_{J'q} \\ &\quad + \sum_{AA'} \bar{V}_{pA} \left[ (\omega - i\eta) \mathbb{1} - (\bar{\mathbf{K}}^{\text{<}} + \bar{\mathbf{C}}^{\text{<}}) \right]_{AA'}^{-1} \tilde{V}_{A'q} \end{aligned} \quad (109)$$

where the indices  $JJ'/AA'$  label forward-time/backward-time multi-particle-hole Intermediate State Configurations (ISCs). The matrices  $\bar{\mathbf{K}}_{JJ'}^> + \bar{\mathbf{C}}_{JJ'}^>$  and  $\bar{\mathbf{K}}_{AA'}^< + \bar{\mathbf{C}}_{AA'}^<$  represent the interactions between the different ISCs and the  $\bar{\mathbf{K}}$ -matrices are diagonal ( $\bar{\mathbf{K}}_{JJ'}^> = \bar{\mathbf{K}}_{JJ}^> \delta_{JJ'}$ ). The quantities  $\tilde{U}_{pJ}/\bar{U}_{Jp}$  and  $\bar{V}_{pJ}/\tilde{V}_A$  represent the coupling matrices that link initial and final single-particle states to the different ISCs. For the occupied-occupied block of the self-energy we have

$$\tilde{\Sigma}_{ij}(\omega) = \tilde{\Sigma}_{ij}^\infty + \sum_{AA'} \bar{V}_{iA} [(\omega - i\eta)\mathbb{1} - (\bar{\mathbf{K}}^> + \bar{\mathbf{C}}^>)]_{AA'}^{-1} \tilde{V}_{A'j}. \quad (110)$$

The occupied block of the coupled-cluster self-energy only contains poles above the real axis and is a consequence of backward time propagation alone. The self-energy of the virtual-virtual block is

$$\tilde{\Sigma}_{ab}(\omega) = \tilde{\Sigma}_{ab}^\infty + \sum_{JJ'} \tilde{U}_{aJ} [(\omega + i\eta)\mathbb{1} - (\bar{\mathbf{K}}^< + \bar{\mathbf{C}}^<)]_{JJ'}^{-1} \bar{U}_{J'b} \quad (111)$$

and contains poles only beneath the real axis resulting from forward time propagation only. The self-energy of the occupied-virtual block contains the combined forward and backward propagation and has poles both above and below the real axis as

$$\begin{aligned} \tilde{\Sigma}_{ia}(\omega) &= \tilde{\Sigma}_{ia}^\infty + \sum_{JJ'} \tilde{U}_{iJ} [(\omega + i\eta)\mathbb{1} - (\bar{\mathbf{K}}^< + \bar{\mathbf{C}}^<)]_{JJ'}^{-1} \bar{U}_{J'a} \\ &+ \sum_{AA'} \bar{V}_{iA} [(\omega - i\eta)\mathbb{1} - (\bar{\mathbf{K}}^> + \bar{\mathbf{C}}^>)]_{AA'}^{-1} \tilde{V}_{A'a}. \end{aligned} \quad (112)$$

As  $\tilde{G}_{ai}(\omega) = 0$ , the self-energy of the virtual-occupied block also vanishes:  $\tilde{\Sigma}_{ai}(\omega) = 0$ . An important limit is when the cluster operator vanishes, *i.e.*  $T = 0$  ( $\tilde{G} \rightarrow G$ ). In this case, the coupled-cluster Dyson equation (Eq. 108) reduces to the electronic Dyson equation, Eq. 28, where  $H_1$  is the bare two-body Coulomb interaction subtracted by the HF potential. The coupled-cluster self-energy reduces to the two-body electronic self-energy.

## IX. DIAGRAMMATIC PERTURBATION EXPANSION OF THE COUPLED-CLUSTER SELF-ENERGY

In this section, we derive the perturbative diagrammatic expansion of the coupled-cluster self-energy functional,  $\tilde{\Sigma}[G_0]$ , to third-order. The number of diagrams in the perturbative

expansion for the coupled-cluster self-energy may be reduced by restricting the diagrammatic expansion to contain only interaction-irreducible diagrams [12]. This results in a combined series that involves renormalization of the propagators and interaction vertices. Diagrams are referred to as interaction-reducible when they can be split into two diagrams by cutting an interaction vertex into two parts [12, 13]. As long as only interaction-irreducible diagrams are included, where all propagators are dressed, the diagrammatic expansion for the coupled-cluster self-energy is equivalent to replacing the perturbation  $\bar{H}_1$  in Eq. 107 with the effective interaction

$$\tilde{\bar{H}}_1 = \sum_{pq} (\tilde{F}_{pq} - f_{pq}) a_p^\dagger a_q + \frac{1}{(2!)^2} \sum_{pq,rs} \tilde{\Xi}_{pq,rs} a_p^\dagger a_q^\dagger a_s a_r + \frac{1}{(3!)^2} \sum_{pqr,stu} \tilde{\chi}_{pqr,stu} a_p^\dagger a_q^\dagger a_r^\dagger a_u a_t a_s + \dots \quad (113)$$

obtained from the normal-ordering of the similarity transformed Hamiltonian with respect to the biorthogonal ground state expectation value (Eq. 93). Obtaining the perturbative expression for the coupled-cluster self-energy in terms of effective interactions resulting from normal-ordering with respect to the reference  $|\Phi_0\rangle$ , requires the relationships between the effective interactions, which are defined in Appendices C and D. The effective interactions arising from normal-ordering with respect to the reference arise when expanding the self-energy with respect to the reference Green's function,  $G_0$ . Therefore, the self-energy expansion with respect to the non-interacting propagator is obtained by the expansion of interaction-irreducible interactions that enter 1PI, skeleton self-energy diagrams.

In the following, we employ the antisymmetrized Hugenholtz-Shavitt-Bartlett diagram convention [51]. Diagrammatically, the effective interactions that arise when normal-ordering the Hamiltonian with respect to the reference state are represented by

$$\begin{aligned} \begin{array}{c} p \\ r \end{array} \bullet \text{---} \text{---} \text{---} \text{---} \text{---} \text{---} \bullet \begin{array}{c} q \\ s \end{array} &= \chi_{pq,rs}, \\ \begin{array}{c} p \\ s \end{array} \bullet \text{---} \text{---} \text{---} \bullet \begin{array}{c} q \\ t \end{array} \text{---} \text{---} \text{---} \bullet \begin{array}{c} r \\ u \end{array} &= \chi_{pqr,stu}, \\ \begin{array}{c} p \\ s \end{array} \bullet \text{---} \text{---} \text{---} \bullet \begin{array}{c} q \\ t \end{array} \text{---} \text{---} \text{---} \bullet \begin{array}{c} r \\ u \end{array} \text{---} \text{---} \text{---} \bullet \begin{array}{c} w \\ v \end{array} &= \chi_{pqrw,stu}, \end{aligned} \quad (114)$$

and so on for the higher-body terms. The effective interactions that arise from normal-ordering the Hamiltonian with respect to the biorthogonal expectation value are obtained





However, since the matrix element  $\chi_{ab,jk} = \langle \Phi_{jk}^{ab} | \bar{H} | \Phi_0 \rangle = 0$  via the amplitude equations, the forward time contribution of the second-order self-energy vanishes. Therefore, we are left with

$$\tilde{\Sigma}_{ij}^{(2)}(\omega) = \frac{1}{2} \sum_{kla} \frac{\chi_{ia,kl} \chi_{kl,ja}}{\omega + \epsilon_a - \epsilon_k - \epsilon_l - i\eta}. \quad (122)$$

Likewise, the second-order contribution to the virtual-virtual block is

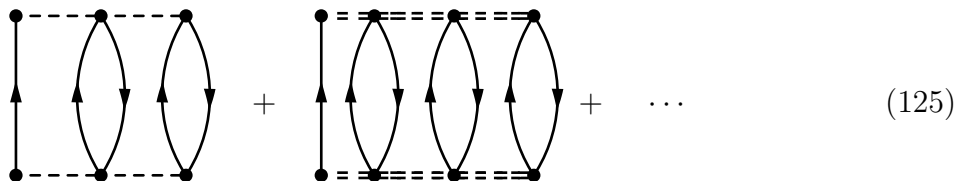
$$\tilde{\Sigma}_{ab}^{(2)}(\omega) = \frac{1}{2} \sum_{cdk} \frac{\chi_{ak,cd} \chi_{cd,bk}}{\omega + \epsilon_k - \epsilon_c - \epsilon_d + i\eta}. \quad (123)$$

In this case, the backward time-contribution vanishes due to the doubles amplitude equations  $\chi_{ac,ij} = 0$ . Turning to the second-order contribution corresponding to hole to particle propagation we have  $\tilde{\Sigma}_{ai}^{(2)} = 0$ . This is because both  $\chi_{bc,ij} = \chi_{ab,jk} = 0$ . However, both time-orderings remain in the particle to hole block

$$\tilde{\Sigma}_{ia}^{(2)}(\omega) = \frac{1}{2} \left( \sum_{bcj} \frac{\chi_{ij,bc} \chi_{bc,aj}}{\omega + \epsilon_j - \epsilon_b - \epsilon_c + i\eta} + \sum_{jkb} \frac{\chi_{ib,jk} \chi_{jk,ab}}{\omega + \epsilon_b - \epsilon_j - \epsilon_k - i\eta} \right). \quad (124)$$

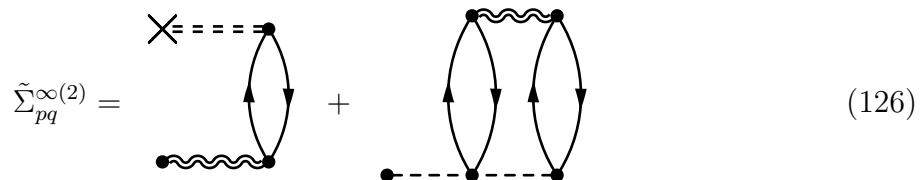
Therefore, at second-order, the perturbative expansion of the coupled-cluster self-energy is exactly that of the spectral form outlined in Subsection VIII B. Summarising, the forward time dynamical contribution to the coupled-cluster self-energy in the occupied-occupied space vanishes as a result of the similarity transformation. These contributions appear instead in the first-order static term,  $\tilde{\Sigma}_{ij}^{\infty(0)}$ . This is because the forward time contributions that would appear in the second-order electronic self-energy are instead contained in the doubles amplitudes  $t_{ij}^{ab}$  that enter the similarity transformation. Therefore, if we included these forward time contributions in the second-order dynamical self-energy, we would be double-counting these contributions. The same structure is observed for the backward time contribution of the coupled-cluster self-energy in the virtual-virtual space which are now contained in the static contribution,  $\tilde{\Sigma}_{ab}^{\infty(0)}$ . The occupied-virtual block of the coupled-cluster self-energy must vanish in order to consistently determine the doubles amplitudes that contain these contributions. When  $T = 0$ , the second-order expression for the coupled-cluster self-energy in Eq. 120 reduces the MP2 self-energy, *i.e.*  $\tilde{\Sigma}_{pq}^{T=0(2)}(\omega) = \Sigma_{pq}^{\text{MP2}}(\omega)$  as  $\chi_{pq,rs} \rightarrow \langle pq || rs \rangle$ .

Other second-order diagrams such as



and so on, containing elements up to  $N$ -body from the similarity transformed Hamiltonian, vanish as a result of having four or more lines below any interaction vertex. The coupled-cluster self-energy diagram of Eq. 119 represents an excitation processes whereby the intermediate scattered states consist of excited states containing two-particle-one-hole (2p1h) and two-hole-one-particle (2h1p) configurations. Likewise, the diagrams of Eq. 125 contains intermediate scattered states of 3p2h/3h2p and 4p3h/4h3p character, which vanish within coupled-cluster theory, but will contribute in the case of a generic  $N$ -body interaction Hamiltonian.

The final second-order interaction-reducible diagrams are those where the two-body effective interaction is contracted with the static self-energy and where the three-body effective interaction is contracted with the two-body interaction:



These are static terms that evaluate to give

$$\tilde{\Sigma}_{pq}^{\infty(2)} = \sum_{kc} \frac{\chi_{pc,qk} \tilde{\Sigma}_{kc}^{\infty(0)}}{(\epsilon_k - \epsilon_c + i\eta)} + \frac{1}{(2!)^2} \sum_{abij} \frac{\chi_{pab,qij} \chi_{ij,ab}}{(\epsilon_i + \epsilon_j - \epsilon_a - \epsilon_b + i\eta)}. \quad (127)$$

The contributions resulting from the contraction of the four-body with the three-body effective interaction and so on vanish as a result of containing four or more lines below the interaction vertex. In Brueckner theory, the first term vanishes because  $\tilde{\Sigma}_{kc}^{\infty(0)} = 0$  [24].

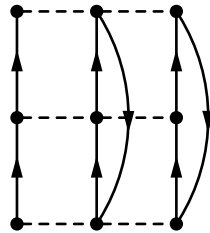
### C. Third-order diagrams

In order to reduce the number of diagrams depicted at third-order [12], we present only the 1PI, skeleton and interaction-irreducible coupled-cluster self-energy diagrams. This restriction requires the self-energy to be written in terms of fully dressed Green's functions

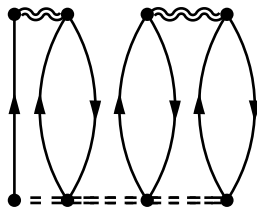
because the self-energy insertions are already included in the propagator renormalization. They are depicted below:

$$\begin{aligned}
 \tilde{\Sigma}^{(3)}[G_0] = & \text{[Diagram 1]} + \text{[Diagram 2]} + \text{[Diagram 3]} + \text{[Diagram 4]} \\
 & + \text{[Diagram 5]} + \text{[Diagram 6]} + \text{[Diagram 7]} + \text{[Diagram 8]} \\
 & + \text{[Diagram 9]} + \text{[Diagram 10]}
 \end{aligned}
 \tag{128}$$

Typical third-order diagrams of the form:



vanish due to the fact that matrix elements of the similarity transformed Hamiltonian with four or more lines below a vertex are zero. Other third-order contributions such as the diagram



are in fact interaction-reducible as they are obtained by contracting the four-body effective interaction with a two-body Green's function. However, these diagrams will appear in the perturbative expansion of the self-energy with respect to  $G_0$ , but they do not contribute to the series of third-order 1PI, skeleton and interaction-irreducible diagrams that enter  $\tilde{\Sigma}[\tilde{G}]$ . When  $T = 0$ , the third-order coupled-cluster self-energy exactly reduces to the two skeleton diagrams of the electronic self-energy as

$$\Sigma^{(3)}[G_0] = \text{Diagram 1} + \text{Diagram 2}$$

where the interaction line is now the antisymmetrized bare Coulomb interaction. Therefore, we have  $\tilde{\Sigma}_{pq}^{T=0(3)}(\omega) = \Sigma_{pq}^{(3)}(\omega)$  as expected.

To demonstrate the evaluation of a typical third-order contribution to the coupled-cluster self-energy, we focus on the third diagram of Eq. 128. In this diagram, from the Feynman rules [1–3, 12, 13], we have two sets of two equally oriented Green's function lines which give rise to a total symmetry factor  $\frac{1}{(2!)^2} = \frac{1}{4}$ . There is also one closed fermion loop giving rise to an overall phase factor of  $-1$ . The diagram evaluates to

$$\begin{aligned} & \text{Diagram} = -\frac{(i)^4}{(2!)^2} \sum_{\substack{rstuvx \\ yzwnol}} \int \frac{d\omega_1 d\omega_2 d\omega_3 d\omega_4}{(2\pi)^4} \chi_{pr,st} G_{su}^0(\omega_1) G_{tv}^0(\omega_2) G_{wr}^0(\omega_1 + \omega_2 - \omega) \\ & \quad \times \chi_{uvx,yzw} G_{yn}^0(\omega_3) G_{zo}^0(\omega_4) \chi_{no,ql} G_{lx}^0(\omega_3 + \omega_4 - \omega) . \end{aligned} \quad (129)$$

The first three diagrams of Eq. 128 encode excitations that contain mixtures of 2p1h/2h1p states. In the case of three-body interactions, it was proposed that these diagrams make up the dominant contribution to the self-energy at third-order [12, 13]. The rest of the diagrams all contain combinations of 3p2h and 2p1h excitations. Higher-body excitations are possible in the case of a generic  $N$ -body interaction, but vanish within coupled-cluster theory due to the structure of the similarity transformed Hamiltonian [14].

## X. SELF-CONSISTENT RENORMALIZATION OF THE COUPLED-CLUSTER SELF-ENERGY

In this section, we construct the renormalized coupled-cluster self-energy through the exact equation-of-motion for the single-particle coupled-cluster Green's function. From this analysis, we also demonstrate how the perturbative series for the self-energy derived in Section IX emerges from the self-consistent formalism.

### A. Equation-of-motion and the renormalized coupled-cluster self-energy

Through the equation-of-motion, the single-particle coupled-cluster Green's function is coupled to the 4-point, 6-point, 8-point and so on Green's functions. In the spin-orbital basis, these higher-point Green's functions are defined as

$$i\tilde{G}_{pq,rs}^{4\text{pt}}(t_1, t_2; t_3, t_4) = \langle \tilde{\Psi}_0 | \mathcal{T} \{ a_q(t_2) a_p(t_1) a_r^\dagger(t_3) a_s^\dagger(t_4) \} | \Phi_0 \rangle , \quad (130\text{a})$$

$$i\tilde{G}_{pqr,stu}^{6\text{pt}}(t_1, t_2, t_3; t_4, t_5, t_6) = \langle \tilde{\Psi}_0 | \mathcal{T} \left\{ a_r(t_3) a_q(t_2) a_p(t_1) a_s^\dagger(t_4) a_t^\dagger(t_5) a_u^\dagger(t_6) \right\} | \Phi_0 \rangle , \quad (130\text{b})$$

$$\begin{aligned} & i\tilde{G}_{pqrs,tuvw}^{8\text{pt}}(t_1, t_2, t_3, t_4; t_5, t_6, t_7, t_8) \\ &= \langle \tilde{\Psi}_0 | \mathcal{T} \left\{ a_s(t_4) a_r(t_3) a_q(t_2) a_p(t_1) a_t^\dagger(t_5) a_u^\dagger(t_6) a_v^\dagger(t_7) a_w^\dagger(t_8) \right\} | \Phi_0 \rangle . \end{aligned} \quad (130\text{c})$$

The 10-point and higher Green's functions are defined analogously. The relationship between the 4-point Green's function, the two-particle-hole Green's function and the two-particle reduced density matrix is given by

$$\tilde{G}_{pq,rs}^{4\text{pt}}(t^+, t; t', t'^+) = \tilde{G}_{pq,rs}^{2\text{ph}}(t - t') \quad (131\text{a})$$

with

$$\tilde{\Gamma}_{pq,rs} = i\tilde{G}_{pq,rs}^{2\text{ph}}(t - t^+) = \langle \tilde{\Psi}_0 | a_r^\dagger a_s^\dagger a_q a_p | \Phi_0 \rangle . \quad (131\text{b})$$

Here, the notation  $t - t^+$  denotes evaluation of the second time argument of the Green's function with a positive infinitesimal, *i.e.*  $t^+ = t + \eta$ , where  $\eta \rightarrow 0$  from above. Analogous

relationships hold between the higher-body Green's functions and corresponding reduced density matrices.

Taking the time-derivative of the first argument of the coupled-cluster Green's function (Eq. 103), using Eq. 50 and the definitions of the higher-order Green's functions, we have

$$\begin{aligned}
\sum_r \left( i \frac{\partial}{\partial t_1} \delta_{pr} - f_{pr} \right) \tilde{G}_{rq}(t_1 - t_2) &= \delta_{pq} \delta(t_1 - t_2) + \sum_r (\bar{h}_{pr} - f_{pr}) \tilde{G}_{rq}(t_1 - t_2) \\
&+ \frac{1}{2!} \sum_{rst} \bar{h}_{pr,st} \tilde{G}_{st,rq}^{4\text{pt}}(t_1, t_1; t_1^+, t_2) \\
&+ \frac{1}{3! \cdot 2!} \sum_{\substack{rs \\ tuv}} \bar{h}_{prs,tuv} \tilde{G}_{tuv,rsq}^{6\text{pt}}(t_1, t_1, t_1; t_1^{++}, t_1^+, t_2) \\
&+ \frac{1}{4! \cdot 3!} \sum_{\substack{rst \\ uvol}} \bar{h}_{prst,uvol} \tilde{G}_{uvol,rstq}^{8\text{pt}}(t_1, t_1, t_1, t_1; t_1^{+++}, t_1^{++}, t_1^+, t_2) \\
&+ \dots
\end{aligned} \tag{132}$$

In contrast to the electronic Green's function where the interaction Hamiltonian is a two-body operator, the coupled-cluster Green's function is coupled all the way up to the  $N$ -body Green's function, since  $\bar{H}$  is an  $N$ -body operator. Using the functional inverse for the 'non-interacting' Green's function and taking the Fourier transformation of this expression, we rewrite the equation-of-motion as the Dyson series

$$\begin{aligned}
\tilde{G}_{pq}(\omega) &= G_{pq}^0(\omega) + \sum_{rs} G_{pr}^0(\omega) (\bar{h}_{rs} - f_{rs}) \tilde{G}_{sq}(\omega) \\
&- \frac{1}{2!} \sum_{rstu} G_{pr}^0(\omega) \bar{h}_{rs,tu} \int_{-\infty}^{\infty} \frac{d\omega_1 d\omega_2}{(2\pi)^2} \tilde{G}_{tu,qs}^{4\text{pt}}(\omega_1, \omega_2; \omega, \omega_1 + \omega_2 - \omega) \\
&+ \frac{1}{3! \cdot 2!} \sum_{\substack{rst \\ uvw}} G_{ps}^0(\omega) \bar{h}_{rst,uvw} \int_{-\infty}^{\infty} \frac{d\omega_1 d\omega_2 d\omega_3 d\omega_4}{(2\pi)^4} \tilde{G}_{uvw,rqt}^{6\text{pt}}(\omega_1, \omega_2, \omega_3; \omega_4, \omega, \omega_1 + \omega_2 + \omega_3 - \omega_4 - \omega) \\
&- \frac{1}{4! \cdot 3!} \sum_{\substack{rst \\ uvol}} G_{pn}^0(\omega) \bar{h}_{nrst,uvol} \\
&\int_{-\infty}^{\infty} \frac{d\omega_1 d\omega_2 d\omega_3 d\omega_4 d\omega_5 d\omega_6}{(2\pi)^6} \tilde{G}_{uvol,qrst}^{8\text{pt}}(\omega_1, \omega_2, \omega_3, \omega_4; \omega, \omega_5, \omega_6, \omega_1 + \omega_2 + \omega_3 + \omega_4 - \omega_5 - \omega_6 - \omega) \\
&+ \dots
\end{aligned} \tag{133}$$

where the continuing series implies coupling of the five-body interaction to the 10-point

Green's function and so on. Therefore, knowledge of the single-particle Green's function requires the knowledge of all  $N$ -point Green's functions. In order to derive the self-consistent expression for the coupled-cluster self-energy, we first introduce expressions for the 4-point, 6-point, 8-point vertices and so on. These interaction vertices contain only 1PI diagrams and are related to the self-consistent equations of motion for the 4-point, 6-point, 8-point Green's functions and so on, respectively. In the frequency domain, the 4-point vertex function is defined as [3, 52]

$$\begin{aligned}
\tilde{G}_{pq,rs}^{4\text{pt}}(\omega_1, \omega_2; \omega_3, \omega_4) &= 2\pi i \left( \delta(\omega_1 - \omega_3)\delta(\omega_2 - \omega_4)\tilde{G}_{pr}(\omega_1)\tilde{G}_{qs}(\omega_2) \right. \\
&\quad \left. - \delta(\omega_1 - \omega_4)\delta(\omega_2 - \omega_3)\tilde{G}_{ps}(\omega_1)\tilde{G}_{qr}(\omega_2) \right) \\
&\quad - \sum_{tuvw} \tilde{G}_{pt}(\omega_1)\tilde{G}_{qu}(\omega_2)\tilde{\Lambda}_{tu,vw}^{4\text{pt}}(\omega_1, \omega_2; \omega_3, \omega_4)\tilde{G}_{vr}(\omega_3)\tilde{G}_{ws}(\omega_4) .
\end{aligned} \tag{134}$$

This equation presents the 4-point Green's function as the sum of the properly antisymmetrized propagation of two independent particles, with  $\tilde{\Lambda}^{4\text{pt}}$  representing their effective interaction. The 4-point vertex,  $\tilde{\Lambda}^{4\text{pt}}$ , is very closely related to the Bethe-Salpeter kernel and 'vertex' of Hedin's equations (see Section XIV). However, it is constructed from antisymmetrized 1PI diagrams as opposed to the two-particle irreducible diagrams (2PI) which enter the BSE. Similarly, the equation-of-motion for the 6-point Green's function may be written as [3, 12, 52]

$$\begin{aligned}
\tilde{G}_{pqr,stu}^{6\text{pt}}(\omega_1, \omega_2, \omega_3; \omega_4, \omega_5, \omega_6) &= \\
&\quad - (2\pi)^2 \mathcal{A}_{\{p\omega_1, q\omega_2, r\omega_3\}} \left[ \delta(\omega_1 - \omega_4)\delta(\omega_2 - \omega_5)\delta(\omega_3 - \omega_6)\tilde{G}_{ps}(\omega_1)\tilde{G}_{qt}(\omega_2)\tilde{G}_{ru}(\omega_3) \right] \\
&\quad - 2\pi i \mathcal{P}_{\{p\omega_1, q\omega_2, r\omega_3\}} \mathcal{P}_{\{s\omega_4, t\omega_5, u\omega_6\}} \\
&\quad \left( \delta(\omega_1 - \omega_4)\tilde{G}_{ps}(\omega_1) \sum_{vwlo} \tilde{G}_{qv}(\omega_2)\tilde{G}_{rw}(\omega_3)\tilde{\Lambda}_{vw,lo}^{4\text{pt}}(\omega_2, \omega_3; \omega_5, \omega_6)\tilde{G}_{lt}(\omega_5)\tilde{G}_{ou}(\omega_6) \right) \\
&\quad + \sum_{\substack{vwl \\ omn}} \tilde{G}_{pv}(\omega_1)\tilde{G}_{qw}(\omega_2)\tilde{G}_{rl}(\omega_3)\tilde{\Lambda}_{vwl,omn}^{6\text{pt}}(\omega_1, \omega_2, \omega_3; \omega_4, \omega_5, \omega_6)\tilde{G}_{os}(\omega_4)\tilde{G}_{mt}(\omega_5)\tilde{G}_{nu}(\omega_6)
\end{aligned} \tag{135}$$

Here, we employ the notation of Ref. [12] where  $\mathcal{A}_{\{p\omega_1, q\omega_2, r\omega_3\}}$  represents the antisymmetric sum of all possible pairs of permutations of the index-frequency pairs and  $\mathcal{P}_{\{p\omega_1, q\omega_2, r\omega_3\}}$  sums all cyclic permutations of each index-frequency pair. The antisymmetrized and cyclic permutation summations are required to ensure that the fermionic exchange symmetry is obeyed during multiparticle propagation. In general, there are  $n!$  terms that contribute to the independent-particle propagation of  $n$  fermions. For a single fermion propagating

independently with respect to the coupled propagating of  $(n - 1)$  interacting fermions gives rise to  $n^2$  equivalent combinations. For the case of the 6-point vertex equation, we have  $3! = 6$  independent-particle propagation terms,  $3^2 = 9$  terms corresponding to the propagation of a single fermion with two interacting fermions [52]. From this equation, we immediately see the emergence of the coupling of the 6-point vertex function to the 4-point vertex. This is a consequence of the fact that the 6-point vertex is related to the functional derivative of the 4-point vertex with respect to the single-particle Green's function. Continuing this process up to the  $N$ -body Green's function and  $2N$ -point vertex function, yields expressions that couple to all propagators and contain the correct permutation symmetry with respect to the Fermi statistics.

All equations involving vertices are exact by definition and inserting the expressions containing the vertex functions, using the definition of the self-energy through the Dyson equation, we obtain the following expression for the irreducible coupled-cluster self-energy

$$\begin{aligned}
\tilde{\Sigma}_{pq}(\omega) = & \left( \bar{h}_{pq} - i \sum_{rs} \bar{h}_{pr,qs} \tilde{G}_{sr}(t - t^+) + \frac{i}{(2!)^2} \sum_{rstu} \bar{h}_{prs,qtu} \tilde{G}_{tu,rs}^{2\text{ph}}(t - t^+) + \dots \right) - f_{pq} \\
& + \frac{1}{2!} \sum_{\substack{stu \\ vw}} \left( \bar{h}_{ps,tu} - i \sum_{on} \bar{h}_{pso,tun} \tilde{G}_{no}(t - t^+) + \frac{i}{(2!)^2} \sum_{one\kappa} \bar{h}_{pson,tue\kappa} \tilde{G}_{e\kappa,on}^{2\text{ph}}(t - t^+) + \dots \right) \\
& \times \int \frac{d\omega_1 d\omega_2}{(2\pi)^2} \tilde{G}_{tv}(\omega_1) \tilde{G}_{uw}(\omega_2) \tilde{\Lambda}_{vw,qt}^{4\text{pt}}(\omega_1, \omega_2; \omega, \omega_1 + \omega_2 - \omega) \tilde{G}_{ls}(\omega_1 + \omega_2 - \omega) \\
& + \frac{1}{3! \cdot 2!} \sum_{\substack{st \\ uvw}} \sum_{\substack{l\sigma \\ \alpha\gamma\kappa}} \left( \bar{h}_{spt,uvw} - i \sum_{\beta\epsilon} \bar{h}_{spt\beta,uvw\epsilon} \tilde{G}_{\epsilon\beta}(t - t^+) + \frac{i}{(2!)^2} \sum_{\beta\epsilon\delta\rho} \bar{h}_{spt\beta\epsilon,uvw\delta\rho} \tilde{G}_{\delta\rho,\beta\epsilon}^{2\text{ph}}(t - t^+) + \dots \right) \\
& \times \int \frac{d\omega_1 d\omega_2 d\omega_3 d\omega_4}{(2\pi)^4} \tilde{G}_{ul}(\omega_1) \tilde{G}_{v\sigma}(\omega_2) \tilde{G}_{w\alpha}(\omega_3) \tilde{\Lambda}_{l\sigma\alpha,\gamma q\kappa}^{6\text{pt}}(\omega_1, \omega_2, \omega_3; \omega_4, \omega, \omega_1 + \omega_2 + \omega_3 - \omega_4 - \omega) \\
& \quad \times \tilde{G}_{\gamma s}(\omega_4) \tilde{G}_{\sigma t}(\omega_1 + \omega_2 + \omega_3 - \omega_4 - \omega) \\
& + \frac{1}{4! \cdot 3!} \sum_{\substack{stu \\ vw}} \sum_{\substack{\sigma g z \\ y\gamma\epsilon\delta}} \left( \bar{h}_{pstu,vwol} - i \sum_{\alpha\beta} \bar{h}_{pstu\alpha,vwol\beta} \tilde{G}_{\beta\alpha}(t - t^+) + \frac{i}{(2!)^2} \sum_{\alpha\beta\gamma\phi} \bar{h}_{pstu\alpha\beta,vwol\gamma\phi} \tilde{G}_{\gamma\phi,\alpha\beta}^{2\text{ph}}(t - t^+) + \dots \right) \\
& \times \int \frac{d\omega_1 d\omega_2 d\omega_3 d\omega_4 d\omega_5 d\omega_6}{(2\pi)^6} \tilde{G}_{v\sigma}(\omega_1) \tilde{G}_{wg}(\omega_2) \tilde{G}_{oz}(\omega_3) \tilde{G}_{ly}(\omega_4) \\
& \quad \times \tilde{\Lambda}_{\sigma g z y, q\gamma\epsilon\delta}^{8\text{pt}}(\omega_1, \omega_2, \omega_3, \omega_4; \omega, \omega_5, \omega_6, \omega_1 + \omega_2 + \omega_3 + \omega_4 - \omega_5 - \omega_6 - \omega) \\
& \quad \times \tilde{G}_{\gamma s}(\omega_5) \tilde{G}_{et}(\omega_6) \tilde{G}_{\delta u}(\omega_1 + \omega_2 + \omega_3 + \omega_4 - \omega_5 - \omega_6 - \omega) \\
& + \dots
\end{aligned} \tag{136}$$

Due to the equation-of-motion for the Green's function this expression continues up to the  $2N$ -point vertex. Remarkably, as a result of the vertex equations, the effective interaction elements appearing here correspond exactly to those of the normal-ordered similarity transformed Hamiltonian defined in Eq. 93. Therefore, we may simplify the above expression to obtain the fully renormalized coupled-cluster self-energy as

$$\begin{aligned}
\tilde{\Sigma}_{pq}(\omega) &= (\tilde{F}_{pq} - f_{pq}) \\
&+ \frac{1}{2!} \sum_{\substack{ps,tu \\ stuv}} \tilde{\Xi}_{ps,tu} \int \frac{d\omega_1 d\omega_2}{(2\pi)^2} \tilde{G}_{tv}(\omega_1) \tilde{G}_{uw}(\omega_2) \tilde{\Lambda}_{vw,ql}^{4\text{pt}}(\omega_1, \omega_2; \omega, \omega_1 + \omega_2 - \omega) \tilde{G}_{ls}(\omega_1 + \omega_2 - \omega) \\
&+ \frac{1}{3! \cdot 2!} \sum_{\substack{st \\ uvw}} \sum_{\substack{l\sigma \\ \alpha\gamma\kappa}} \tilde{\chi}_{spt,uvw} \int \frac{d\omega_1 d\omega_2 d\omega_3 d\omega_4}{(2\pi)^4} \tilde{G}_{ul}(\omega_1) \tilde{G}_{v\sigma}(\omega_2) \tilde{G}_{w\alpha}(\omega_3) \\
&\quad \times \tilde{\Lambda}_{l\sigma\alpha,\gamma\kappa}^{6\text{pt}}(\omega_1, \omega_2, \omega_3; \omega_4, \omega, \omega_1 + \omega_2 + \omega_3 - \omega_4 - \omega) \tilde{G}_{\gamma s}(\omega_4) \tilde{G}_{\sigma t}(\omega_1 + \omega_2 + \omega_3 - \omega_4 - \omega) \\
&+ \frac{1}{4! \cdot 3!} \sum_{\substack{stu \\ vwol}} \sum_{\substack{\sigma g z \\ y\gamma\epsilon\delta}} \tilde{\chi}_{pstu,vwol} \int \frac{d\omega_1 d\omega_2 d\omega_3 d\omega_4 d\omega_5 d\omega_6}{(2\pi)^6} \tilde{G}_{v\sigma}(\omega_1) \tilde{G}_{wg}(\omega_2) \tilde{G}_{oz}(\omega_3) \tilde{G}_{ly}(\omega_4) \\
&\quad \times \tilde{\Lambda}_{\sigma g zy, q\gamma\epsilon\delta}^{8\text{pt}}(\omega_1, \omega_2, \omega_3, \omega_4; \omega, \omega_5, \omega_6, \omega_1 + \omega_2 + \omega_3 + \omega_4 - \omega_5 - \omega_6 - \omega) \\
&\quad \times \tilde{G}_{\gamma s}(\omega_5) \tilde{G}_{et}(\omega_6) \tilde{G}_{\delta u}(\omega_1 + \omega_2 + \omega_3 + \omega_4 - \omega_5 - \omega_6 - \omega) \\
&+ \dots
\end{aligned} \tag{137}$$

The diagrammatic representation of this equation is given by

$$\begin{aligned}
\tilde{\Sigma}[\tilde{G}] &= \text{diagram 1} + \text{diagram 2} + \text{diagram 3} + \dots \\
&\quad + \dots
\end{aligned} \tag{138}$$

where the higher-order diagrams are represented by propagators coupled to the five-body interaction and the 10-point vertex function and so on. Here, we have introduced the diagrammatic notation for the ‘vertex’ functions,  $\tilde{\Lambda}^{4/6/8\text{pt}}$ . Diagrammatically, through the vertices, the renormalized self-energy is expressed as the sum of all 1PI, interaction-irreducible skeleton diagrams. From the Feynman rules, we see that the correct pre-factors of the self-energy are reproduced. The first vertex diagram has one set of two equally oriented Green's function lines therefore giving a total symmetry factor of  $\frac{1}{2!} = \frac{1}{2}$ . The second vertex diagram

contains one set of three and one set of two equally oriented Green's function lines giving rise to the total symmetry factor of  $\frac{1}{3!2!} = \frac{1}{12}$ . The third vertex diagram contains one set of four and one set of three equally oriented Green's function lines giving rise to the total symmetry factor of  $\frac{1}{4!3!} = \frac{1}{144}$ , and so on. This results in the self-consistently renormalized series for the self-energy functional (up to third order)

$$\begin{aligned}
 \tilde{\Sigma}[\tilde{G}] = & \text{[Diagram 1]} + \text{[Diagram 2]} + \text{[Diagram 3]} + \text{[Diagram 4]} \\
 & + \text{[Diagram 5]} + \text{[Diagram 6]} + \text{[Diagram 7]} + \text{[Diagram 8]} \\
 & + \text{[Diagram 9]} + \text{[Diagram 10]} + \text{[Diagram 11]} + \text{[Diagram 12]} + \dots
 \end{aligned}
 \tag{139}$$

Subsequently we observe the renormalization of both propagators and interaction vertices



Again,  $\tilde{\Xi}_{ab,ij} = \chi_{ab,ij} = 0$  due to the coupled-cluster amplitude equations. Using the expression for the effective two-body interaction, the corresponding second-order self-consistent coupled-cluster self-energy takes the form

$$\begin{aligned}
\tilde{\Sigma}^{(2)}[\tilde{G}] = & \text{Diagram 1} = \text{Diagram 2} + \text{Diagram 3} + \text{Diagram 4} \\
& + \text{Diagram 5} + \dots
\end{aligned}
\tag{143}$$

and so on for the terms containing the higher-body de-excitation amplitudes. Here, we have introduced the mixed Feynman-Goldstone diagram notation to represent the Green's functions and interaction-irreducible matrix elements. The dressed propagators are to be identified as Green's functions, whilst undressed fermion lines contracting with the  $\lambda$ -matrices are to be interpreted as Goldstone diagrams that contribute to the effective interaction,  $\tilde{\chi}_{pq,rs}$ . The three-body effective interaction is similarly defined as

$$\begin{aligned}
\tilde{\chi}_{pqr,stu} = & \text{Diagram 1} + \text{Diagram 2} + \text{Diagram 3} + \dots
\end{aligned}
\tag{144}$$

and so on. The higher-body terms are constructed analogously by contracting the higher-order effective interaction matrix elements  $\{\chi\}$  with the corresponding  $\lambda$ -matrices. As an example, using the Green's function residues and poles defined in Section VIII, we evaluate the second-order self-consistent contribution to the renormalized coupled-cluster self-energy

to give

$$\begin{aligned} \tilde{\Sigma}_{pq}^{(2)}[\tilde{G}](\omega) = & \frac{1}{2} \sum_{\substack{rst \\ uvw}} \tilde{\Xi}_{pr,tu} \left( \sum_{\mu_1 \mu_2 \nu_1} \frac{(\tilde{Y}_t^{\mu_1} \tilde{Y}_u^{\mu_2} \tilde{X}_r^{\nu_1}) \bar{Y}_s^{\mu_1} \bar{Y}_v^{\mu_2} \bar{X}_w^{\nu_1}}{\omega + \varepsilon_{\nu_1}^{N-1} - \varepsilon_{\mu_1}^{N+1} - \varepsilon_{\mu_2}^{N+1} + i\eta} \right. \\ & \left. + \sum_{\nu_1 \nu_2 \mu_1} \frac{\bar{X}_t^{\nu_1} \bar{X}_u^{\nu_2} \bar{Y}_r^{\mu_1} (\tilde{X}_s^{\nu_1} \tilde{X}_v^{\nu_2} \tilde{Y}_w^{\mu_1})}{\omega + \varepsilon_{\mu_1}^{N+1} - \varepsilon_{\nu_1}^{N-1} - \varepsilon_{\nu_2}^{N-1} - i\eta} \right) \tilde{\Xi}_{sv,qw}. \end{aligned} \quad (145)$$

Here, the space spanned by the indices  $\mu$  and  $\nu$  is much larger than the spin-orbital space as they index the removal/addition poles of the Green's function and are directly connected to charged excitation processes. Hence, the resolvents appearing in Eq. 145

$$\tilde{G}_{tur,svw}^{2p1h/2h1p}(\omega) = \sum_{\mu_1 \mu_2 \nu_1} \frac{(\tilde{Y}_t^{\mu_1} \tilde{Y}_u^{\mu_2} \tilde{X}_r^{\nu_1}) \bar{Y}_s^{\mu_1} \bar{Y}_v^{\mu_2} \bar{X}_w^{\nu_1}}{\omega + \varepsilon_{\nu_1}^{N-1} - \varepsilon_{\mu_1}^{N+1} - \varepsilon_{\mu_2}^{N+1} + i\eta} + \sum_{\nu_1 \nu_2 \mu_1} \frac{\bar{X}_t^{\nu_1} \bar{X}_u^{\nu_2} \bar{Y}_r^{\mu_1} (\tilde{X}_s^{\nu_1} \tilde{X}_v^{\nu_2} \tilde{Y}_w^{\mu_1})}{\omega + \varepsilon_{\mu_1}^{N+1} - \varepsilon_{\nu_1}^{N-1} - \varepsilon_{\nu_2}^{N-1} - i\eta} \quad (146)$$

are viewed as spectral representations of correlated simultaneous charged excitation processes involving three-particles.

## B. Aside on the vertex functions

The vertex functions are introduced to provide us with a formally exact, closed-form equation for the coupled-cluster self-energy. However, they are clearly related to the equation-of-motion of their corresponding higher-body Green's function. For example, by taking the time-derivative of the first argument of the 4-point coupled-cluster Green's function, using the biorthogonal Heisenberg equation-of-motion and taking the Fourier transform, we have [3]

$$\begin{aligned} \tilde{G}_{pq,rs}^{4pt}(\omega_1, \omega_2; \omega_3, \omega_4) = & 2\pi i \left( \delta(\omega_1 - \omega_3) \delta(\omega_2 - \omega_4) G_{pr}^0(\omega_1) \tilde{G}_{qs}(\omega_2) - \delta(\omega_1 - \omega_4) \delta(\omega_2 - \omega_3) G_{ps}^0(\omega_1) \tilde{G}_{qr}(\omega_2) \right) \\ & + \sum_{ut} G_{pu}^0(\omega_1) (\bar{h}_{ut} - f_{ut}) \tilde{G}_{ut,rs}^{4pt}(\omega_1, \omega_2; \omega_3, \omega_4) \\ & - \frac{1}{2!} \sum_{utvw} G_{pu}^0(\omega_1) \bar{h}_{ut,vw} \int \frac{d\omega d\omega'}{(2\pi)^2} \tilde{G}_{vwq,rts}^{6pt}(\omega, \omega', \omega_2; \omega_3, \omega + \omega' - \omega_1, \omega_4) \\ & + \frac{1}{3! \cdot 2!} \sum_{\substack{utv \\ wl\sigma}} G_{pu}^0(\omega_1) \bar{h}_{utv,wl\sigma} \int \frac{d\omega d\omega' d\omega'' d\omega'''}{(2\pi)^4} \tilde{G}_{wl\sigma q,rtvs}^{8pt}(\omega, \omega', \omega'', \omega_2; \omega_3, \omega'', \omega + \omega' + \omega'' - \omega_1 - \omega''', \omega_4) \\ & + \dots \end{aligned} \quad (147)$$



with

$$\text{wavy line} = \text{wavy line} + \text{crossed-out wavy line} + \text{loop with dashed line} + \text{two loops with dashed line} + \dots \quad (150)$$

Now, retaining only terms up to second-order (diagrams containing up to two interaction lines), we insert Eqs 149 and 150 into Eq. 148 to obtain the second-order perturbative expansion of the self-energy as

$$\tilde{\Sigma}^{(2)}[G_0] = \text{crossed-out wavy line} + \text{square loop with wavy line} + \text{loop with wavy line and dashed line} + \text{loop with two wavy lines and dashed line} \quad (151)$$

This is exactly the expression obtained at second order in the perturbative expansion as presented in Section IX. All higher-order perturbative diagrams are obtained from the self-consistent expression by successive diagrammatic expansion of exact propagators and interaction vertices.

## XI. THE COUPLED-CLUSTER GROUND STATE ENERGY

In this section, we demonstrate how the coupled-cluster correlation energy may be obtained from the coupled-cluster self-energy. The coupled-cluster ground state energy is given by the expectation value

$$\begin{aligned} E_0^{\text{CC}} &= \langle \Phi_0 | \bar{H} | \Phi_0 \rangle \\ &= \sum_{pq} \bar{h}_{pq} \gamma_{pq}^{\text{ref}} + \frac{1}{(2!)^2} \sum_{pq,rs} \bar{h}_{pq,rs} \Gamma_{pq,rs}^{\text{ref}} + \frac{1}{(3!)^2} \sum_{pqr,stu} \bar{h}_{pqr,stu} \Gamma_{pqr,stu}^{\text{ref}} + \dots, \end{aligned} \quad (152)$$

From Eq. 152, we have

$$\begin{aligned} E_0^{\text{CC}} &= \sum_i \bar{h}_{ii} + \frac{1}{2} \sum_{ij} \bar{h}_{ij,ij} \\ &= E_0^{\text{ref}} + \frac{1}{4} \sum_{ijab} \langle ij || ab \rangle (t_{ij}^{ab} + 2t_i^a t_j^b) + \sum_{ia} f_{ia} t_i^a \\ &= E_0^{\text{ref}} + E_c^{\text{CC}}. \end{aligned} \quad (153)$$

All additional higher-body terms evaluate to zero due to the structure of the coupled-cluster similarity transformed Hamiltonian as all matrix elements with four or more lines below the

interaction vertex vanish [14]. The ground state energy is also given by the coupled-cluster Lagrangian via

$$\begin{aligned}
\mathcal{L}_0^{\text{CC}} &= \langle \tilde{\Psi}_0 | \bar{H} | \Phi_0 \rangle \\
&= \sum_{pq} \bar{h}_{pq} \gamma_{pq}^{\text{ref}} + \frac{1}{(2!)^2} \sum_{pq,rs} \bar{h}_{pq,rs} \Gamma_{pq,rs}^{\text{ref}} + \frac{1}{(3!)^2} \sum_{pqr,stu} \bar{h}_{pqr,stu} \Gamma_{pqr,stu}^{\text{ref}} + \dots \\
&+ \sum_{pq} \bar{h}_{pq} \langle \Lambda | a_p^\dagger a_q | \Phi_0 \rangle + \frac{1}{(2!)^2} \sum_{pq,rs} \bar{h}_{pq,rs} \langle \Lambda | a_p^\dagger a_q^\dagger a_s a_r | \Phi_0 \rangle \\
&+ \frac{1}{(3!)^2} \sum_{pqr,stu} \bar{h}_{pqr,stu} \langle \Lambda | a_p^\dagger a_q^\dagger a_r^\dagger a_u a_t a_s | \Phi_0 \rangle + \dots
\end{aligned} \tag{154}$$

where  $\langle \Lambda | = \langle \Phi_0 | \Lambda$  is the state obtained from application of the de-excitation operator onto the reference. From the equation-of-motion for the single-particle CC Green's function (Eq. 132), it appears that the total ground-state energy cannot be obtained from the self-energy because

$$\begin{aligned}
\frac{1}{2} \lim_{\eta \rightarrow 0^+} \sum_{pq} \int_{-\infty}^{\infty} \frac{d\omega}{2\pi i} e^{i\eta\omega} \tilde{\Sigma}_{pq}(\omega) \tilde{G}_{qp}(\omega) &= \frac{1}{2} \sum_{pq} (\bar{h}_{pq} - f_{pq}) \langle \Phi_0 | (\mathbb{1} + \Lambda) a_p^\dagger a_q | \Phi_0 \rangle \\
&+ \frac{1}{(2!)^2} \sum_{pq,rs} \bar{h}_{pq,rs} \langle \Phi_0 | (\mathbb{1} + \Lambda) a_p^\dagger a_q^\dagger a_s a_r | \Phi_0 \rangle \\
&+ \frac{1}{3! \cdot (2!)^2} \sum_{pqr,stu} \bar{h}_{pqr,stu} \langle \Phi_0 | (\mathbb{1} + \Lambda) a_p^\dagger a_q^\dagger a_r^\dagger a_u a_t a_s | \Phi_0 \rangle \\
&+ \dots
\end{aligned} \tag{155}$$

which equates to

$$\begin{aligned}
\frac{1}{2} \lim_{\eta \rightarrow 0^+} \sum_{pq} \int_{-\infty}^{\infty} \frac{d\omega}{2\pi i} e^{i\eta\omega} \tilde{\Sigma}_{pq}(\omega) \tilde{G}_{qp}(\omega) &= \frac{1}{2} \langle \Phi_0 | (\mathbb{1} + \Lambda) (\bar{h}_1 - F) | \Phi_0 \rangle + \langle \Phi_0 | (\mathbb{1} + \Lambda) \bar{V} | \Phi_0 \rangle \\
&+ \frac{3}{2} \langle \Phi_0 | (\mathbb{1} + \Lambda) \bar{W} | \Phi_0 \rangle + \dots
\end{aligned} \tag{156}$$

The correct prefactors of the coupled-cluster Lagrangian in Eq. 154 are not generated by the equation-of-motion for the single-particle Green's function. Therefore the amplitude equations are not correctly reproduced from the equation-of-motion. This is analogous to the fact that the ground state energy of a three-body hermitian interaction Hamiltonian is not obtainable from the equation-of-motion for the single-particle Green's function [12].

However, the coupled-cluster ground state energy is still accessible from the coupled-cluster self-energy by noting that we may write the coupled-cluster single-particle Green's function as the sum of two contributions:

$$\begin{aligned}\tilde{G}_{pq}(t_1, t_2) &= i\tilde{G}_{pq}^{\text{ref}}(t_1, t_2) + \tilde{G}_{pq}^{\Lambda}(t_1, t_2) \\ i\tilde{G}_{pq}^{\text{ref}}(t_1, t_2) &= \langle \Phi_0 | \mathcal{T} \{ a_p(t_1) a_q^\dagger(t_2) \} | \Phi_0 \rangle \\ i\tilde{G}_{pq}^{\Lambda}(t_1, t_2) &= \langle \Lambda | \mathcal{T} \{ a_p(t_1) a_q^\dagger(t_2) \} | \Phi_0 \rangle .\end{aligned}$$

Focusing on the equation-of-motion for  $\tilde{G}_{pq}^{\text{ref}}$ , we have the following expression

$$\begin{aligned}\sum_r \left( i \frac{\partial}{\partial t_1} \delta_{pr} - f_{pr} \right) \tilde{G}_{rq}^{\text{ref}}(t_1 - t_2) &= \delta_{pq} \delta(t_1 - t_2) + \sum_r (\bar{h}_{pr} - f_{pr}) \tilde{G}_{rq}^{\text{ref}}(t_1 - t_2) \\ &+ \frac{1}{2!} \sum_{rst} \bar{h}_{pr, st} \tilde{G}_{st, rq}^{4\text{pt}, \text{ref}}(t_1, t_1; t_1^+, t_2) \\ &+ \frac{1}{3! \cdot 2!} \sum_{\substack{rs \\ tuv}} \bar{h}_{prs, tuv} \tilde{G}_{tuv, rsq}^{6\text{pt}, \text{ref}}(t_1, t_1, t_1; t_1^{++}, t_1^+, t_2) \\ &+ \dots \\ &= \delta_{pq} \delta(t_1 - t_2) + \sum_r \int_{-\infty}^{\infty} \frac{d\omega}{2\pi} e^{-i\omega(t_1 - t_2)} \tilde{\Sigma}_{pr}^*(\omega) \tilde{G}_{rq}^{\text{ref}}(\omega).\end{aligned}\tag{157}$$

where  $\tilde{\Sigma}^*$  is an 'effective' self-energy and all Green's functions are defined in terms of expectation values over the reference,  $|\Phi_0\rangle$ . Taking the limit as  $t_2 \rightarrow t_1^+$ , the trace and multiplying by  $\frac{-i}{2}$ , we have

$$-\frac{i}{2} \lim_{\eta \rightarrow 0^+} \sum_{pq} \int_{-\infty}^{\infty} \frac{d\omega}{2\pi} e^{i\eta\omega} \tilde{\Sigma}_{pq}^*(\omega) \tilde{G}_{qp}^{\text{ref}}(\omega) = \frac{1}{2} \sum_{pq} (\bar{h}_{pq} - f_{pq}) \gamma_{pq}^{\text{ref}} + \frac{1}{(2!)^2} \sum_{pq, rs} \bar{h}_{pq, rs} \Gamma_{pq, rs}^{\text{ref}}\tag{158}$$

as all three-body and higher terms vanish. Using Eqs 153 and 158, the ground-state coupled-cluster energy is given by

$$E_0^{\text{CC}} = -\frac{i}{2} \lim_{\eta \rightarrow 0^+} \sum_{pq} \int_{-\infty}^{\infty} \frac{d\omega}{2\pi} e^{i\eta\omega} \tilde{\Sigma}_{pq}^*(\omega) \tilde{G}_{qp}^{\text{ref}}(\omega) + \frac{1}{2} \sum_i (\bar{h}_{ii} + f_{ii}) .\tag{159}$$

As the ‘effective’ self-energy  $\tilde{\Sigma}^*$  also consists of a static and dynamical part, we have

$$\begin{aligned}
-\frac{i}{2} \lim_{\eta \rightarrow 0^+} \sum_{pq} \int_{-\infty}^{\infty} \frac{d\omega}{2\pi} e^{i\eta\omega} \tilde{\Sigma}_{pq}^*(\omega) \tilde{G}_{qp}^{\text{ref}}(\omega) &= \frac{1}{2} \sum_{pq} \tilde{\Sigma}_{pq}^{*,\infty} \gamma_{qp}^{\text{ref}} \\
&- \frac{i}{2} \lim_{\eta \rightarrow 0^+} \sum_{ij} \int_{-\infty}^{\infty} \frac{d\omega}{2\pi} e^{i\eta\omega} \tilde{\Sigma}_{ij}^{*,c}(\omega) \tilde{G}_{ji}^{\text{ref}}(\omega) \\
&- \frac{i}{2} \lim_{\eta \rightarrow 0^+} \sum_{ab} \int_{-\infty}^{\infty} \frac{d\omega}{2\pi} e^{i\eta\omega} \tilde{\Sigma}_{ab}^{*,c}(\omega) \tilde{G}_{ba}^{\text{ref}}(\omega),
\end{aligned} \tag{160}$$

where we have used  $\tilde{G}_{ia}^{\text{ref}}(\omega) = \tilde{G}_{ai}^{\text{ref}}(\omega) = 0$ . The poles of the occupied-occupied block of the self-energy and Green’s function lie above the real axis and the poles of the virtual-virtual block of the self-energy and Green’s function lie below the real axis. Therefore, from the residue theorem, the integrals over frequency vanish and we are left only with the static contribution

$$-\frac{i}{2} \lim_{\eta \rightarrow 0^+} \sum_{pq} \int_{-\infty}^{\infty} \frac{d\omega}{2\pi} e^{i\eta\omega} \tilde{\Sigma}_{pq}^*(\omega) \tilde{G}_{qp}^{\text{ref}}(\omega) = \frac{1}{2} \sum_{pq} \tilde{\Sigma}_{pq}^{*,\infty} \gamma_{pq}^{\text{ref}}. \tag{161}$$

Since the ‘effective’ self-energy  $\tilde{\Sigma}^*$  is defined through the equation-of-motion for  $\tilde{G}^{\text{ref}}$ , where all expectation values are taken over the reference alone, we find that the static contribution to the effective self-energy is exactly the first term of the renormalized coupled-cluster self-energy (see Section X) where no de-excitation amplitudes are present,  $\tilde{\Sigma}_{pq}^{*,\infty} = \tilde{\Sigma}_{pq}^{\infty(0)}$ . Using the definition of  $\tilde{\Sigma}_{pq}^{\infty(0)}$  from Eq. 115, we find (for a general reference state  $|\Phi_0\rangle$ )

$$\begin{aligned}
\frac{1}{2} \sum_{pq} \tilde{\Sigma}_{pq}^{\infty(0)} \gamma_{pq}^{\text{ref}} &= \frac{1}{2} \sum_i \tilde{\Sigma}_{ii}^{\infty(0)} \\
&= \frac{1}{4} \sum_{ijab} \langle ij || ab \rangle (t_{ij}^{ab} + 2t_i^a t_j^b) + \frac{1}{2} \sum_{ia} f_{ia} t_i^a + \frac{1}{2} \sum_{iaj} \langle ij || aj \rangle t_j^a.
\end{aligned} \tag{162}$$

The resulting coupled-cluster ground state energy obtained is given by

$$\begin{aligned}
E_0^{\text{CC}} &= \frac{1}{2} \sum_i (h_{ii} + f_{ii}) + \frac{1}{2} \sum_{ia} h_{ia} t_i^a + \frac{1}{2} \sum_i \tilde{\Sigma}_{ii}^{\infty(0)} \\
&= E_0^{\text{ref}} + \frac{1}{4} \sum_{ijab} \langle ij || ab \rangle (t_{ij}^{ab} + 2t_i^a t_j^b) + \sum_{ia} f_{ia} t_i^a.
\end{aligned} \tag{163}$$

where we have used  $\bar{h}_{ii} = h_{ii} + \sum_a h_{ia} t_i^a$  and  $\tilde{\Sigma}_{ii}^{\infty(0)}$  defined in Eq. 117. This is exactly the expression obtained with ground state coupled-cluster theory. Therefore, within the Green’s function formalism, the coupled-cluster correlation energy is generally given by the

expression

$$E_c^{\text{CC}} = \frac{1}{2} \sum_i \left( \tilde{\Sigma}_{ii}^{\infty(0)} + \sum_a h_{ia} t_i^a \right). \quad (164)$$

In the Breuckner basis, the second term vanishes and the correlation energy is simply given by the first term of the static contribution to the coupled-cluster self-energy [24]. Hence, the coupled-cluster ground state correlation energy is completely determined by the coupled-cluster self-energy. From Eq. 164, we find that the coupled-cluster ground state energy obtained at any level of approximation of the CC self-energy gives the same ground state energy as that obtained at the same level of approximation of the ground state coupled-cluster equations.

## XII. THE COUPLED-CLUSTER DYSON SUPERMATRIX AND SELF-ENERGY APPROXIMATIONS

In this section, we provide a brief outline of the coupled-cluster quasiparticle equation and Dyson supermatrix. Standard Green's function theory is centered around the frequency-dependent quasiparticle equation, which gives access to the poles and residues of the Green's function. This allows us to directly combine coupled-cluster theory with the methodology employed in the Green's function formalism, leading us to introduce several approximations for the coupled-cluster self-energy that preserve its correct spectral form.

Starting from the spectral form of the CC self-energy, given in Eq. 109, the coupled-cluster quasiparticle equation can be written in terms of the unfolded coupled-cluster Dyson supermatrix eigenvalue problem [24]

$$\begin{pmatrix} \mathbf{f} + \tilde{\Sigma}^{\infty} & \tilde{\mathbf{U}} & \tilde{\mathbf{V}} \\ \tilde{\mathbf{U}} & \bar{\mathbf{K}}^> + \bar{\mathbf{C}}^> & 0 \\ \tilde{\mathbf{V}} & 0 & \bar{\mathbf{K}}^< + \bar{\mathbf{C}}^< \end{pmatrix} \begin{pmatrix} \bar{\mathbf{A}} \\ \bar{\mathbf{W}}^+ \\ \bar{\mathbf{W}}^- \end{pmatrix} = \begin{pmatrix} \bar{\mathbf{A}} \\ \bar{\mathbf{W}}^+ \\ \bar{\mathbf{W}}^- \end{pmatrix} \varepsilon. \quad (165)$$

Here we have employed matrix notation for the coupling and interactions between the forward and backward time multi-particle-hole ISCs. The eigenvalues,  $\varepsilon$ , are the exact addition and removal energies of the system. Since the coupled-cluster self-energy is non-hermitian, the coupled-cluster Dyson supermatrix has distinct left and right eigenvectors. However, the

CC Dyson supermatrix is pseudo-hermitian due to the similarity transformed Hamiltonian  $\bar{H}$ , ensuring that it possesses a real spectrum. The quasiparticle renormalization factor is found from the inverse of the overlap of the eigenvectors as

$$\begin{aligned} Z_\nu &= \left( \sum_p \tilde{A}_p^\nu \bar{A}_p^\nu + \sum_J \tilde{W}_J^{+,\nu} \bar{W}_J^{+,\nu} + \sum_A \tilde{W}_A^{-,\nu} \bar{W}_A^{-,\nu} \right)^{-1} \\ &= \left( 1 - \frac{\partial \tilde{\Sigma}_{\nu\nu}(\omega)}{\partial \omega} \Big|_{\omega=\varepsilon_\nu} \right)^{-1}, \end{aligned} \quad (166)$$

where  $(\tilde{\mathbf{A}} \ \tilde{\mathbf{W}}^+ \ \tilde{\mathbf{W}}^-)$  is the left eigenvector solution.

By introducing the coupled-cluster Dyson supermatrix, we preserve the correct analytical structure of the self-energy required to obtain the correct convergence of the Feynman-Dyson diagrammatic perturbation expansion [51]. This forms the basis of the Algebraic Diagrammatic Construction method [13, 37]. In the following subsections, we construct the upfolded Dyson supermatrices for different 2p1h/2h1p CC self-energy approximations that preserve the correct analytic structure. These approximations allow us to leverage the connections between Green's function and coupled-cluster theory.

### A. Second-order perturbative and self-consistent approximations

From the second-order perturbative coupled-cluster self-energy (Eq. 120), we see that  $J/A$  are restricted to the space of 2p1h/2h1p excitations such that:

$$\begin{aligned} \tilde{U}_{p,abi}^{(0)} &= \frac{1}{\sqrt{2}} \chi_{pi,ab} \\ \bar{U}_{abi,q}^{(0)} &= \frac{1}{\sqrt{2}} \chi_{ab,qi} \\ \tilde{V}_{ija,q}^{(0)} &= \frac{1}{\sqrt{2}} \chi_{ij,qa} \\ \bar{V}_{p,ija}^{(0)} &= \frac{1}{\sqrt{2}} \chi_{pa,ij} \end{aligned} \quad (167)$$

The ISC interaction matrices are given by  $\bar{\mathbf{K}}_{abi,cdj}^{>(0)} = (\epsilon_a + \epsilon_b - \epsilon_i) \delta_{ac} \delta_{bd} \delta_{ij}$  and  $\bar{\mathbf{K}}_{ija,klb}^{<(0)} = (\epsilon_i + \epsilon_j - \epsilon_a) \delta_{ik} \delta_{jl} \delta_{ab}$ , respectively. This leads to the following upfolded CC Dyson supermatrix

$$\tilde{\mathbf{D}}^{\text{CC}(2)} = \begin{pmatrix} f_{pq} + \tilde{\Sigma}_{pq}^{\infty(0)} + \tilde{\Sigma}_{pq}^{\infty(2)} & \tilde{U}_{p,abi}^{(0)} & \bar{V}_{p,ija}^{(0)} \\ \bar{U}_{abi,q}^{(0)} & \bar{\mathbf{K}}_{abi,cdj}^{>(0)} & 0 \\ \tilde{V}_{ija,q}^{(0)} & 0 & \bar{\mathbf{K}}_{ija,klb}^{<(0)} \end{pmatrix}. \quad (168)$$

Alternatively, we also carry out this procedure for the second-order self-consistent, renormalized coupled-cluster self-energy given in Eq. 145. This self-energy also consists of 2p1h/2h1p excitation character and gives rise to the following coupling matrices:

$$\begin{aligned}
\tilde{U}_{p,\mu_1\mu_2\nu_1}^{\text{sc}(2)} &= \frac{1}{\sqrt{2}} \sum_{rtu} \tilde{\Xi}_{pr,tu} \tilde{Y}_t^{\mu_1} \tilde{Y}_u^{\mu_2} \tilde{X}_r^{\nu_1} \\
\bar{U}_{\mu_1\mu_2\nu_1,q}^{\text{sc}(2)} &= \frac{1}{\sqrt{2}} \sum_{svw} \tilde{\Xi}_{sv,qw} \bar{Y}_s^{\mu_1} \bar{Y}_v^{\mu_2} \bar{X}_w^{\nu_1} \\
\bar{V}_{p,\nu_1\nu_2\mu_1}^{\text{sc}(2)} &= \frac{1}{\sqrt{2}} \sum_{rtu} \tilde{\Xi}_{pr,tu} \bar{X}_t^{\nu_1} \bar{X}_u^{\nu_2} \bar{Y}_r^{\mu_1} \\
\tilde{V}_{\nu_1\nu_2\mu_1,q}^{\text{sc}(2)} &= \frac{1}{\sqrt{2}} \sum_{svw} \tilde{\Xi}_{sv,qw} \tilde{X}_s^{\nu_1} \tilde{X}_v^{\nu_2} \tilde{Y}_w^{\mu_1} .
\end{aligned} \tag{169}$$

The interaction matrices become  $\bar{\mathbf{K}}_{\mu_1\mu_2\nu_1,\mu_3\mu_4\nu_2}^> = (\varepsilon_{\mu_1}^{N+1} + \varepsilon_{\mu_2}^{N+1} - \varepsilon_{\nu_1}^{N-1})\delta_{\mu_1\mu_3}\delta_{\mu_2\mu_4}\delta_{\nu_1\nu_2}$  and  $\bar{\mathbf{K}}_{\nu_1\nu_2\mu_1,\nu_3\nu_4\mu_2}^< = (\varepsilon_{\nu_1}^{N-1} + \varepsilon_{\nu_2}^{N-1} - \varepsilon_{\mu_1}^{N+1})\delta_{\nu_1\nu_3}\delta_{\nu_2\nu_4}\delta_{\mu_1\mu_2}$ . Within this approximation, the resulting coupled-cluster Dyson supermatrix is given by

$$\tilde{\mathbf{D}}^{\text{CCsc}(2)} = \begin{pmatrix} f_{pq} + \tilde{\Sigma}_{pq}^{\infty\text{CCSD}} & \tilde{U}_{p,\mu_1\mu_2\nu_1}^{\text{sc}(2)} & \bar{V}_{p,\nu_1\nu_2\mu_1}^{\text{sc}(2)} \\ \bar{U}_{\mu_1\mu_2\nu_1,q}^{\text{sc}(2)} & \bar{\mathbf{K}}_{\mu_1\mu_2\nu_1,\mu_3\mu_4\nu_2}^> & 0 \\ \tilde{V}_{\nu_1\nu_2\mu_1,q}^{\text{sc}(2)} & 0 & \bar{\mathbf{K}}_{\nu_1\nu_2\mu_1,\nu_3\nu_4\mu_2}^< \end{pmatrix}. \tag{170}$$

The static contribution,  $\tilde{\Sigma}_{pq}^{\infty\text{CCSD}}$ , is taken within the CCSD approximation to be consistent with the treatment of 2p1h/2h1p excitations contained in the second-order self-energy:

$$\tilde{\Sigma}_{pq}^{\infty\text{CCSD}} = \tilde{\Sigma}_{pq}^{\infty(0)} + \sum_{ia} \lambda_a^i \chi_{pa,qi} + \frac{1}{(2!)^2} \sum_{ijab} \lambda_{ab}^{ij} \chi_{pab,qij} . \tag{171}$$

The solution of Eq. 170 requires iterative diagonalization, whereby the coupling and interaction matrices are updated at each step. The zeroth-order iteration is taken as the second-order perturbative supermatrix defined in Eq. 168 and the resulting eigenvectors and eigenvalues are subsequently fed into the definition of the coupling and interaction matrices. This process is repeated until convergence of the spectrum of  $\tilde{\mathbf{D}}^{\text{CCsc}(2)}$  is achieved.

## B. Coupled-cluster self-energy approximations including the complete set of 2p1h/2h1p interactions

Both the perturbative and second-order coupled-cluster self-energies contain interactions between ISC that are fundamentally of 2p1h/2h1p excitation character. Therefore,

at second-order, the coupled-cluster self-energy is fundamentally restricted to the space of 2p1h/2h1p excitations and we can include the complete set of interactions by defining the interaction matrices [24]

$$\begin{aligned}\bar{\mathbf{K}}_{iab,jcd}^{>,2p1h(0)} + \bar{\mathbf{C}}_{iab,jcd}^{>,2p1h(0)} &= \langle \Phi_i^{ab} | \bar{H}_N | \Phi_j^{cd} \rangle \\ \bar{\mathbf{K}}_{ija,klb}^{<,2h1p(0)} + \bar{\mathbf{C}}_{ija,klb}^{<,2h1p(0)} &= - \langle \Phi_{kl}^b | \bar{H}_N | \Phi_{ij}^a \rangle .\end{aligned}\quad (172)$$

This approximation corresponds to allowing all particles to propagate independently, and to interact pairwise via the static component of the perturbative CC-BSE kernel and via the combined three-body interaction of the similarity transformed Hamiltonian [24]. This results in the 2p1h(0) coupled-cluster self-energy approximation

$$\begin{aligned}\tilde{\Sigma}_{pq}^{2p1h(0)}(\omega) &= \tilde{\Sigma}_{pq}^{\infty(0)} + \tilde{\Sigma}_{pq}^{\infty(2)} \\ &+ \frac{1}{(2!)^2} \sum_{\substack{kla \\ mnb}} \chi_{pa,kl} [(\omega - i\eta) \mathbb{1} - (\bar{\mathbf{K}}_{kla,mnb}^{<,2h1p(0)} + \bar{\mathbf{C}}_{kla,mnb}^{<,2h1p(0)})]^{-1} \chi_{mn,qb} \\ &+ \frac{1}{(2!)^2} \sum_{\substack{iab \\ jcd}} \chi_{pi,ab} [(\omega + i\eta) \mathbb{1} - (\bar{\mathbf{K}}_{iab,jcd}^{>,2p1h(0)} + \bar{\mathbf{C}}_{iab,jcd}^{>,2p1h(0)})]^{-1} \chi_{cd,qj} .\end{aligned}\quad (173)$$

Hence, we have the unfolded CC Dyson supermatrix structure as

$$\bar{\mathbf{D}}^{\text{CC},2p1h(0)} = \begin{pmatrix} f_{pq} + \tilde{\Sigma}_{pq}^{\infty(0)} + \tilde{\Sigma}_{pq}^{\infty(2)} & \frac{1}{\sqrt{2}} \tilde{U}_{p,abi}^{(0)} & \frac{1}{\sqrt{2}} \tilde{V}_{p,ija}^{(0)} \\ \frac{1}{\sqrt{2}} \tilde{U}_{cdj,q}^{(0)} & \bar{\mathbf{K}}_{iab,jcd}^{>,2p1h(0)} + \bar{\mathbf{C}}_{iab,jcd}^{>,2p1h(0)} & 0 \\ \frac{1}{\sqrt{2}} \tilde{V}_{klb,q}^{(0)} & 0 & \bar{\mathbf{K}}_{ija,klb}^{<,2h1p(0)} + \bar{\mathbf{C}}_{ija,klb}^{<,2h1p(0)} \end{pmatrix} .\quad (174)$$

This matrix is very closely related to IP/EA-EOM-CC theory truncated to the space of 2p1h/2h1p excitations, but is the supermatrix is defined over the complete spin-orbital space [24].

Similarly, we further generalize the second-order coupled-cluster self-energy approximation by allowing the interaction matrices to be composed of the full effective interactions arising when normal-ordering  $\bar{H}$  with respect to the biorthogonal ground state expectation value as [24, 53]

$$\begin{aligned}\bar{\mathbf{K}}_{iab,jcd}^{>,2p1h} + \bar{\mathbf{C}}_{iab,jcd}^{>,2p1h} &= \tilde{F}_{ac} \delta_{ij} \delta_{bd} - \tilde{F}_{ad} \delta_{ij} \delta_{bc} + \tilde{F}_{bd} \delta_{ac} \delta_{ij} - \tilde{F}_{bc} \delta_{ad} \delta_{ij} - \tilde{F}_{ji} \delta_{ac} \delta_{bd} + \tilde{F}_{ji} \delta_{ad} \delta_{bc} \\ &+ \tilde{\Xi}_{ja,ci} \delta_{bd} + \tilde{\Xi}_{jb,di} \delta_{ac} + \tilde{\Xi}_{ab,cd} \delta_{ij} - \tilde{\Xi}_{ja,di} \delta_{bc} - \tilde{\Xi}_{jb,ci} \delta_{ad} + \tilde{\chi}_{jab,cid}\end{aligned}\quad (175a)$$

$$\begin{aligned}
(\bar{\mathbf{K}}_{ija,klb}^{<,2h1p} + \bar{\mathbf{C}}_{ija,klb}^{<,2h1p}) &= \tilde{F}_{ik}\delta_{ab}\delta_{jl} - \tilde{F}_{il}\delta_{ab}\delta_{jk} + \tilde{F}_{jl}\delta_{ab}\delta_{ik} - \tilde{F}_{jk}\delta_{ab}\delta_{il} + \tilde{F}_{ba}\delta_{il}\delta_{jk} - \tilde{F}_{ba}\delta_{ik}\delta_{jl} \\
&+ \tilde{\Xi}_{ib,al}\delta_{jk} + \tilde{\Xi}_{jb,ak}\delta_{il} - \tilde{\Xi}_{ij,kl}\delta_{ab} - \tilde{\Xi}_{ib,ak}\delta_{jl} - \tilde{\Xi}_{jb,al}\delta_{ik} + \tilde{\chi}_{ijb,kal} .
\end{aligned} \tag{175b}$$

The CC Dyson supermatrix within this approximation is given by [24]

$$\tilde{\mathbf{D}}^{\text{CC},2p1h} = \begin{pmatrix} f_{pq} + \tilde{\Sigma}_{pq}^{\infty\text{CCSD}} & \tilde{\Xi}_{pi,ab} & \tilde{\Xi}_{pa,ij} \\ \tilde{\Xi}_{cd,qj} & \bar{\mathbf{K}}_{iab,jcd}^{>,2p1h} + \bar{\mathbf{C}}_{iab,jcd}^{>,2p1h} & 0 \\ \tilde{\Xi}_{kl,qb} & 0 & \bar{\mathbf{K}}_{ija,klb}^{<,2h1p} + \bar{\mathbf{C}}_{ija,klb}^{<,2h1p} \end{pmatrix}. \tag{176}$$

The coupled-cluster Dyson supermatrix approximations, defined in Eqs. 174 and 176, circumvent the need to perform self-consistent calculations as the interaction matrices correspond to a specific time-ordered 2p1h/2h1p Green's function [53, 54] (an example of which is defined in Eq. 146). However, the self-consistent expansion of the coupled-cluster self-energy is required to correctly define the BSE kernel.

### XIII. RELATIONSHIP TO IP/EA-EOM-CC AND $G_0W_0$ APPROXIMATIONS

In this section, we provide an overview of the connections between approximations for the coupled-cluster self-energy, IP/EA-EOM-CC and  $G_0W_0$  theory. Subsequently, we arrive at CC- $G_0W_0$  theory given by Eq. 198.

#### A. Equation-of-motion coupled-cluster theory

The IP-EOM-CC method was presented in Section VI. The electron removal energies are obtained from the IP-EOM-CC eigenvalue problem given in Eq. 90. Restricting the IP-EOM-CC supermatrix to contain only 2h1p interactions gives the IP-EOM-CCSD approximation:

$$\bar{\mathbf{H}}^{\text{IP-EOM-CCSD}} = - \begin{pmatrix} \langle \Phi_i | \bar{H}_N | \Phi_j \rangle & \langle \Phi_i | \bar{H}_N | \Phi_{kl}^a \rangle \\ \langle \Phi_{mn}^b | \bar{H}_N | \Phi_j \rangle & \langle \Phi_{mn}^b | \bar{H}_N | \Phi_{kl}^a \rangle \end{pmatrix}. \tag{177}$$

By identifying that the upper left block is  $-\langle \Phi_i | \bar{H}_N | \Phi_j \rangle = f_{ji} + \tilde{\Sigma}_{ji}^{\infty(0)}$ , that in the Brueckner basis,  $\langle \Phi_i | \bar{H}_N | \Phi_{kl}^a \rangle = \chi_{kl,ia}$  and  $\langle \Phi_{mn}^b | \bar{H}_N | \Phi_j \rangle = \chi_{jb,mn}$ , we re-write the IP-EOM-CCSD

supermatrix as

$$\bar{\mathbf{H}}^{\text{IP-EOM-CCSD}} = \begin{pmatrix} f_{ji} + \tilde{\Sigma}_{ji}^{\infty(0)} & -\chi_{kl,ia} \\ -\chi_{jb,mn} & \bar{\mathbf{K}}_{kla,mnb}^{<,2h1p(0)} + \bar{\mathbf{C}}_{kla,mnb}^{<,2h1p(0)} \end{pmatrix}, \quad (178)$$

where we have used Eq. 172 to identify the interaction matrices as the lower right block of the IP-EOM-CCSD supermatrix. Downfolding this supermatrix into the single-particle occupied-occupied subspace, we have [24]

$$\bar{H}_{ij}^{\text{EOM-CCSD}}(\omega) = f_{ji} + \tilde{\Sigma}_{ji}^{\infty(0)} + \frac{1}{4} \sum_{\substack{kla \\ mnb}} \chi_{ja,kl} (\omega \mathbb{1} - (\bar{\mathbf{K}}^{<,2h1p(0)} + \bar{\mathbf{C}}^{<,2h1p(0)}))_{kla,mnb}^{-1} \chi_{mn,ib}. \quad (179)$$

Transposing Eq. 179, we identify the effective EOM-CCSD ‘non-Dyson self-energy’ as:

$$\begin{aligned} \bar{\Sigma}_{ij}^{\text{EOM-CCSD}}(\omega) &= \bar{H}_{ji}^{\text{EOM-CCSD}}(\omega) - f_{ij} \\ &= \tilde{\Sigma}_{ij}^{\infty(0)} + \frac{1}{4} \sum_{\substack{kla \\ mnb}} \chi_{ia,kl} (\omega \mathbb{1} - (\bar{\mathbf{K}}^{<,2h1p(0)} + \bar{\mathbf{C}}^{<,2h1p(0)}))_{kla,mnb}^{-1} \chi_{mn,jb}. \end{aligned} \quad (180)$$

By comparison with Eq. 173, we see that the IP-EOM-CCSD effective self-energy is simply the transpose of the 2p1h(0) coupled-cluster self-energy restricted to the occupied-occupied block, as first demonstrated in Ref. [24]. However, the contribution  $\tilde{\Sigma}_{ij}^{\infty(2)}$  does not appear in IP-EOM-CCSD theory. It arises from the correct treatment of the static component in the perturbative expansion of the coupled-cluster self-energy.

## B. The $G_0W_0$ self-energy and CC- $G_0W_0$ theory

The dynamical  $G_0W_0$  self-energy is given by [4, 26, 55, 56]

$$\Sigma_{pq}^{G_0W_0}(\omega) = \sum_{av} \frac{W_{p,av} W_{av,q}}{\omega - \Omega_\nu - \epsilon_a + i\eta} + \sum_{iv} \frac{W_{p,iv} W_{iv,q}}{\omega + \Omega_\nu - \epsilon_i - i\eta}, \quad (181)$$

where the coupling and interaction matrix elements  $W_{p,q\nu}$  and  $\Omega_\nu$  are usually found by solution of the RPA equations

$$\begin{pmatrix} \mathbf{A} & \mathbf{B} \\ -\mathbf{B}^* & -\mathbf{A}^* \end{pmatrix} \begin{pmatrix} \mathbf{X} \\ \mathbf{Y} \end{pmatrix} = \mathbf{\Omega} \begin{pmatrix} \mathbf{X} \\ \mathbf{Y} \end{pmatrix} \quad (182)$$

where

$$A_{ia,jb} = (\epsilon_a - \epsilon_i) \delta_{ab} \delta_{ij} + \langle ia || bj \rangle \quad (183a)$$

$$B_{ia,jb} = \langle ij||ab \rangle . \quad (183b)$$

$$W_{p,q\nu} = \sum_{ia} \left( \langle pa||qi \rangle X_{ia}^\nu + \langle pi||qa \rangle Y_{ia}^\nu \right) . \quad (183c)$$

In the  $G_0W_0$  approximation, the exchange interaction is separated from the direct interaction and one is left with only the direct RPA (dRPA) equations. Here, we instead choose to work with the antisymmetrized RPA equations to more easily exploit the connections to coupled-cluster theory. The exchange contributions may be trivially removed from our equations to recover the  $G_0W_0$  approximation using dRPA. If the Tamm-Dancoff approximation (TDA) is made for the RPA equations whereby the  $\mathbf{B}$  coupling block of Eq. 182 is neglected, the coupling elements become

$$W_{p,q\nu}^{\text{TDA}} = \sum_{ia} \langle pa||qi \rangle X_{ia}^\nu . \quad (184)$$

Conventionally, the RPA equations are formulated employing real spin-orbitals, which we shall also assume here [26, 28]. In terms of the unfolded Dyson supermatrix representation, the  $G_0W_0$  quasiparticle equation takes the form

$$\mathbf{D}^{G_0W_0} = \begin{pmatrix} f_{pq} & W_{p,av} & W_{p,iv} \\ W_{av,q} & \Lambda_{av,b\nu'}^{G_0W_0>} & 0 \\ W_{iv,q} & 0 & \Lambda_{iv,j\nu'}^{G_0W_0<} \end{pmatrix} \quad (185)$$

with

$$\begin{aligned} \Lambda_{av,b\nu'}^{G_0W_0>} &= (\epsilon_a + \Omega_\nu) \delta_{ab} \delta_{\nu\nu'} \\ \Lambda_{iv,j\nu'}^{G_0W_0<} &= (\epsilon_i - \Omega_\nu) \delta_{ij} \delta_{\nu\nu'} . \end{aligned} \quad (186)$$

where the index  $\nu$  is a quasi-boson index that spans a set of values much larger than the spin-orbital index. The RPA eigenvalue problem can be re-written in terms of effective coupled-cluster doubles amplitudes by identifying  $\mathbf{T} = \mathbf{YX}^{-1}$ . Using this expression in the RPA equations (Eq. 182) leads to the ring CCD (rCCD) approximation [24, 38, 57]

$$\mathbf{B}^* + \mathbf{A}^* \mathbf{T} + \mathbf{TA} + \mathbf{TBT} = \mathbf{0} , \quad (187)$$

with the RPA Hamiltonian written as

$$H_{ia,jb}^{\text{RPA}} = (\epsilon_a - \epsilon_i) \delta_{ab} \delta_{ij} + \langle ia||bj \rangle + \sum_{kc} \langle ik||bc \rangle (t_{jk}^{ca})_{\text{rCCD}} . \quad (188)$$

As a result, the RPA eigenvalue problem becomes

$$\sum_{jb} H_{ia,jb}^{\text{RPA}} X_{jb}^{\nu} = \Omega_{\nu} X_{ia}^{\nu} . \quad (189)$$

where the rCCD doubles amplitudes do not retain fermionic anti-symmetry [38].

To demonstrate the connection between the  $G_0W_0$  approximation and the coupled-cluster self-energy, we restrict our analysis of the coupled-cluster self-energy to the space of 2h1p/2p1h excitations. In doing so, we introduce the CC- $G_0W_0$  Dyson supermatrix as

$$\tilde{\mathbf{D}}^{\text{CC-}G_0W_0} = \begin{pmatrix} f_{pq} + \tilde{\Sigma}_{pq}^{\infty\text{rCCD}} & \chi_{pi,ab}^{\text{rCCD}} & \chi_{pa,ij}^{\text{rCCD}} \\ \chi_{ab,qi}^{\text{rCCD}} & \bar{\Lambda}_{iab,jcd}^{G_0W_0>} & 0 \\ \chi_{ij,qa}^{\text{rCCD}} & 0 & \bar{\Lambda}_{ija,klb}^{G_0W_0<} \end{pmatrix} \quad (190)$$

where the effective interactions  $\{\chi_{pq,rs}^{\text{rCCD}}\}$  are found from the two-body matrix elements of  $\bar{H}$ , but are formed from only the rCCD diagrams and amplitudes. For example, the element  $\chi_{ia,kl}^{\text{rCCD}}$  is given by

$$\chi_{ia,kl}^{\text{rCCD}} = \langle ia || kl \rangle + \sum_{cm} \langle im || kc \rangle (t_{ml}^{ca})_{\text{rCCD}} . \quad (191)$$

The interaction matrices are defined as

$$\bar{\Lambda}_{iab,jcd}^{G_0W_0>} = (\epsilon_a \delta_{bd} \delta_{ij} + H_{ib,jd}^{\text{RPA}}) \delta_{ac} \quad (192a)$$

$$\bar{\Lambda}_{ija,klb}^{G_0W_0<} = (\epsilon_i \delta_{jl} \delta_{ab} - H_{ja,lb}^{\text{RPA}}) \delta_{ik} . \quad (192b)$$

The static contribution,  $\tilde{\Sigma}_{pq}^{\infty\text{rCCD}}$ , can be evaluated exactly within the rCCD approximation and is given by

$$\tilde{\Sigma}_{pq}^{\infty\text{rCCD}} = \tilde{\Sigma}_{pq}^{\infty(0)\text{rCCD}} + \frac{1}{(2!)^2} \sum_{ijab} \chi_{pab,qij}^{\text{rCCD}} (\lambda_{ab}^{ij})_{\text{rCCD}} , \quad (193)$$

where  $(\lambda_{ab}^{ij})_{\text{rCCD}}$  are the rCCD de-excitation amplitudes obtained from the rCCD Lagrangian [27]. There are no singles amplitudes in the coupled-cluster doubles approximation. The three-body interaction elements can be found in Ref. [14], an example of which is the element

$$\chi_{iab,jkl}^{\text{rCCD}} = \sum_n \chi_{in,jk}^{\text{rCCD}} (t_{nl}^{ab})_{\text{rCCD}} + \sum_c \chi_{ia,ck}^{\text{rCCD}} (t_{jl}^{cb})_{\text{rCCD}} . \quad (194)$$

The resolvents of the interaction matrices in CC- $G_0W_0$  theory are given by

$$[(\omega - i\eta)\mathbb{1} - \bar{\Lambda}^{G_0W_0<}]_{kla,mnb}^{-1} = \sum_{\nu} \frac{X_{la}^{\nu} X_{nb}^{\nu*} \delta_{km}}{\omega - \epsilon_k + \Omega_{\nu} - i\eta} \quad (195)$$

and

$$[(\omega + i\eta)\mathbb{1} - \bar{\Lambda}^{G_0W_0>}]_{iab,jcd}^{-1} = \sum_{\nu} \frac{X_{ib}^{\nu} X_{jd}^{\nu*} \delta_{ac}}{\omega - \epsilon_a - \Omega_{\nu} + i\eta}. \quad (196)$$

By defining

$$\begin{aligned} \bar{W}_{p,q\nu} &= \sum_{ia} \chi_{pa,qi}^{\text{rCCD}} X_{ia}^{\nu} \\ \bar{W}_{q\nu,p} &= \sum_{ia} \chi_{qi,pa}^{\text{rCCD}} X_{ia}^{\nu*} \\ \tilde{W}_{p,q\nu} &= \sum_{ia} \chi_{pi,qa}^{\text{rCCD}} X_{ia}^{\nu} \\ \tilde{W}_{q\nu,p} &= \sum_{ia} \chi_{qa,pi}^{\text{rCCD}} X_{ia}^{\nu*}, \end{aligned} \quad (197)$$

we re-write the CC- $G_0W_0$  approximation as

$$\tilde{\Sigma}_{pq}^{\text{CC-}G_0W_0}(\omega) = \tilde{\Sigma}_{pq}^{\infty\text{rCCD}} + \sum_{a\nu} \frac{\tilde{W}_{p,a\nu} \tilde{W}_{a\nu,q}}{\omega - \epsilon_a - \Omega_{\nu} + i\eta} + \sum_{k\nu} \frac{\bar{W}_{p,k\nu} \bar{W}_{k\nu,q}}{\omega - \epsilon_k + \Omega_{\nu} - i\eta}. \quad (198)$$

From the rCCD amplitude equations, we identify the screened interaction appearing in the  $G_0W_0$  self-energy (Eq. 181) as follows

$$\begin{aligned} \bar{W}_{i,k\nu} &= \sum_{la} \chi_{ia,kl}^{\text{rCCD}} X_{la}^{\nu} \\ &= \sum_{la} \langle ia||kl \rangle X_{la}^{\nu} + \sum_{cm,la} \langle im||kc \rangle (t_{ml}^{ca})_{\text{rCCD}} X_{la}^{\nu}. \end{aligned} \quad (199)$$

Using the rCCD equations for the amplitudes:  $(t_{ml}^{ca})_{\text{rCCD}} = \sum_{\nu'} Y_{mc}^{\nu'} (X^{-1})_{la}^{\nu'}$ , yields

$$\bar{W}_{i,k\nu} = \sum_{la} \left( \langle ia||kl \rangle X_{la}^{\nu} + \langle il||ka \rangle Y_{la}^{\nu} \right) = W_{i,k\nu}, \quad (200)$$

which is exactly the expression for the screened interaction of Eq. 183c. The second coupling term is actually composed from TDA RPA screening alone as

$$\begin{aligned} \bar{W}_{k\nu,j} &= \sum_{nb} \chi_{kn,jb}^{\text{rCCD}} X_{nb}^{\nu*} = \sum_{nb} \langle kn||jb \rangle X_{nb}^{\nu*} \\ &= \left( \sum_{nb} \langle jb||kn \rangle X_{nb}^{\nu} \right)^* \\ &= W_{j,k\nu}^{\text{TDA}*} \end{aligned} \quad (201)$$

from Eq. 184. The absence of the full RPA screening in the dynamical contribution of the CC- $G_0W_0$  self-energy is a result of the rCCD amplitude equations. Combining both results together, we have

$$\begin{aligned}\tilde{\Sigma}_{ij}^{\text{CC-}G_0W_0}(\omega) &= \frac{1}{2} \sum_{kab} \langle ik || ab \rangle (t_{jk}^{ab})_{\text{rCCD}} + \frac{1}{(2!)^2} \sum_{ijab} \chi_{iab,jkl}^{\text{rCCD}} (\lambda_{ab}^{kl})_{\text{rCCD}} \\ &+ \sum_{k\nu} \frac{W_{i,k\nu} W_{j,k\nu}^{*\text{TDA}}}{\omega - \epsilon_k + \Omega_\nu - i\eta},\end{aligned}\quad (202)$$

as  $\tilde{W}_{a\nu,j} = 0$  vanishes due to the rCCD amplitude equations. This expression shares some similarities with the approximate analysis presented in Ref. [28] on comparing the IP-EOM-CCSD and  $G_0W_0$  approximations. The appearance of the static term in CC- $G_0W_0$  is necessary in order to fully account for the negation of the full RPA screening in the TDA screened interaction,  $W_{j,k\nu}^{*\text{TDA}}$ .

For the virtual-virtual block, we have

$$\begin{aligned}\tilde{\Sigma}_{ab}^{\text{CC-}G_0W_0}(\omega) &= -\frac{1}{2} \sum_{ijc} \langle ij || bc \rangle (t_{ij}^{ac})_{\text{rCCD}} + \frac{1}{(2!)^2} \sum_{klcd} \chi_{acd,bkl}^{\text{rCCD}} (\lambda_{cd}^{kl})_{\text{rCCD}} \\ &+ \sum_{c\nu} \frac{W_{a,c\nu}^{\text{TDA}} W_{b,c\nu}^*}{\omega - \epsilon_a - \Omega_\nu + i\eta}.\end{aligned}\quad (203)$$

The occupied-virtual block contains the combination of both time-orderings with the second-order static contribution as

$$\begin{aligned}\tilde{\Sigma}_{ia}^{\text{CC-}G_0W_0}(\omega) &= \frac{1}{(2!)^2} \sum_{klcd} \chi_{icd,akl}^{\text{rCCD}} (\lambda_{cd}^{kl})_{\text{rCCD}} + \sum_{c\nu} \frac{W_{i,c\nu}^{\text{TDA}} W_{a,c\nu}^*}{\omega - \Omega_\nu - \epsilon_c + i\eta} \\ &+ \sum_{k\nu} \frac{W_{i,k\nu} W_{a,k\nu}^{*\text{TDA}}}{\omega + \Omega_\nu - \epsilon_k - i\eta},\end{aligned}\quad (204)$$

with  $\tilde{\Sigma}_{ai}^{\text{CC-}G_0W_0} = 0$  as required by the coupled-cluster similarity transformation. Finally, from Eq. 152, the ground state correlation energy in CC- $G_0W_0$  theory is the RPA correlation energy [24, 38]

$$E_c^{\text{CC-}G_0W_0} = \frac{1}{2} \sum_i \tilde{\Sigma}_{ii}^{\infty\text{rCCD}} = \frac{1}{4} \sum_{ij,ab} \langle ij || ab \rangle (t_{ij}^{ab})_{\text{rCCD}}. \quad (205)$$

Through this reformulation of the  $G_0W_0$  approximation in the framework of coupled-cluster theory, we may now include ‘vertex’ corrections that go beyond the  $G_0W_0$  approximation, whilst maintaining the correct spectral form of the self-energy. This is achieved by simply

modifying the doubles excitation and de-excitation amplitudes that enter the approximation. For example, using Eq. 190, one may use the full CCSD singles and doubles excitation and de-excitation amplitudes instead of the rCCD amplitudes as a simple way to extend the  $G_0W_0$  approximation to include effects of singles excitations and go beyond RPA screening by including the complete set of interactions,  $\langle \Phi_j^a | \bar{H}_N | \Phi_i^b \rangle$ , between singly excited configurations in the definition of the interaction matrices defined in  $\bar{\Lambda}_{iab,jcd}^{G_0W_0>} / \bar{\Lambda}_{ija,klb}^{G_0W_0<}$  [24].

#### XIV. THE COUPLED-CLUSTER BETHE-SALPETER EQUATION

Within the Green's function formalism, the Bethe-Salpeter equation describes two-particle correlation processes and gives access to neutral and two-particle excitation energies. The coupled-cluster Bethe-Salpeter equation is written as

$$\begin{aligned} \tilde{L}_{pq,rs}(t_1, t_2; t_3, t_4) &= \tilde{L}_{pq,rs}^0(t_1, t_2; t_3, t_4) \\ &+ \sum_{tuvw} \int dt dt' dt'' dt''' \tilde{L}_{pt,ru}^0(t_1, t; t_3, t') \tilde{\Xi}_{uv,tw}(t', t''; t, t''') \tilde{L}_{wq,vs}(t''', t_2; t'', t_4) \end{aligned} \quad (206)$$

where  $\tilde{L}_{pq,rs}^0(t_1, t_2; t_3, t_4) = -i\tilde{G}_{ps}(t_1, t_4)\tilde{G}_{qr}(t_2, t_3)$  corresponds to the propagation of two-independent particles [3]. The correlated four-point linear response function  $\tilde{L}$  is expressed as the functional derivative of the single-particle Green's function with respect to a fictitious external potential,  $U$ , via Schwinger's functional derivative technique (see Appendix E)

$$\begin{aligned} \tilde{L}_{pq,rs}(t_1, t_2; t_3, t_4) &= -i \left. \frac{\delta \tilde{G}_{pr}(t_1, t_3)}{\delta U_{sq}(t_4, t_2)} \right|_{U=0} \\ &= \tilde{G}_{pq,rs}^{4pt}(t_1, t_2; t_3, t_4) - i\tilde{G}_{pr}(t_1, t_3)\tilde{G}_{qs}(t_2, t_4) . \end{aligned} \quad (207)$$

It is important to note that the coupled-cluster Bethe-Salpeter equation is not an equation for the coupled-cluster representation of the electronic 4-point electronic response function, defined as

$$\bar{L}_{pq,rs}(t_1, t_2; t_3, t_4) = \bar{G}_{pq,rs}^{4pt}(t_1, t_2; t_3, t_4) - i\bar{G}_{pr}(t_1, t_3)\bar{G}_{qs}(t_2, t_4)$$

where

$$i\bar{G}_{pq,rs}^{4pt}(t_1, t_2; t_3, t_4) = \langle \tilde{\Psi}_0 | \mathcal{T} \{ \bar{a}_q(t_2) \bar{a}_p(t_1) \bar{a}_r^\dagger(t_3) \bar{a}_s^\dagger(t_4) \} | \Phi_0 \rangle$$

is the coupled-cluster representation of the electronic 4-point Green's function. This is because the coupled-cluster representation of the electronic 4-point electronic response function can only be obtained by direct computation using quantities obtained from ground state and EE-EOM-CC theory, which remains largely unexplored. Instead, the coupled-cluster BSE naturally arises as a result of the coupling between the SP-CCGF and the four-point response function through the coupled-cluster self-energy.

In the real time-domain, the kernel of the Bethe-Salpeter kernel is given by the functional derivative of the self-energy with respect to the Green's function as

$$\tilde{\Xi}_{pq,rs}(t_1, t_2; t_3, t_4) = i \frac{\delta \tilde{\Sigma}_{pr}(t_1, t_3)}{\delta \tilde{G}_{sq}(t_4, t_2)}. \quad (208)$$

The kernel is composed of two-particle irreducible (2PI) diagrams [3]. The BSE is fundamentally different from the corresponding Dyson equation for the single-particle Green's function because it cannot be cast in a closed form equation for the ph/hp response function. The ph/hp response function is defined as [37]

$$\tilde{L}_{pq,rs}^{\text{ph}}(t_1, t_2) = \tilde{L}_{pq,rs}(t_1, t_2; t_1^+, t_2^+). \quad (209)$$

Now, restricting the BSE to that of the ph/hp sector, we have

$$\begin{aligned} \tilde{L}_{pq,rs}^{\text{ph}}(t_1, t_2) &= \tilde{L}_{pq,rs}^{\text{ph}(0)}(t_1, t_2) \\ &+ \sum_{tuvw} \int dt dt' dt'' dt''' \tilde{L}_{pt,ru}^0(t_1, t; t_1^+, t') \tilde{\Xi}_{uv,tw}(t', t''; t, t''') \tilde{L}_{wq,vs}(t''', t_2; t'', t_2^+). \end{aligned} \quad (210)$$

It is the presence of the kernel,  $\tilde{\Xi}$ , that means we cannot send the time arguments in the propagators to the corresponding ones for the ph/hp propagator [58–63]. Therefore, we do not have a closed equation for the ph/hp response function as Eq. 210 is not a functional of  $\tilde{L}^{\text{ph}}$ . This is because the BSE contains a fundamental coupling between the particle-hole, particle-particle and hole-hole response functions via the kernel.

### A. Relationship between the BSE kernel and the 4-point vertex function

The BSE kernel  $\tilde{\Xi}$ , and the 4-point vertex function  $\tilde{\Lambda}^{4\text{pt}}$ , are closely related. From Eq. 134 for the 4-point vertex function, in the real-time domain, we have

$$\begin{aligned} \tilde{G}_{pq,rs}^{4\text{pt}}(t_1, t_2; t_3, t_4) &= i\tilde{G}_{pr}(t_1, t_3)\tilde{G}_{qs}(t_2, t_4) - i\tilde{G}_{ps}(t_1, t_4)\tilde{G}_{qr}(t_2, t_3) \\ &- \sum_{tuvw} \int dt dt' dt'' dt''' \tilde{G}_{pt}(t_1, t') \tilde{G}_{qu}(t_2, t'') \tilde{\Lambda}_{tu,vw}^{4\text{pt}}(t', t''; t, t''') \tilde{G}_{vr}(t, t_3) \tilde{G}_{ws}(t''', t_4). \end{aligned} \quad (211)$$

This equation can be rewritten using the definition of the 4-point response function  $\tilde{L}$  and its non-interacting counterpart  $\tilde{L}_0$ , as

$$\begin{aligned} \tilde{L}_{pq,rs}(t_1, t_2; t_3, t_4) &= \tilde{L}_{pq,rs}^0(t_1, t_2; t_3, t_4) \\ &+ \sum_{tuvw} \int dt dt' dt'' dt''' \tilde{L}_{pv,rt}^0(t_1, t; t_3, t') \tilde{\Lambda}_{tu,vw}^{4\text{pt}}(t', t''; t, t''') \tilde{L}_{wq,us}^0(t''', t_2; t'', t_4). \end{aligned} \quad (212)$$

Comparison of Eq. 212 with Eq. 206, we see that the 4-point vertex function is the reducible BSE kernel. With this identification, we can immediately write the relationship between the BSE kernel and 4-point vertex as

$$\begin{aligned} \tilde{\Lambda}_{pq,rs}^{4\text{pt}}(t_1, t_2; t_3, t_4) &= \tilde{\Xi}_{pq,rs}(t_1, t_2; t_3, t_4) \\ &+ \sum_{tuvw} \int dt dt' dt'' dt''' \tilde{\Xi}_{pv,rt}(t_1, t; t_3, t') \tilde{L}_{tu,vw}^0(t', t''; t, t''') \tilde{\Lambda}_{wq,us}^{4\text{pt}}(t''', t_2; t'', t_4). \end{aligned} \quad (213)$$

Using this relationship, we have

$$\begin{aligned} \tilde{L} &= \tilde{L}_0 + \tilde{L}_0 \tilde{\Lambda}^{4\text{pt}} \tilde{L}_0 \\ &= \tilde{L}_0 + \tilde{L}_0 (\tilde{\Xi} + \tilde{\Xi} \tilde{L}_0 \tilde{\Lambda}^{4\text{pt}}) \tilde{L}_0 \\ &= \tilde{L}_0 + \tilde{L}_0 \tilde{\Xi} (\tilde{L}_0 + \tilde{L}_0 \tilde{\Lambda}^{4\text{pt}} \tilde{L}_0) \\ &= \tilde{L}_0 + \tilde{L}_0 \tilde{\Xi} \tilde{L} \end{aligned} \quad (214)$$

which is the Bethe-Salpeter equation (Eq. 206). Since the 4-point vertex is the reducible kernel of the BSE, it consists of 1PI diagrams and hence appears in the self-consistent expansion for the self-energy. As a result, the 4-point vertex can be viewed as the functional derivative of  $\tilde{\Sigma}$  with respect to  $\tilde{G}$ :  $\tilde{\Lambda}^{4\text{pt}} \sim i \frac{\delta \tilde{\Sigma}}{\delta \tilde{G}}$ . The irreducible BSE kernel  $\tilde{\Xi}$ , consists only of 2PI diagrams as the BSE performs the geometric series summation of these terms.

## B. The coupled-cluster Bethe-Salpeter kernel

By taking the functional derivative of the coupled-cluster self-energy defined in Eq. 138 with respect to the coupled-cluster Green's function we generate the coupled-cluster BSE kernel. Diagrammatically, this functional derivative is found by cutting the Green's function and interaction lines in the Feynman series for the renormalized coupled-cluster self-energy. To do so, we first analyze the variation of the interaction lines with respect to the Green's function. In the real-time domain, the static component of the self-energy is given by

$$\begin{aligned}\tilde{\Sigma}_{pq}^{\infty}(t_1, t_3) &= \tilde{\Sigma}_{pq}^{\infty} \delta(t_1, t_3) \\ &= \left( \bar{h}_{pq} - i \sum_{rs} \bar{h}_{pr,qs} \tilde{G}_{sr}(t_1 - t_1^+) + \frac{i}{4} \sum_{rs,tu} \bar{h}_{prs,qtu} \tilde{G}_{tu,rs}^{2\text{ph}}(t_1 - t_1^+) + \dots \right) \delta(t_1, t_3) .\end{aligned}\quad (215)$$

The functional derivative of the static component with respect to the exact Green's function is therefore

$$\begin{aligned}i \frac{\delta \tilde{\Sigma}_{pr}^{\infty}(t_1, t_3)}{\delta \tilde{G}_{sq}(t_4, t_2)} &= \left( \bar{h}_{pq,rs} - i \sum_{rs,tu} \bar{h}_{pqt,rsu} \tilde{G}_{ut}(t_1 - t_1^+) + \dots \right) \delta(t_1, t_3) \delta(t_1, t_2) \delta(t_1^+, t_4) \\ &\quad + \tilde{\chi}_{pq,rs}^c(t_1, t_2; t_1^+, t_4) \delta(t_1, t_3) ,\end{aligned}\quad (216)$$

where  $\tilde{\Xi}_{pq,rs}^c(t_1, t_2; t_1^+, t_4)$  represents the contribution that is dependent on functional derivatives involving the  $\tilde{\Lambda}^{\text{npt}}$ -vertices and is explicitly related to multiparticle correlation effects. This additional term  $\tilde{\Xi}^c$  is similar in origin to the functional derivative of  $W$  with respect to the Green's function in the  $GW$  approximation that arises in deriving the electronic  $GW$ -BSE kernel. The first term inside the brackets is simply the series for the two-body effective interaction (see Appendix B) [24] and so we have

$$i \frac{\delta \tilde{\Sigma}_{pr}^{\infty}(t_1, t_3)}{\delta \tilde{G}_{sq}(t_4, t_2)} = \tilde{\Xi}_{pq,rs} \delta(t_1, t_3) \delta(t_1, t_2) \delta(t_1^+, t_4) + \tilde{\Xi}_{pq,rs}^c(t_1, t_2; t_1^+, t_4) \delta(t_1, t_3) .\quad (217)$$

Therefore, at first-order, the functional derivative is the static two-body effective interaction and arises due to 'independent particle' propagation. The additional term  $\tilde{\chi}^c$  must also be accounted for and is a dynamical contribution.

To derive the additional component  $\tilde{\chi}^c$  we adopt a simplified notation whereby the spin-orbital indices and time/frequency arguments are removed. With this notation, we write

the 4-point and 6-point vertex equations from Eqs 134 and 135 as

$$\tilde{G}^{4\text{pt}} = i\mathcal{A}\{\tilde{G}\tilde{G}\} - \tilde{G}\tilde{G}\tilde{\Lambda}^{4\text{pt}}\tilde{G}\tilde{G} \quad (218)$$

and

$$\tilde{G}^{6\text{pt}} = -\mathcal{A}\{\tilde{G}\tilde{G}\tilde{G}\} - i\mathcal{P}\{\tilde{G}\tilde{G}\tilde{G}\tilde{\Lambda}^{4\text{pt}}\tilde{G}\tilde{G}\} + \tilde{G}\tilde{G}\tilde{G}\tilde{\Lambda}^{6\text{pt}}\tilde{G}\tilde{G}\tilde{G} . \quad (219)$$

where  $\mathcal{A}$  generates the correct fermionic symmetry associated with independent-particle propagation and  $\mathcal{P}$  is the cyclic permutation symmetry required to correctly describe fermionic statics of two correlated particles propagating with respect to a third independent-particle. Using this simplified notation, the static component of the self-energy becomes

$$\tilde{\Sigma}^\infty = \bar{h}^{1b} - i\bar{h}^{2b}\tilde{G} + \frac{i}{4}\bar{h}^{3b}\tilde{G}^{4\text{pt}} - \frac{i}{(3!)^2}\bar{h}^{4b}\tilde{G}^{6\text{pt}} + \dots \quad (220)$$

where  $\bar{h}^{nb}$  represent the  $n$ -body matrix elements of the similarity transformed Hamiltonian. As demonstrated in Ref. [24], the contribution of the functional derivative  $\frac{\delta\tilde{\Sigma}^\infty}{\delta\tilde{G}}$  due to anti-symmetrized independent-particle propagation gives the static two-body effective interaction,  $\tilde{\chi}^{2b}$ . The functional derivatives of the higher-body Green's functions with respect to the single-particle propagator (removing the anti-symmetrized independent-particle propagation) gives rise to the general structure

$$\frac{\delta}{\delta\tilde{G}}\left(\tilde{G}^{4\text{pt}} - i\mathcal{A}\{\tilde{G}\tilde{G}\}\right) = -2\tilde{G}\tilde{\Lambda}^{4\text{pt}}\tilde{G}\tilde{G} - \tilde{G}\tilde{G}\frac{\delta\tilde{\Lambda}^{4\text{pt}}}{\delta\tilde{G}}\tilde{G}\tilde{G} \quad (221a)$$

with

$$\begin{aligned} \frac{\delta}{\delta\tilde{G}}\left(\tilde{G}^{6\text{pt}} + \mathcal{A}\{\tilde{G}\tilde{G}\tilde{G}\}\right) &= -(3!)^2i\tilde{G}\tilde{G}\tilde{\Lambda}^{4\text{pt}}\tilde{G}\tilde{G} - 3^2i\tilde{G}\tilde{G}\tilde{G}\frac{\delta\tilde{\Lambda}^{4\text{pt}}}{\delta\tilde{G}}\tilde{G}\tilde{G} + 3\tilde{G}\tilde{G}\tilde{\Lambda}^{6\text{pt}}\tilde{G}\tilde{G}\tilde{G} \\ &+ \tilde{G}\tilde{G}\tilde{G}\frac{\delta\tilde{\Lambda}^{6\text{pt}}}{\delta\tilde{G}}\tilde{G}\tilde{G}\tilde{G} \end{aligned} \quad (221b)$$

and so on for the higher derivatives. In these equations, the pre-factors represent the number of equivalent terms generated by the different functional derivatives with respect to permutation of the fermionic states. Therefore, the functional derivative of the static component of the coupled-cluster self-energy gives rise to

$$\begin{aligned} i\frac{\delta\tilde{\Sigma}^\infty}{\delta\tilde{G}} &= \tilde{\Xi}^{2b} + \frac{1}{(2!)^2}\bar{h}^{3b}\left(2!\tilde{G}\tilde{\Lambda}^{4\text{pt}}\tilde{G}\tilde{G} + \tilde{G}\tilde{G}\frac{\delta\tilde{\Lambda}^{4\text{pt}}}{\delta\tilde{G}}\tilde{G}\tilde{G}\right) \\ &+ \frac{1}{(3!)^2}\bar{h}^{4b}\left(- (3!)^2i\tilde{G}\tilde{G}\tilde{\Lambda}^{4\text{pt}}\tilde{G}\tilde{G} - 3^2i\tilde{G}\tilde{G}\tilde{G}\frac{\delta\tilde{\Lambda}^{4\text{pt}}}{\delta\tilde{G}}\tilde{G}\tilde{G} + 3\tilde{G}\tilde{G}\tilde{\Lambda}^{6\text{pt}}\tilde{G}\tilde{G}\tilde{G}\right) \\ &+ \tilde{G}\tilde{G}\tilde{G}\frac{\delta\tilde{\Lambda}^{6\text{pt}}}{\delta\tilde{G}}\tilde{G}\tilde{G}\tilde{G} + \dots \end{aligned} \quad (222)$$

Collecting like terms together along with the higher-order contributions arising from functional derivatives of the higher-order Green's functions we have

$$\begin{aligned}
i\frac{\delta\tilde{\Sigma}^\infty}{\delta\tilde{G}} &= \tilde{\Xi}^{2b} + \frac{1}{2!}\left(\bar{h}^{3b} - i\bar{h}^{4b}\tilde{G} + \dots\right)\left(\tilde{G}\tilde{\Lambda}^{4\text{pt}}\tilde{G}\tilde{G}\right) + \frac{1}{(2!)^2}\left(\bar{h}^{3b} - i\bar{h}^{4b}\tilde{G} + \dots\right)\left(\tilde{G}\tilde{G}\frac{\delta\tilde{\Lambda}^{4\text{pt}}}{\delta\tilde{G}}\tilde{G}\tilde{G}\right) \\
&+ \frac{1}{(3!)^2}\left(\bar{h}^{4b} - i\bar{h}^{5b}\tilde{G} + \dots\right)\left(3\tilde{G}\tilde{G}\tilde{\Lambda}^{6\text{pt}}\tilde{G}\tilde{G}\tilde{G} + \tilde{G}\tilde{G}\tilde{G}\frac{\delta\tilde{\Lambda}^{6\text{pt}}}{\delta\tilde{G}}\tilde{G}\tilde{G}\tilde{G}\right) + \dots
\end{aligned} \tag{223}$$

Identifying the expressions in brackets as the effective interactions that arise when normal-ordering the similarity transformed Hamiltonian with respect to the biorthogonal ground state expectation value, we find

$$\begin{aligned}
i\frac{\delta\tilde{\Sigma}^\infty}{\delta\tilde{G}} &= \tilde{\Xi}^{2b} + \frac{1}{2!}\tilde{\chi}^{3b}\left(\tilde{G}\tilde{\Lambda}^{4\text{pt}}\tilde{G}\tilde{G}\right) + \frac{1}{(2!)^2}\tilde{\chi}^{3b}\left(\tilde{G}\tilde{G}\frac{\delta\tilde{\Lambda}^{4\text{pt}}}{\delta\tilde{G}}\tilde{G}\tilde{G}\right) + \frac{1}{3! \cdot 2!}\tilde{\chi}^{4b}\tilde{G}\tilde{G}\tilde{\Lambda}^{6\text{pt}}\tilde{G}\tilde{G}\tilde{G} \\
&+ \frac{1}{(3!)^2}\tilde{\chi}^{4b}\tilde{G}\tilde{G}\tilde{G}\frac{\delta\tilde{\Lambda}^{6\text{pt}}}{\delta\tilde{G}}\tilde{G}\tilde{G}\tilde{G} + \dots
\end{aligned} \tag{224}$$

where the series continues with the higher-order effective interactions contracting with higher-order vertices in this schematic derivation. At first-order, the explicitly frequency-dependent contribution gives rise to the following diagrams, which correspond to the second term of the right hand side of Eq. 224

$$\begin{aligned}
\tilde{\Xi}_{pq,rs}^{c(1)} &= \begin{array}{c} \text{Diagram 1: A wavy line with index } q \text{ connects two vertices. The left vertex is connected to a dashed line with index } p \text{ and } r. \text{ The right vertex is connected to a dashed line with index } s. \text{ Two solid lines with arrows form a loop between the two vertices.} \end{array} + \begin{array}{c} \text{Diagram 2: A wavy line with index } q \text{ connects two vertices. The left vertex is connected to a dashed line with index } p \text{ and } s. \text{ The right vertex is connected to a dashed line with index } r. \text{ Two solid lines with arrows form a loop between the two vertices.} \end{array}
\end{aligned} \tag{225}$$

where we have re-inserted the spin-orbital indices and accounted for the different external index permutations. Diagrammatically, this term arises from cutting the Green's function lines in the following diagram contributing to the static component of the self-energy:

$$\begin{aligned}
\tilde{\Sigma}_{pr}^{\infty(c,1)} &= \begin{array}{c} \text{Diagram: A wavy line with index } q \text{ connects two vertices. The left vertex is connected to a dashed line with index } p \text{ and } r. \text{ The right vertex is connected to a dashed line with index } p \text{ and } r. \text{ Two solid lines with arrows form a loop between the two vertices.} \end{array}
\end{aligned} \tag{226}$$

This diagram appears when expanding the 4-point Green's function in the expression for  $\tilde{\Sigma}^\infty$  through the four-point vertex equation (Eq. 134). The resulting contribution is explicitly

dynamical. A similar expression holds for the two-body effective interaction elements

$$i \frac{\delta \tilde{\Xi}_{pq,rs}}{\delta \tilde{G}_{ut}(t_4, t_2)} \delta(t_1, t_3) = \tilde{\chi}_{pqt,rsu} \delta(t_1, t_3) \delta(t_1, t_2) \delta(t_1^+, t_4) + \tilde{\chi}_{pqt,rsu}^c(t_1, t_2; t_1^+ t_4) \delta(t_1, t_3) . \quad (227)$$

Using our simplified notation, we find

$$\begin{aligned} i \frac{\delta \tilde{\Xi}^{2b}}{\delta \tilde{G}} &= \tilde{\chi}^{3b} + \frac{1}{2!} \tilde{\chi}^{4b} \left( \tilde{G} \tilde{\Lambda}^{4\text{pt}} \tilde{G} \tilde{G} \right) + \frac{1}{(2!)^2} \tilde{\chi}^{4b} \left( \tilde{G} \tilde{G} \frac{\delta \tilde{\Lambda}^{4\text{pt}}}{\delta \tilde{G}} \tilde{G} \tilde{G} \right) + \frac{1}{3! \cdot 2!} \tilde{\chi}^{5b} \tilde{G} \tilde{G} \Lambda^{6\text{pt}} \tilde{G} \tilde{G} \tilde{G} \\ &+ \frac{1}{(3!)^2} \tilde{\chi}^{5b} \tilde{G} \tilde{G} \tilde{G} \frac{\delta \Lambda^{6\text{pt}}}{\delta \tilde{G}} \tilde{G} \tilde{G} \tilde{G} + \dots \end{aligned} \quad (228)$$

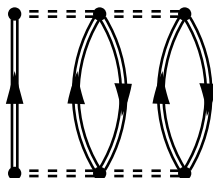
and so on for the derivatives of higher-body interactions. In the case of a three-body Hamiltonian, this derivative would only generate the bare three-body interaction,  $i \frac{\delta \tilde{\Xi}^{2b}}{\delta \tilde{G}} = \tilde{\chi}^{3b} = \bar{h}^{3b}$ , as there are no higher-body interactions present. Using these results, the corresponding expansion for the coupled-cluster BSE kernel is given by the following series of Feynman diagrams (up to second-order)

$$\begin{aligned} \tilde{\Xi}_{pq,rs}[\tilde{G}] &= \begin{array}{c} p \\ \bullet \end{array} \text{---} \text{---} \text{---} \begin{array}{c} q \\ \bullet \end{array} + \begin{array}{c} p \\ \bullet \end{array} \begin{array}{c} \text{---} \text{---} \text{---} \\ \text{---} \text{---} \text{---} \\ \bullet \end{array} \begin{array}{c} s \\ \bullet \end{array} + \begin{array}{c} p \\ \bullet \end{array} \begin{array}{c} \text{---} \text{---} \text{---} \\ \text{---} \text{---} \text{---} \\ \bullet \end{array} \begin{array}{c} q \\ \bullet \end{array} + \begin{array}{c} p \\ \bullet \end{array} \begin{array}{c} \text{---} \text{---} \text{---} \\ \text{---} \text{---} \text{---} \\ \bullet \end{array} \begin{array}{c} q \\ \bullet \end{array} \\ &+ \begin{array}{c} p \\ \bullet \end{array} \begin{array}{c} \text{---} \text{---} \text{---} \\ \text{---} \text{---} \text{---} \\ \bullet \end{array} \begin{array}{c} q \\ \bullet \end{array} + \begin{array}{c} p \\ \bullet \end{array} \begin{array}{c} \text{---} \text{---} \text{---} \\ \text{---} \text{---} \text{---} \\ \bullet \end{array} \begin{array}{c} q \\ \bullet \end{array} + \begin{array}{c} p \\ \bullet \end{array} \begin{array}{c} \text{---} \text{---} \text{---} \\ \text{---} \text{---} \text{---} \\ \bullet \end{array} \begin{array}{c} q \\ \bullet \end{array} + \begin{array}{c} p \\ \bullet \end{array} \begin{array}{c} \text{---} \text{---} \text{---} \\ \text{---} \text{---} \text{---} \\ \bullet \end{array} \begin{array}{c} q \\ \bullet \end{array} \\ &+ \dots \end{aligned} \quad (229)$$

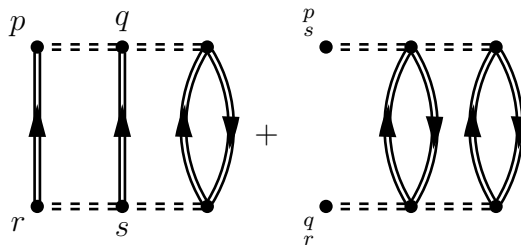
We obtain the perturbative expansion,  $\tilde{\Xi}[G_0]$ , to second-order by inserting Eq. 150 into Eq. 229 whilst replacing all effective interactions and Green's functions by their reference counterparts:  $\tilde{\chi} \rightarrow \chi$ ,  $\tilde{G} \rightarrow G_0$ . As can be seen from the general diagrammatic series, the

CC-BSE kernel reduces to the electronic BSE kernel when  $T = 0$  and the effects of the similarity transformation are removed. The second, third and fourth diagrams of the first line of Eq. 229 arise by cutting the Green's function lines of the second-order dynamical self-energy diagram of Eq. 143. The fifth and sixth diagrams of Eq. 229 appear when taking the functional derivative of the two-body effective interaction lines appearing in the second-order self-energy diagram. They are the first-order contributions according to Eq. 227. The final two diagrams of Eq. 229 are those that arise due to derivatives of the static component of the self-energy as outlined in Eq. 225.

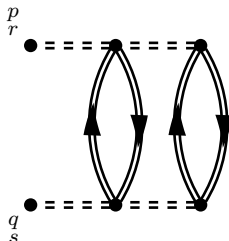
We can also take the functional derivative of the vanishing second-order self-energy diagram (see Section IX)



and find that this gives rise to the BSE kernel diagrams



However, as these diagrams have four Green's function lines below the three-body vertex, they also vanish due to the coupled-cluster similarity transformation. If we take the functional derivative of the two-body interaction in Eq. 226, at first-order we generate the complementary exchange diagram



which also vanishes. At first-order, the functional derivative of the three-body effective interaction in Eq. 226 gives rise to the diagram



which explicitly contains the 4-body effective interaction. Depending on the ordering of the external indices, this diagram may not vanish and will give a non-zero contribution to the CC-BSE kernel.

From our analysis, we see that the diagrams of the Bethe-Salpeter kernel generated by an  $N$ -body interaction result from functional derivatives of different components of the self-energy. We note that the corresponding expression for the 6-point vertex function is obtained by functional derivative of the BSE kernel with respect to the single-particle Green's function,  $\tilde{\Lambda}^{6\text{pt}} \sim i \frac{\delta \tilde{\Xi}}{\delta G}$ , and so on for the higher-order vertices. These relationships arise as the 6-point Green's function is generated from the functional derivative of the 4-point Green's function and so on (see Appendix E).

Using the general analysis presented in this work, we can generate the diagrammatic series for the coupled-cluster BSE kernel order-by-order. When restricted to the TDA, the perturbative expansion of the coupled-cluster BSE kernel derived here is closely related to the EE-EOM-CC eigenvalue problem. To conclude this section, we write the terms appearing in the second-order perturbative expansion of the CC-BSE kernel as

$$\begin{aligned}
\tilde{\Xi}_{pq,rs}^{(2)}(\omega) = & \chi_{pq,rs} + \sum_{kc} \frac{\chi_{pqc,rsk} \tilde{\Sigma}_{kc}^{\infty(0)}}{\epsilon_k - \epsilon_c} + \frac{1}{(2!)^2} \sum_{abij} \frac{\chi_{pqab,rsij} \chi_{ij,ab}}{\epsilon_i - \epsilon_j - \epsilon_a - \epsilon_b} + \sum_{kc} \frac{\chi_{pk,sc} \chi_{cq,rk}}{\omega - (\epsilon_c - \epsilon_k) + i\eta} \\
& + \sum_{kc} \frac{\chi_{pc,ks} \chi_{kq,rc}}{\omega - (\epsilon_k - \epsilon_c) - i\eta} - \frac{1}{2} \sum_{kl} \frac{\chi_{pq,kl} \chi_{kl,rs}}{\omega - (\epsilon_k + \epsilon_l) - i\eta} + \frac{1}{2} \sum_{cd} \frac{\chi_{pq,cd} \chi_{cd,rs}}{\omega - (\epsilon_c + \epsilon_d) + i\eta} \\
& + \frac{1}{2} \sum_{abk} \frac{(\chi_{abq,rks} \chi_{pk,ab} + \chi_{pkq,abs} \chi_{ab,rk} + \chi_{pab,rks} \chi_{kq,ab} + \chi_{pab,rsk} \chi_{qk,ab})}{\omega + \epsilon_k - \epsilon_a - \epsilon_b + i\eta} \\
& + \frac{1}{2} \sum_{kla} \frac{(\chi_{klq,ras} \chi_{pa,kl} + \chi_{paq,klr} \chi_{kl,ra} + \chi_{pkl,ras} \chi_{aq,kl} + \chi_{pkl,rsa} \chi_{qa,kl})}{\omega + \epsilon_a - \epsilon_k - \epsilon_l - i\eta}.
\end{aligned} \tag{231}$$

Here, the first three terms arise due to the perturbative expansion of the two-body effective interaction (see Eq. 150). The remaining terms correspond to the remaining diagrams of Eq. 229 where the Green's function and interaction lines are replaced by  $G_0$  and  $\chi$  equivalents. We clearly see the similarity between the fourth, fifth, sixth and seventh terms of Eq. 231 and those obtained within the second-order perturbative approximation for the electronic BSE kernel [25, 60–62]. Using Eq. 231 for the CC-BSE kernel, we can formulate closed equations for the particle-hole response function which give access to neutral excitation energies.

## XV. CONCLUSIONS AND OUTLOOK

In summary, we have presented the general diagrammatic theory of the irreducible self-energy and Bethe-Salpeter kernel that is generated by a general  $N$ -body hermitian or non-hermitian interaction Hamiltonian. We have centered our analysis around the non-hermitian coupled-cluster similarity transformed Hamiltonian.

To generate a consistent theory of the coupled-cluster self-energy, we define the single-particle Green's function  $\tilde{G}$ , of a general  $N$ -body non-hermitian interaction within the biorthogonal quantum theory. We extend the Gell-Mann and Low theorem to include adiabatic generation of the right and left ground states of a pseudo-hermitian Hamiltonian, which leads to the perturbative expansion of the non-hermitian single-particle Green's function. Using the Gell-Mann and Low theorem, we introduce the non-hermitian Dyson equation and generate the perturbative expansion for the coupled-cluster self-energy,  $\tilde{\Sigma}[G_0]$ . From the equation-of-motion for the single-particle coupled-cluster Green's function we reveal the structure of the self-consistent renormalized coupled-cluster self-energy,  $\tilde{\Sigma}[\tilde{G}]$  and demonstrate how the perturbative self-energy is generated from this functional. The analysis presented in this work clearly demonstrates the emergence of different effective interactions that appear when expanding the self-energy with respect to either the non-interacting or the exact Green's function. These interactions correspond to those appearing when normal-ordering the Hamiltonian with respect to the reference or exact ground state. Further, we show how the electronic self-energy emerges when the similarity transformation of the electronic structure Hamiltonian is removed.

We subsequently derive the coupled-cluster Dyson supermatrix from the spectral representation of the coupled-cluster self-energy and present several approximate expressions for the coupled-cluster self-energy that are restricted to the space of 2p1h/2h1p excitations. In the process, we have firmly demonstrated the relationship and connections between the coupled-cluster self-energy, IP/EA-EOM-CC theory and the  $G_0W_0$  approximation. This analysis lead us to introduce CC- $G_0W_0$  theory which combines aspects of the  $G_0W_0$  approximation with the coupled-cluster self-energy presented in Section X. This is a novel approximation that will be explored in future work. Our formulation also allows us to explore approximations beyond  $G_0W_0$  theory by using the full CCSD singles and doubles

excitation and de-excitation amplitudes in place of the rCCD amplitudes. Use of the full CCSD amplitudes goes beyond RPA screening by including the complete set of interactions,  $\langle \Phi_j^a | \bar{H}_N | \Phi_i^b \rangle$ , between singly excited configurations [24].

Finally, we derive the coupled-cluster BSE kernel in terms of the functional derivative of the coupled-cluster self-energy with respect to the single-particle coupled-cluster Green's function. We demonstrate that diagrams of the CC-BSE kernel are generated both by cutting Green's function lines in self-energy diagrams whilst also taking derivatives of the interaction vertices. These diagrams are closely related to the terms that arise within EE-EOM-CCSD theory once further approximations are made in defining an effective kernel that depends only on a single frequency [58, 61, 62].

Our formalism provides the theoretical foundation for many possible implementations as a result of different approximations of the coupled-cluster amplitude equations. A potential further application of the formalism presented in this work would be to generate the self-energy and Bethe-Salpeter kernel for the transcorrelated Hamiltonian [64–67]. The theory presented in this work provides a unified and complete description of the seemingly disconnected approaches of coupled-cluster theory and the Green's function formalism. Our findings should form the basis for improved formulations of Green's function theory for systems of many interacting particles.

## Appendix A: Proof of Extended Gell-Mann and Low Theorem

From the ‘adiabatic switching on’ procedure, we have the time-evolution operator in the interaction picture as

$$U_\eta(0, -\infty) = \mathcal{T} \left\{ \exp \left( -i \int_{-\infty}^0 dt \bar{H}_1(t) e^{-\eta|t|} \right) \right\} \quad (\text{A1})$$

If the limit

$$\lim_{\eta \rightarrow 0} \frac{U_\eta(0, -\infty) |\Phi_0\rangle}{\langle \tilde{\Phi}_0 | U_\eta(0, -\infty) | \Phi_0 \rangle} \equiv \frac{|\Psi_0\rangle}{\langle \tilde{\Phi}_0 | \Psi_0 \rangle} \quad (\text{A2})$$

exists then:

$$\bar{H} \frac{|\Psi_0\rangle}{\langle \tilde{\Phi}_0 | \Psi_0 \rangle} = E \frac{|\Psi_0\rangle}{\langle \tilde{\Phi}_0 | \Psi_0 \rangle}. \quad (\text{A3})$$

Therefore, the quantity  $\frac{|\Psi_0\rangle}{\langle\tilde{\Phi}_0|\Psi_0\rangle}$  is an eigenstate of the full Hamiltonian,  $\bar{H}$ .

**Proof:** Consider the quantity

$$\begin{aligned} (\bar{H}_0 - E^{(0)}) |\Psi_0(\eta)\rangle &= (\bar{H}_0 - E^{(0)}) U_\eta(0, -\infty) |\Phi_0\rangle \\ &= [H_0, U_\eta(0, -\infty)] |\Phi_0\rangle . \end{aligned} \quad (\text{A4})$$

In the biorthogonal Interaction picture, we have that

$$i \frac{\partial}{\partial t} \bar{H}_1(t) = [\bar{H}_1(t), \bar{H}_0] \quad (\text{A5})$$

Evaluating the commutators arising in Eq. A4, we have

$$\begin{aligned} (\bar{H}_0 - E^{(0)}) |\Psi_0(\eta)\rangle &= - \sum_{n=1}^{\infty} \frac{(-i)^{n-1}}{n!} \int_{-\infty}^0 dt_1 \cdots \int_{-\infty}^0 dt_n e^{-\eta|t_1+\dots+t_n|} \\ &\quad \times \left( \sum_{i=1}^n \frac{\partial}{\partial t_i} \right) \mathcal{T} \{ \bar{H}_1(t_1) \dots \bar{H}_1(t_n) \} |\Phi_0\rangle \end{aligned} \quad (\text{A6})$$

Performing integration by parts with respect to  $t_1$ , we have

$$(\bar{H}_0 - E^{(0)}) |\Psi_0(\eta)\rangle = -\bar{H}_1 |\Psi_0(\eta)\rangle + i\eta g \frac{\partial}{\partial g} |\Psi_0(\eta)\rangle \quad (\text{A7})$$

where we have assumed that the interaction  $\bar{H}_1$  is proportional to an arbitrary coupling constant,  $g$ , which allows us to identify [1, 39]

$$\frac{(-i)^{n-1}}{(n-1)!} g^n = ig \frac{\partial}{\partial g} \left( \frac{(-i)^n}{n!} g^n \right) . \quad (\text{A8})$$

Therefore, we have

$$(\bar{H} - E^{(0)}) |\Psi_0(\eta)\rangle = i\eta g \frac{\partial}{\partial g} |\Psi_0(\eta)\rangle \quad (\text{A9})$$

and projecting on both sides with  $\frac{\langle\tilde{\Phi}_0|}{\langle\tilde{\Phi}_0|\Psi_0(\eta)\rangle}$ , we get

$$\frac{\langle\tilde{\Phi}_0|\bar{H}_1|\Psi_0(\eta)\rangle}{\langle\tilde{\Phi}_0|\Psi_0(\eta)\rangle} = i\eta g \frac{\partial}{\partial g} \left( \log \langle\tilde{\Phi}_0|\Psi_0(\eta)\rangle \right) = \Delta E(\eta) . \quad (\text{A10})$$

However, we also have that

$$(\bar{H} - E^{(0)}) \frac{|\Psi_0(\eta)\rangle}{\langle\tilde{\Phi}_0|\Psi_0(\eta)\rangle} = \frac{i\eta g}{\langle\tilde{\Phi}_0|\Psi_0(\eta)\rangle} \frac{\partial}{\partial g} |\Psi_0(\eta)\rangle \quad (\text{A11})$$

by multiplying Eq A9 by  $\frac{1}{\langle \tilde{\Phi}_0 | \Psi_0(\eta) \rangle}$ . This equation can be rearranged to give

$$\left( \bar{H} - E^{(0)} - i\eta g \frac{\partial}{\partial g} \right) \frac{|\Psi_0(\eta)\rangle}{\langle \tilde{\Phi}_0 | \Psi_0(\eta) \rangle} = \frac{|\Psi_0(\eta)\rangle}{\langle \tilde{\Phi}_0 | \Psi_0(\eta) \rangle} \times \left( i\eta g \frac{\partial}{\partial g} \log \langle \tilde{\Phi}_0 | \Psi_0(\eta) \rangle \right) \quad (\text{A12})$$

However, by Eq. A10, we may rearrange the expression to give

$$(\bar{H} - E^{(0)} - \Delta E(\eta)) \frac{|\Psi_0(\eta)\rangle}{\langle \tilde{\Phi}_0 | \Psi_0(\eta) \rangle} = i\eta g \frac{\partial}{\partial g} \frac{|\Psi_0(\eta)\rangle}{\langle \tilde{\Phi}_0 | \Psi_0(\eta) \rangle} \quad (\text{A13})$$

Now, we are in a position to take the limit as  $\eta \rightarrow 0$ . By assumption, the right hand side is finite to all orders in perturbation theory. Therefore, the multiplication by  $\eta$  as  $\eta \rightarrow 0$  sends the right hand side to zero. As a result, we have

$$(\bar{H} - E) \lim_{\eta \rightarrow 0} \frac{|\Psi_0(\eta)\rangle}{\langle \tilde{\Phi}_0 | \Psi_0(\eta) \rangle} = 0 \quad (\text{A14})$$

and hence we have the extended Gell-Mann and Low theorem. By analogy, we also have

$$(\bar{H}^\dagger - E) \lim_{\eta \rightarrow 0} \frac{|\tilde{\Psi}_0(\eta)\rangle}{\langle \tilde{\Phi}_0 | \tilde{\Psi}_0(\eta) \rangle} = 0 \quad (\text{A15})$$

for the left eigenstate.

## Appendix B: Pseudo-hermitian quantum mechanics and coupled-cluster theory

Biorthogonal quantum mechanics may be viewed in terms of the conventional quantum theory in the case where the Hilbert space is endowed with a nontrivial metric,  $\tau$ . We can make the choice that arbitrary associated states may be related to arbitrary states of the Hilbert space  $\mathcal{H}$ , through the metric,  $\tau$ . This requires the metric  $\tau$ , to be an invertible transformation (linear hermitian automorphism) on  $\mathcal{H}$  [44]. As a result, we write an arbitrary associated state as

$$|\tilde{\Psi}\rangle = \tau |\Psi\rangle \quad (\text{B1})$$

from an arbitrary state  $|\Psi\rangle$ . This definition requires the Hamiltonian to be  $\tau$ -pseudo-hermitian [40, 43, 44], namely

$$\bar{H}^\dagger = \tau \bar{H} \tau^{-1}. \quad (\text{B2})$$

To construct a pseudo-hermitian quantum theory, we must introduce the  $\tau$ -inner product defined as

$$\langle \Psi, \Phi \rangle_\tau := \langle \Phi | \tau | \Psi \rangle = \langle \tilde{\Phi} | \Psi \rangle. \quad (\text{B3})$$

The  $\tau$ -inner product is invariant under the evolution generated by a  $\tau$ -pseudo-hermitian Hamiltonian. A diagonalizable non-hermitian Hamiltonian possesses a *real* spectrum *if and only if* it is pseudo-Hermitian with respect to a linear hermitian automorphism (metric) of the form

$$\tau = OO^\dagger, \quad (\text{B4})$$

where  $O : \mathcal{H} \rightarrow \mathcal{H}$  is a linear operator [44]. Consider a pseudo-canonical transformation that leaves the Schrödinger equation

$$i\frac{\partial}{\partial t} |\Psi_S(t)\rangle = \bar{H} |\Psi_S(t)\rangle \quad (\text{B5})$$

form invariant. This requires the transformation to be of the form

$$\bar{H} \rightarrow \tilde{H} = A\bar{H}A^{-1}. \quad (\text{B6})$$

A diagonalizable Hamiltonian  $\bar{H}$  possesses a real spectrum if and only if there is a pseudo-canonical transformation that maps  $\bar{H}$  into a hermitian operator. If  $\bar{H}$  has a real spectrum then it is  $\tau$ -pseudo-hermitian of the form

$$\bar{H}^\dagger = (OO^\dagger)\bar{H}(OO^\dagger)^{-1}. \quad (\text{B7})$$

However, via the pseudo-canonical transformation we have

$$\tilde{H}^\dagger = (A^{-1})^\dagger \bar{H}^\dagger A^\dagger = (A^{-1})^\dagger (OO^\dagger) \bar{H} (OO^\dagger)^{-1} A^\dagger \quad (\text{B8})$$

Now, if we let  $A = O^\dagger$ , we have

$$\tilde{H}^\dagger = (A^{-1})^\dagger (A^\dagger A) \bar{H} (A^\dagger A)^{-1} A^\dagger = A\bar{H}A^{-1} = \tilde{H} \quad (\text{B9})$$

and hence  $\tilde{H}$  is hermitian. Therefore, a diagonalizable non-hermitian Hamiltonian possesses real eigenvalues if and only if it is pseudo-hermitian with respect to the  $\tau$ -inner product [44].

For example, in coupled-cluster theory the relationship between the hermitian electronic structure Hamiltonian  $H$ , and the similarity transformed non-hermitian Hamiltonian  $\bar{H}$  is given by

$$H = e^T \bar{H} e^{-T}. \quad (\text{B10})$$

By defining  $A = O^\dagger = e^T$ , we find that the similarity transformed Hamiltonian is necessarily pseudo-hermitian with respect to the metric defined by

$$\tau = (e^T)^\dagger e^T. \quad (\text{B11})$$

Clearly this metric is hermitian and possesses an inverse. Therefore, coupled-cluster theory can either be formulated in the language of biorthogonal quantum theory or in terms of a psuedo-hermitian quantum theory with a non trivial metric defined by Eq. B11.

### Appendix C: Normal-ordered Similarity Transformed Hamiltonian

The similarity transformed Hamiltonian is written as

$$\bar{H} = e^{-T} H e^T = \sum_{pq} \bar{h}_{pq} a_p^\dagger a_q + \frac{1}{(2!)^2} \sum_{pq,rs} \bar{h}_{pq,rs} a_p^\dagger a_q^\dagger a_s a_r + \frac{1}{(3!)^2} \sum_{pqr,stu} \bar{h}_{pqr,stu} a_p^\dagger a_q^\dagger a_r^\dagger a_u a_t a_s + \dots \quad (\text{C1})$$

Normal-ordering this Hamiltonian with respect to the reference determinant gives the expression

$$\begin{aligned} \bar{H} = \langle \Phi_0 | \bar{H} | \Phi_0 \rangle + \sum_{pq} F_{pq} \{ a_p^\dagger a_q \}_0 + \frac{1}{(2!)^2} \sum_{pq,rs} \chi_{pq,rs} \{ a_p^\dagger a_q^\dagger a_s a_r \}_0 \\ + \frac{1}{(3!)^2} \sum_{pqr,stu} \chi_{pqr,stu} \{ a_p^\dagger a_q^\dagger a_r^\dagger a_u a_t a_s \}_0 + \dots \end{aligned} \quad (\text{C2})$$

where the effective interaction matrix elements are given by [24]

$$F_{pq} = \bar{h}_{pq} - i \sum_{rs} \bar{h}_{pr,qs} G_{sr}^0(t - t^+) + \frac{i}{(2!)^2} \sum_{rs,tu} \bar{h}_{prs,qtu} G_{tu,rs}^{2\text{ph},(0)}(t - t^+) + \dots \quad (\text{C3a})$$

$$\chi_{pq,rs} = \bar{h}_{pq,rs} - i \sum_{tu} \bar{h}_{pqt,rsu} G_{ut}^0(t - t^+) + \frac{i}{(2!)^2} \sum_{tuwv} \bar{h}_{pqtu,rsuv} G_{wv,tu}^{2\text{ph},(0)}(t - t^+) + \dots \quad (\text{C3b})$$

and so on for the three-body and higher effective interactions. Here,  $-iG_{pq}^0(t - t^+) = \langle \Phi_0 | a_q^\dagger a_p | \Phi_0 \rangle$  and  $iG_{pq,rs}^{2\text{ph},(0)}(t - t^+) = \langle \Phi_0 | a_r^\dagger a_s^\dagger a_q a_p | \Phi_0 \rangle$  are the reference one- and two-particle reduced density matrices, respectively. The higher-order contributions are given by contracting higher-body matrix elements with reference reduced density matrices. However, we can also write the similarity transformed Hamiltonian as

$$\begin{aligned} \bar{H} = \langle \tilde{\Psi}_0 | \bar{H} | \Phi_0 \rangle + \sum_{pq} \tilde{F}_{pq} \{ a_p^\dagger a_q \} + \frac{1}{(2!)^2} \sum_{pq,rs} \tilde{\Xi}_{pq,rs} \{ a_p^\dagger a_q^\dagger a_s a_r \} \\ + \frac{1}{(3!)^2} \sum_{pqr,stu} \tilde{\chi}_{pqr,stu} \{ a_p^\dagger a_q^\dagger a_r^\dagger a_u a_t a_s \} + \dots \end{aligned} \quad (\text{C4})$$

where  $E_0^{\text{CC}} = \langle \tilde{\Psi}_0 | \bar{H} | \Phi_0 \rangle = \langle \Phi_0 | \bar{H} | \Phi_0 \rangle$  from the coupled-cluster Lagrangian. The normal-ordered effective interactions become

$$\begin{aligned} \tilde{F}_{pq} &= \bar{h}_{pq} - i \sum_{rs} \bar{h}_{pr,qs} \tilde{G}_{sr}(t-t^+) + \frac{i}{(2!)^2} \sum_{rs,tu} \bar{h}_{prs,qtu} \tilde{G}_{tu,rs}^{2\text{ph}}(t-t^+) + \dots \\ &= F_{pq} + \sum_{ai} \chi_{pa,qi} \lambda_a^i + \frac{1}{(2!)^2} \sum_{ijab} \chi_{pab,qij} \lambda_{ab}^{ij} + \dots \end{aligned} \quad (\text{C5a})$$

$$\begin{aligned} \tilde{\Xi}_{pq,rs} &= \bar{h}_{pq,rs} - i \sum_{tu} \bar{h}_{pqt,rsu} \tilde{G}_{ut}(t-t^+) + \frac{i}{(2!)^2} \sum_{tuwv} \chi_{pqtu,rsuw} \tilde{G}_{wv,tu}^{2\text{ph}}(t-t^+) + \dots \\ &= \chi_{pq,rs} + \sum_{ia} \chi_{pqa,rsi} \lambda_a^i + \frac{1}{(2!)^2} \sum_{ijab} \chi_{pqab,rsij} \lambda_{ab}^{ij} + \dots \end{aligned} \quad (\text{C5b})$$

and so on for the three-body and higher effective interactions. Here,  $-i\tilde{G}_{pq}(t-t^+) = \langle \tilde{\Psi}_0 | a_q^\dagger a_p | \Phi_0 \rangle$  and  $i\tilde{G}_{pq,rs}^{2\text{ph}}(t-t^+) = \langle \tilde{\Psi}_0 | a_r^\dagger a_s^\dagger a_q a_p | \Phi_0 \rangle$  are the biorthogonal one- and two-particle reduced density matrices, respectively. The higher-order contributions are given by contracting higher-body matrix elements with biorthogonal reduced density matrices.

#### Appendix D: Expansion of interaction-irreducible vertices

Here, we present the diagrammatic expansion of the interaction-irreducible one-body vertex. The derivation for higher-order interaction vertices is analogous. The one-body interaction-irreducible vertex is given by

$$\tilde{F}_{pq} = \bar{h}_{pq} - i \sum_{rs} \bar{h}_{pr,qs} \tilde{G}_{sr}(t-t^+) + \frac{i}{(2!)^2} \sum_{rstu} \bar{h}_{prs,qtu} \tilde{G}_{tu,rs}^{2\text{ph}}(t-t^+) + \dots \quad (\text{D1})$$

Using the Dyson equation for the single-particle Green's function

$$\tilde{G}_{pq}(t-t') = G_{pq}^0(t-t') + \int dt_1 dt_2 \sum_{vw} G_{pv}^0(t-t_1) \tilde{\Sigma}_{vw}(t_1-t_2) \tilde{G}_{wq}(t_2-t') \quad (\text{D2})$$

and expanding the equal time two-particle Green's function as the antisymmetrized sum of the first two terms from independent-particle propagation

$$\tilde{G}_{tu,rs}^{2\text{ph}}(t-t^+) \approx i\tilde{G}_{tr}(t-t^+) \tilde{G}_{us}(t-t^+) - i\tilde{G}_{ts}(t-t^+) \tilde{G}_{ur}(t-t^+), \quad (\text{D3})$$

we insert the Dyson equation into Eqs D1 and D3 to obtain



a non-local fictitious external potential  $U$ , that couples to the system, we can write the single-particle coupled-cluster Green's function as

$$i\tilde{G}_{pr}(t_1, t_3) = \frac{\langle \tilde{\Psi}_0 | \mathcal{T} \{ S a_p(t_1) a_r^\dagger(t_3) \} | \Phi_0 \rangle}{\langle \tilde{\Psi}_0 | S | \Phi_0 \rangle} \quad (\text{E1})$$

where

$$S = \mathcal{T} \left\{ \exp \left( -i \int dt dt' \sum_{vw} U_{vw}(t, t') a_v^\dagger(t) a_w(t') \right) \right\} \quad (\text{E2})$$

We can therefore define

$$\begin{aligned} \tilde{L}_{pq,rs}(t_1, t_2; t_3, t_4) &= -i \frac{\delta \tilde{G}_{pr}(t_1, t_3)}{\delta U_{sq}(t_4, t_2)} \\ &= \tilde{G}_{pq,rs}^{4\text{pt}}(t_1, t_2; t_3, t_4) - i \tilde{G}_{pr}(t_1, t_3) \tilde{G}_{qs}(t_2, t_4) \end{aligned} \quad (\text{E3})$$

This result immediately yields the Bethe-Salpeter equation as the inverse is defined as

$$\tilde{L}_{pq,rs}^{-1}(t_1, t_2; t_3, t_4) = i \frac{\delta U_{pr}(t_1, t_3)}{\delta \tilde{G}_{sq}(t_4, t_2)} \quad (\text{E4})$$

which leads to

$$\tilde{L}_{pq,rs}^{0,-1}(t_1, t_2; t_3, t_4) = \tilde{L}_{pq,rs}^{-1}(t_1, t_2; t_3, t_4) + i \frac{\delta \tilde{\Sigma}_{pr}(t_1, t_3)}{\delta \tilde{G}_{sq}(t_4, t_2)}. \quad (\text{E5})$$

Therefore, we identify the BSE kernel as

$$\tilde{\Xi}_{pq,rs}(t_1, t_2; t_3, t_4) = i \frac{\delta \tilde{\Sigma}_{pr}(t_1, t_3)}{\delta \tilde{G}_{sq}(t_4, t_2)}. \quad (\text{E6})$$

Finally we write the integral form of the coupled-cluster BSE:

$$\begin{aligned} \tilde{L}_{pq,rs}(t_1, t_2; t_3, t_4) &= \tilde{L}_{pq,rs}^0(t_1, t_2; t_3, t_4) \\ &+ \sum_{tuvw} \int dt dt' dt'' dt''' \tilde{L}_{pt,ru}^0(t_1, t; t_3, t') \tilde{\Xi}_{uv,tw}(t', t''; t, t''') \tilde{L}_{wq,vs}(t''', t_2; t'', t_4). \end{aligned} \quad (\text{E7})$$

Using the functional derivative technique, the relationship between the 4-point and 6-point Green's functions is as follows:

$$\tilde{G}_{pqr,stu}^{6\text{pt}}(t_1, t_2, t_3; t_4, t_5, t_6) = -i \frac{\delta \tilde{G}_{pq,st}^{4\text{pt}}(t_1, t_2; t_4, t_5)}{\delta U_{ur}(t_6, t_3)} + i \tilde{G}_{pq,st}^{4\text{pt}}(t_1, t_2; t_4, t_5) \tilde{G}_{ru}(t_3, t_6). \quad (\text{E8})$$

Therefore, the 6-point vertex is related to the functional derivative of the 4-point vertex/irreducible BSE kernel. Analogous relationships hold for the higher-order vertices.

---

[1] A. Fetter and J. D. Walecka, *Quantum Theory of Many Particle Systems* (McGraw-Hill, 1971).

- [2] G. D. Mahan, *Many-particle physics* (Springer Science & Business Media, 2000).
- [3] G. Stefanucci and R. Van Leeuwen, *Nonequilibrium many-body theory of quantum systems: A modern introduction* (Cambridge University Press, 2013).
- [4] L. Hedin, [Physical Review \*\*139\*\*, A796 \(1965\)](#).
- [5] C. Barbieri and A. Carbone, An Advanced Course in Computational Nuclear Physics: Bridging the Scales from Quarks to Neutron Stars , 571 (2017).
- [6] F. Aryasetiawan and O. Gunnarsson, [Reports on Progress in Physics \*\*61\*\*, 237 \(1998\)](#).
- [7] M. S. Hybertsen and S. G. Louie, [Physical Review B \*\*34\*\*, 5390 \(1986\)](#).
- [8] M. Rohlfing and S. G. Louie, [Physical Review B \*\*62\*\*, 4927 \(2000\)](#).
- [9] P. Romaniello, S. Guyot, and L. Reining, [The Journal of Chemical Physics \*\*131\*\*, 154111 \(2009\)](#).
- [10] P. Romaniello, F. Bechstedt, and L. Reining, [Physical Review B \*\*85\*\*, 155131 \(2012\)](#).
- [11] S. Hirata, A. E. Doran, P. J. Knowles, and J. Ortiz, [The Journal of Chemical Physics \*\*147\*\*, 044108 \(2017\)](#).
- [12] A. Carbone, A. Cipollone, C. Barbieri, A. Rios, and A. Polls, [Physical Review C \*\*88\*\*, 054326 \(2013\)](#).
- [13] F. Raimondi and C. Barbieri, [Physical Review C \*\*97\*\*, 054308 \(2018\)](#).
- [14] I. Shavitt and R. J. Bartlett, *Many-body methods in chemistry and physics: MBPT and coupled-cluster theory* (Cambridge university press, 2009).
- [15] T. Helgaker, P. Jorgensen, and J. Olsen, *Molecular electronic-structure theory* (John Wiley & Sons, 2013).
- [16] M. Nooijen and J. G. Snijders, [International Journal of Quantum Chemistry \*\*44\*\*, 55 \(1992\)](#).
- [17] M. Nooijen and J. G. Snijders, [International Journal of Quantum Chemistry \*\*48\*\*, 15 \(1993\)](#).
- [18] B. Peng and K. Kowalski, [Physical Review A \*\*94\*\*, 062512 \(2016\)](#).
- [19] B. Peng and K. Kowalski, [Journal of Chemical Theory and Computation \*\*14\*\*, 4335 \(2018\)](#).
- [20] A. Shee and D. Zgid, [Journal of Chemical Theory and Computation \*\*15\*\*, 6010 \(2019\)](#).
- [21] B. Peng, N. P. Bauman, S. Gulania, and K. Kowalski, in *Annual Reports in Computational Chemistry*, Vol. 17 (Elsevier, 2021) pp. 23–53.
- [22] A. Shee, C.-N. Yeh, and D. Zgid, [Journal of Chemical Theory and Computation \*\*18\*\*, 664 \(2022\)](#).
- [23] O. J. Backhouse and G. H. Booth, [Journal of Chemical Theory and Computation \*\*18\*\*, 6622](#)

- (2022).
- [24] C. J. N. Coveney and D. P. Tew, [arXiv preprint arXiv:2309.10451](#) (2023).
- [25] E. Monino and P.-F. Loos, [The Journal of Chemical Physics](#) **159** (2023).
- [26] J. Tölle and G. Kin-Lic Chan, [The Journal of Chemical Physics](#) **158** (2023).
- [27] V. Rishi, A. Perera, and R. J. Bartlett, [The Journal of Chemical Physics](#) **153**, 234101 (2020).
- [28] M. F. Lange and T. C. Berkelbach, [Journal of Chemical Theory and Computation](#) **14**, 4224 (2018).
- [29] J. J. Phillips and D. Zgid, [The Journal of Chemical Physics](#) **140**, 241101 (2014).
- [30] D. Neuhauser, R. Baer, and D. Zgid, [Journal of Chemical Theory and Computation](#) **13**, 5396 (2017).
- [31] A. A. Kananenka, A. R. Welden, T. N. Lan, E. Gull, and D. Zgid, [Journal of Chemical Theory and Computation](#) **12**, 2250 (2016).
- [32] L. Reining, [Wiley Interdisciplinary Reviews: Computational Molecular Science](#) **8**, e1344 (2018).
- [33] O. J. Backhouse and G. H. Booth, [Journal of Chemical Theory and Computation](#) **16**, 6294 (2020).
- [34] O. J. Backhouse, M. Nusspickel, and G. H. Booth, [Journal of Chemical Theory and Computation](#) **16**, 1090 (2020).
- [35] P. Pokhilko, S. Iskakov, C.-N. Yeh, and D. Zgid, [The Journal of Chemical Physics](#) **155**, 024119 (2021).
- [36] C. J. Scott, O. J. Backhouse, and G. H. Booth, [The Journal of Chemical Physics](#) **158** (2023).
- [37] J. Schirmer, *Many-body methods for atoms, molecules and clusters*, Vol. 94 (Springer, 2018).
- [38] G. E. Scuseria, T. M. Henderson, and D. C. Sorensen, [The Journal of Chemical Physics](#) **129**, 231101 (2008).
- [39] M. Gell-Mann and F. E. Low, [Physical Review](#) **95**, 1300 (1954).
- [40] D. C. Brody, [Journal of Physics A: Mathematical and Theoretical](#) **47**, 035305 (2013).
- [41] J. Southall, D. Hodgson, R. Purdy, and A. Beige, [Symmetry](#) **14**, 1816 (2022).
- [42] D. C. Brody, [Journal of Physics A: Mathematical and Theoretical](#) **49**, 10LT03 (2016).
- [43] W. Pauli, [Reviews of Modern Physics](#) **15**, 175 (1943).
- [44] A. Mostafazadeh, [Journal of Mathematical Physics](#) **43**, 3944 (2002).
- [45] C. M. Bender, D. C. Brody, and H. F. Jones, [Physical Review Letters](#) **89**, 270401 (2002).

- [46] Y.-G. Miao and Z.-M. Xu, *Physics Letters A* **380**, 1805 (2016).
- [47] R. A. Chiles and C. E. Dykstra, *The Journal of Chemical Physics* **74**, 4544 (1981).
- [48] N. C. Handy, J. A. Pople, M. Head-Gordon, K. Raghavachari, and G. W. Trucks, *Chemical Physics Letters* **164**, 185 (1989).
- [49] D. P. Tew, *The Journal of Chemical Physics* **145** (2016).
- [50] J. Gauss and J. F. Stanton, *The Journal of Chemical Physics* **103**, 3561 (1995).
- [51] S. Hirata, I. Grabowski, J. V. Ortiz, and R. J. Bartlett, *Physical Review A* **109**, 052220 (2024).
- [52] R. D. Mattuck and A. Theumann, *Advances in Physics* **20**, 721 (1971).
- [53] G. Riva, P. Romaniello, and J. A. Berger, *Physical Review Letters* **131**, 216401 (2023).
- [54] G. Riva, P. Romaniello, and J. A. Berger, *Physical Review B* **110**, 115140 (2024).
- [55] T. C. Berkelbach, *The Journal of Chemical Physics* **149**, 041103 (2018).
- [56] S. J. Bintrim and T. C. Berkelbach, *The Journal of Chemical Physics* **154**, 041101 (2021).
- [57] G. E. Scuseria, T. M. Henderson, and I. W. Bulik, *The Journal of Chemical Physics* **139**, 104113 (2013).
- [58] G. Strinati, *La Rivista del Nuovo Cimento (1978-1999)* **11**, 1 (1988).
- [59] P. Romaniello, D. Sangalli, J. Berger, F. Sottile, L. G. Molinari, L. Reining, and G. Onida, *The Journal of Chemical Physics* **130** (2009).
- [60] D. Zhang, S. N. Steinmann, and W. Yang, *The Journal of Chemical Physics* **139** (2013).
- [61] D. Sangalli, P. Romaniello, G. Onida, and A. Marini, *The Journal of Chemical Physics* **134** (2011).
- [62] E. Rebolini and J. Toulouse, *The Journal of Chemical Physics* **144** (2016).
- [63] V. Olevano, J. Toulouse, and P. Schuck, *The Journal of Chemical Physics* **150** (2019).
- [64] N. Handy, *The Journal of Chemical Physics* **51**, 3205 (1969).
- [65] S. Tsuneyuki, *Progress of Theoretical Physics Supplement* **176**, 134 (2008).
- [66] S. McArdle and D. P. Tew, *arXiv preprint arXiv:2006.11181* (2020).
- [67] N. Lee and A. J. Thom, *Journal of Chemical Theory and Computation* **19**, 5743 (2023).